

A COMPARISON ON PROTEIN, BACTERIAL ANTI-ADHESIVE AND ANTI-  
BACTERIAL PROPERTIES OF ZWITTERIONIC BLOCK COPOLYMER  
MICELLE CONTAINING ULTRA-THIN FILMS OF VARYING  
COMPOSITIONS

A THESIS SUBMITTED TO  
THE GRADUATE SCHOOL OF NATURAL AND APPLIED SCIENCES  
OF  
MIDDLE EAST TECHNICAL UNIVERSITY

BY

SİNEM ULUSAN

IN PARTIAL FULFILLMENT OF THE REQUIREMENTS  
FOR  
THE DEGREE OF MASTER OF SCIENCE  
IN  
CHEMISTRY

JANUARY 2019



Approval of the thesis:

**A COMPARISON ON PROTEIN, BACTERIAL ANTI-ADHESIVE AND  
ANTI-BACTERIAL PROPERTIES OF ZWITTERIONIC BLOCK  
COPOLYMER MICELLE CONTAINING ULTRA-THIN FILMS OF  
VARYING COMPOSITIONS**

submitted by **SİNEM ULUSAN** in partial fulfillment of the requirements for the degree of **Master of Science in Chemistry Department, Middle East Technical University** by,

Prof. Dr. Halil Kalıpçılar  
Dean, Graduate School of **Natural and Applied Sciences**

\_\_\_\_\_

Prof. Dr. Cihangir Tanyeli  
Head of Department, **Chemistry**

\_\_\_\_\_

Assoc. Prof. Dr. İrem Erel Göktepe  
Supervisor, **Chemistry, METU**

\_\_\_\_\_

Prof. Dr. Sreeparna Banerjee  
Co-Supervisor, **Department of Biological Sciences, METU**

\_\_\_\_\_

**Examining Committee Members:**

Prof. Dr. Levent Toppare  
Department of Chemistry, METU

\_\_\_\_\_

Assoc. Prof. Dr. İrem Erel Göktepe  
Department of Chemistry, METU

\_\_\_\_\_

Prof. Dr. Kezban Ulubayram  
Dept. of Basic Pharmaceutical Sciences, Hacettepe University

\_\_\_\_\_

Assoc. Prof. Dr. Özgül Persil Çetinkol  
Department of Chemistry, METU

\_\_\_\_\_

Assist. Prof. Dr. Antoine Marion  
Department of Chemistry, METU

\_\_\_\_\_

Date: 15.01.2019

**I hereby declare that all information in this document has been obtained and presented in accordance with academic rules and ethical conduct. I also declare that, as required by these rules and conduct, I have fully cited and referenced all material and results that are not original to this work.**

Name, Last name: Sinem Ulsan

Signature:

## ABSTRACT

### A COMPARISON ON PROTEIN, BACTERIAL ANTI-ADHESIVE AND ANTI-BACTERIAL PROPERTIES OF ZWITTERIONIC BLOCK COPOLYMER MICELLE CONTAINING ULTRA-THIN FILMS OF VARYING COMPOSITIONS

Ulusan, Sinem

M. S., Department of Chemistry

Supervisor: Assoc. Prof. Dr. İrem Erel Göktepe

Co-Supervisor: Prof. Dr. Sreeparna Banerjee

January 2019, 97 pages

In this study preparation of ultra-thin coatings of zwitterionic block copolymer micelles and a comparison of their protein adsorption, adhesiveness and anti-bacterial properties as well as adhesiveness against osteoblast-like cells were studied. Zwitterionic block copolymer micelles were obtained through pH-induced self-assembly of poly[3-dimethyl (methacryloyloxyethyl) ammonium propane sulfonate-*b*-2-(diisopropylamino)ethyl methacrylate] ( $\beta$ PDMA-*b*-PDPA) at pH 7.5.  $\beta$ PDMA-*b*-PDPA micelles with zwitterionic  $\beta$ PDMA-corona and pH-responsive PDPA-core were then used as building blocks to prepare either 1-layer or layer-by-layer (LbL) assembled multilayer films together with Hyaluronic Acid (HA), Tannic Acid (TA) or poly(sodium 4-styrene sulfonate) (PSS). Protein adsorption tests showed that 3-layer  $\beta$ PDMA-*b*-PDPA micelles/HA films were the most effective in reducing the adhesion of BSA, lysozyme, ferritin, and casein. In contrast,  $\beta$ PDMA-*b*-PDPA micelles/TA films were the most attractive surfaces for protein adsorption. Bacterial anti-adhesive tests against a model Gram-negative bacterium, *Escherichia coli* and a model Gram-positive bacterium, *Staphylococcus aureus* were in good agreement with the protein adsorption properties of the films. The differences in the anti-adhesive properties between these three different film systems were discussed within

the context of chemical nature and the functional chemical groups of the polyanions, layer number and surface morphology of the films. Multilayers were found to lose their anti-adhesiveness in the long-term. However, by taking advantage of the pH-responsive hydrophobic micellar cores, an anti-bacterial agent could be loaded into the micelles and multilayers could exhibit anti-bacterial activity in the long-term especially at moderately acidic conditions. In contrast to anti-adhesive properties, no significant differences were recorded in the anti-bacterial properties or osteoblast adhesive properties between the different film types.

**Keywords:** LbL, polyzwitterions, anti-bacterial, anti-adhesive, surface morphology, pH-responsive micellization

## ÖZ

### **BLOK KOPOLİMER MİSEL İÇEREN ÇOK İNCE FİLMLEİN, BAKTERİ VE PROTEİN TUTUNMASI VE ANTİ-BAKTERİYEL ÖZELLİKLERİNİN KARŞILAŞTIRILMASI**

Uluslan, Sinem  
Yüksek Lisans, Kimya Bölümü  
Tez Yöneticisi: Doç. Dr. İrem Erel Göktepe  
Yardımcı Tez Yöneticisi: Prof. Dr. Sreeparna Banerjee  
Ocak 2019, 97 sayfa

Bu çalışmada zwitteriyonik blok kopolimer miseller kullanılarak, hazırlanmış ultra ince filmlerin, bakteri ve protein tutunması, anti-bakteriyel özellikleri ve aynı zamanda osteoblast-benzeri hücre tutunması özellikleri rapor edilmiştir. Zwitteriyonik blok kopolimer miceller poli[3-dimetil(metakriloyiloksietil) amonyum propan sülfonat-*b*-2 (diizopropilamino)etil metakrilat] ( $\beta$ PDMA-*b*-PDPA) polimerinin asidik suda çözünüp (pH 3), yavaş yavaş pH ın 7.5 a yükseltilmesiyle hazırlanmıştır. pH a bağlı olarak sudaki çözünürlüğü etkilenen PDPA bloğu ortam bazik olduğunda sudaki çözünürlüğünü kaybedip hidrofobik yapıdaki koru ve zwitteriyonik blok  $\beta$ PDMA da zwitteriyonik koronası olan miselleri kendiliğinden oluşturmuşlardır. Daha sonra bu miseller üç farklı polianyon (Hyaluronik asit, Tanik asit ya da poli(stiren-4-sülfonat)) ile birlikte kullanılarak katman katman filmler oluşturulmuştur. Protein kaynağı olarak BSA, lizozim, ferritin ve kaseinin kullanıldığı deney sonuçlarına göre 3-katman  $\beta$ PDMA-*b*-PDPA misel/HA sisteminde protein tutunmasının en az, 3-katman  $\beta$ PDMA-*b*-PDPA misel/TA yüzeylerinde protein tutunmasının en fazla olduğu görülmüştür. Bakteri tutunması deneylerinde Gram + bakteri olan *Staphylococcus aureus* ve Gram – bakteri olan *Escherichia coli*, model alınmıştır. Bakteri tutunması deney sonuçları, protein tutunma deney

sonuçlarıyla uyum göstermiştir. Farklı yüzeylerin hem bakteri hem de protein tutunmasına karşı özellikleri, kullanılan polianyonlar ve kimyasal yapıları, yüzey morfolojileri ve katman sayıları gibi ölçütler göze alınarak kıyaslanıp karşılaştırılmıştır. Bu filmler kısa süre boyunca kararlı kalsalar da uzun süreçte kararlılıklarını yitirmişlerdir. Fakat hidrofobik kor içerisine yüklenen ve hidrofobik bir antibiyotik olan Triklosan sayesinde, uzun sürede filmlerden pH a bağlı olarak ilaç salımı ve anti-bakteriyel özellikler de kontrol edilmiştir. Tutunma deneylerinden farklı olarak anti-bakteriyel açıdan veya osteoblast tutunması açısından yüzeyler arasında ciddi farklar gözlenmemiştir.

**Anahtar Kelimeler:** Katman katman, polizwitteriyonlar, anti-bakteriyel, yapışmaz, yüzey morfolojisi, pH a bağlı miselleşme

To my precious family and Dearest Ebrar...

## ACKNOWLEDGMENTS

Foremost, I would like to express my gratitude and appreciation to my advisor, Assoc. Prof. Dr. İrem Erel Göktepe for her endless help, guidance, patience and support throughout my thesis. Her interdisciplinary studies enable me to combine Chemistry and Biological Sciences in my studies, which I believe will provide non-negligible advantages throughout my academic career.

I would like to thank to my co-advisor, Prof. Dr. Sreeparna Banerjee, from Biological Sciences Department, for her immense patience, guidance, tutorship and inspiration. Without her belief in me, I would not gain experience in biological sciences. I am appreciated and honored to be their graduate student. I am thankful to them for training me and directing me to think like scientist.

I would like to thank to Prof. Dr. Vural Bütün for supplying the polymer used in this study. I also thank to my thesis defense committee members, Prof. Dr. Levent Toppare, Prof. Dr. Kezban Ulubayram, Assoc. Prof. Dr. Özgül Persil Çetinkol and Assist. Prof. Dr. Antoine Marion for their guidance.

I would like to thank to Prof. Dr. Saim Özkar and Prof. Dr. Mahinur Akkaya, for their support and advices since I was an undergraduate student. Also I would like to thank to Prof. Dr. Mayda Gürsel, Prof. Dr. Mesut Muyan, Prof Dr. Gazi Huri and Ayşegül Özgür Gezer for their supports. I would like to thank Prof. Dr. Cihangir Tanyeli for helping me to start thinking on how to solve a scientific problem. I owe my first research experience to him and his graduate students, especially Dr. Seda Karahan, who trained me with her endless patience and love. I also would like to thank Eda Karadeniz, Şevki Can Cevher, Melek Parlak and Nalan Korkmaz Çokol for their help and support whenever I need.

I would like to thank to my dear labmates in biology department, especially Dr. Sinem Tunçer, for helping and training me. Also I would like to express my love to my dear friends and labmates, Burak Kızıl, Esin Gülce Seza, Betül Taşkoparan, Melis Çolakoğlu, Aydan Torun, Çağdaş Ermiş, İsmail Güderer, Hoşnaz Tuğral, Ayşe Güniz Sirt and Caner Yener for making our working environment enjoyable and

supporting me after every negative data and encouraging me after every positive data. I also would like to thank Aliye Ezgi Güleç and Hepşen Hazal Hüsnügil. I also thank to our non-official lab member Hülya Çöpoğlu for her supports. I am so happy to know all of them...

I would like to thank to my labmates in chemistry department, especially Dr. Bora Onat for his help and guidance. I would like to thank to my dear friend Majid Akbar for his support, friendship and immediate help whenever I need. I am so glad for mood-lifting activities organized by Majid together with Yusuf Samet Aytekin, Gencay Çelik, Ansab Alvi (Mufti), Muhammet Tahir Ansari (Lancer), Mustafa Yaşa and Mohammad Ali Rahimi. I am thankful to my dear labmates and friends, Eda Çağlı, Dilara Gündoğdu, Meltem Haktanıyan and Nihan Saraçoğulları for being there, helping me out, and supporting me. I also would like to thank to our undergraduate members Esmâ Uğur and Gökçe Tidim for being supportive to me.

I am thankful to my dear friends, Aslı Çetin, Soner Öztürk, Asena Şanlı, Züleyha Bingül, Kağan Gültekin, Milad Fathi, Tuğrul Almammadov, Özge İbiş, Elif Serel Yılmaz, Alim Yolalmaz, Serra Karaman and Merve Bozdemir for being a part in my life, for being with me everytime I need.

I also would like to thank to all of my friends from METU-Scout Team for all camping memories and I would like to express my sadness and passion for my dear friend Ali Baran Göğüş, who passed away very short time ago...

I would like to express my endless love to my family, İsmail Bayram Ulusan, Elmas Ulusan, Gizem Özge Ulusan and especially Furkan Utku Ulusan for being supportive to me and caring me. I cannot explain how much they mean to me with words.

Finally, I would like to express my immense, endless and biggest love to my dearie niece, Ebrar Selvi Ergin for being my niece. I love her more than everything and thank to her for motivating me even with her existence. I apologize to her because of not sparing enough time to have better memories together...

All above, I would like to express my deepest respect and love to Mustafa Kemal Atatürk for his idealism.

The content of this thesis is reprinted with permission from {Ulusan S.; Bütün V.; Banerjee S.; Erel-Goktepe, I. *Langmuir*, 2018 DOI:10.1021/acs.langmuir.8b01735}.  
Copyright {2018} American Chemical Society.

## TABLE OF CONTENT

ABSTRACT .....	v
ÖZ .....	vii
ACKNOWLEDGMENTS .....	x
TABLE OF CONTENT .....	xiii
LIST OF SCHEMES .....	xv
LIST OF FIGURES .....	xvi
LIST OF ABBREVIATIONS .....	xix
CHAPTERS	
1. INTRODUCTION .....	1
1.1. The Importance of Anti-adhesiveness on Biomaterial Surfaces .....	1
1.2. Surface Modification of Biomaterials using Polymers .....	3
1.2.1. Coating of the Biomaterial Surfaces using Anti-adhesive Polymers .....	3
1.2.1.1. History of Polyzwitterions .....	7
1.2.1.2. Types of Polybetaines Based on Functional Groups .....	9
1.2.2. Releasing Anti-microbial Agents from Polymer Coatings .....	12
1.2.3. Physical/Chemical Immobilization of Antimicrobial Agents into the Polymer Coatings to Kill the Bacteria upon Contact .....	13
1.3. Layer-by-Layer Self-assembly Technique .....	14
1.3.1. Layer-by-Layer Self-assembly of Polybetaines .....	18
1.3.2. Block Copolymer Micelle Containing LbL Films .....	19
1.3.3. Anti-Adhesive and Antibacterial LbL Films.....	20
1.3.4. Surface Coatings Promoting Osteoblast Adhesion .....	21
1.4. Aim of the Thesis .....	22
2. EXPERIMENTAL .....	25
2.1. Materials.....	25
2.2. Preparation and characterization of $\beta$ PDMA- <i>b</i> -PDPA micelles.....	26
2.3. Deposition and characterization of multilayers.....	27

2.4.	Growth conditions for bacteria.....	28
2.5.	Cell culture and imaging .....	28
2.6.	Transformation of <i>E. coli</i> K12 to stably express GFP .....	29
2.7.	Light Microscopy .....	29
2.8.	Fluorescent Microscopy .....	29
2.9.	Kirby-Bauer Test.....	30
2.10.	Protein Adsorption Tests .....	30
2.10.1.	Determination of protein adsorption by measuring protein amount via microBCA assay .....	30
2.10.2.	Determination of protein adsorption by ellipsometry .....	31
2.11.	Counting of viable surface-adherent bacteria .....	31
2.12.	Crystal violet Staining Assay .....	32
2.13.	Hydrophobicity Plots .....	32
2.14.	Statistical Analysis .....	33
3.	RESULTS & DISCUSSION .....	35
3.1.	Preparation and Characterization of Multilayers .....	35
3.2.	Stability of Multilayers.....	45
3.3.	Protein Adsorption onto Multilayers.....	51
3.4.	Anti-adhesive and Anti-bacterial Properties of the Multilayers.....	58
3.4.1.	Bacterial Anti-adhesive Properties of Multilayers .....	58
3.4.2.	Anti-bacterial Activity of Multilayers .....	65
3.5.	Osteoblast-like Cell (SaOS-2) Adhesion Properties of Multilayers.....	69
4.	CONCLUSIONS .....	73

## LIST OF SCHEMES

<b>Scheme 1.</b> Possible repeating unit architectures for polyzwitterions .....	6
<b>Scheme 2.</b> Widely used cationic and anionic moieties for zwitterionic polybetaines. 9	
<b>Scheme 3.</b> Chemical Structures of $\beta$ PDMA- <i>b</i> -PDPA, HA, TA, and PSS.....	36
<b>Scheme 4.</b> pH dependent micellization of $\beta$ PDMA- <i>b</i> -PDPA.....	37
<b>Scheme 5.</b> Chemical structure of Triclosan and representation for Triclosan loaded $\beta$ PDMA- <i>b</i> -PDPA micelles .....	66

## LIST OF FIGURES

<b>Figure 1.</b> The process of biofilm formation and components of a mature biofilm .....	2
<b>Figure 2.</b> The chemical structure of HEMA .....	4
<b>Figure 3.</b> The chemical structures of PEG or OEG <b>(A)</b> and PEGMA <b>(B)</b> .....	5
<b>Figure 4.</b> The chemical structure of PAOX .....	5
<b>Figure 5.</b> Examples for polycarboxybetaines; poly(carboxybetaineacrylamide) (PCBAA) <b>(A)</b> , poly(carboxybetaine methacrylate) (PCBMA) <b>(B)</b> .....	10
<b>Figure 6.</b> An example for a polysulfobetaine, poly(sulfobetainemethacrylate) (PSBMA) .....	11
<b>Figure 7.</b> An example for a polyphosphobetaine, poly(methacryloyloxyethyl phosphorylcholine) (PMPC) .....	12
<b>Figure 8.</b> The schematic representation of LbL self-assembly process .....	15
<b>Figure 9.</b> Schematic representation of the interactions between the layers when the driving force for the construction is hydrogen bonding <b>(A)</b> or electrostatic interactions <b>(B)</b> .....	16
<b>Figure 10.</b> Controlling film thickness during LbL self-assembly .....	17
<b>Figure 11.</b> Controlling film properties at the post-assembly step .....	18
<b>Figure 12.</b> Number-average hydrodynamic size distribution of $\beta$ PDMA- <i>b</i> -PDPA at pH 3 and pH 7.5 <b>(A)</b> , TEM image of $\beta$ PDMA- <i>b</i> -PDPA micelles at pH 7.5 <b>(B)</b> , Zeta potential distribution of $\beta$ PDMA- <i>b</i> -PDPA micelles at pH 7.5 <b>(C)</b> .....	38
<b>Figure 13.</b> LbL growth of $\beta$ PDMA- <i>b</i> -PDPA micelles with HA <b>(A)</b> , TA <b>(B)</b> and PSS <b>(C)</b> at pH 7.5 .....	39
<b>Figure 14.</b> Comparison of layer-by-layer growth of $\beta$ PDMA- <i>b</i> -PDPA micelles/HA <b>(A)</b> ; $\beta$ PDMA- <i>b</i> -PDPA micelles/TA <b>(B)</b> and $\beta$ PDMA- <i>b</i> -PDPA micelles/PSS <b>(C)</b> at pH 7.5, pH 8 and pH 8.5. ....	40
<b>Figure 15.</b> AFM height images and roughness values of 3-layer $\beta$ PDMA- <i>b</i> -PDPA micelles/HA, $\beta$ PDMA- <i>b</i> -PDPA micelles/TA and $\beta$ PDMA- <i>b</i> -PDPA micelles/PSS films .....	43

<b>Figure 16.</b> AFM height images (same z-scales) and roughness values of 3-layers $\beta$ PDMA- <i>b</i> -PDPA micelles/HA, $\beta$ PDMA- <i>b</i> -PDPA micelles/TA and $\beta$ PDMA- <i>b</i> -PDPA micelles/PSS films .....	43
<b>Figure 17.</b> Static contact angles of $\beta$ PDMA- <i>b</i> -PDPA micelles/HA (square), $\beta$ PDMA- <i>b</i> -PDPA micelles/TA (circle) and $\beta$ PDMA- <i>b</i> -PDPA micelles/PSS (triangle) films. ....	45
<b>Figure 18.</b> Fraction retained at the surface of $\beta$ PDMA- <i>b</i> -PDPA micelles/HA, $\beta$ PDMA- <i>b</i> -PDPA micelles/TA and $\beta$ PDMA- <i>b</i> -PDPA micelles/PSS films after immersion into PBS at pH 7.5 (A); pH 5.5 (B) at 37°C .....	46
<b>Figure 19.</b> Fraction retained at the surface of $\beta$ PDMA- <i>b</i> -PDPA micelles/HA, $\beta$ PDMA- <i>b</i> -PDPA micelles/TA and $\beta$ PDMA- <i>b</i> -PDPA micelles/PSS films after immersion into bacterial culture medium at pH 7.5 (A) and pH 5.5 (B) at 37°C.....	47
<b>Figure 20.</b> Fraction retained at the surface of $\beta$ PDMA- <i>b</i> -PDPA micelles/HA, $\beta$ PDMA- <i>b</i> -PDPA micelles/TA and $\beta$ PDMA- <i>b</i> -PDPA micelles/PSS films after immersion into PBS at pH 7.5 (A) and pH 5.5 (B) for 24 hours at 37°C .....	49
<b>Figure 21.</b> Fraction retained at the surface of $\beta$ PDMA- <i>b</i> -PDPA micelles/HA, $\beta$ PDMA- <i>b</i> -PDPA micelles/TA and $\beta$ PDMA- <i>b</i> -PDPA micelles/PSS films after immersion into bacterial culture medium at pH 7.5 (A) and pH 5.5 (B) for 24 hours at 37°C.....	50
<b>Figure 22.</b> Protein adsorption onto modified or unmodified slides. Amount of BSA adsorbed onto $\beta$ PDMA- <i>b</i> -PDPA micelles/HA, $\beta$ PDMA- <i>b</i> -PDPA micelles/TA and $\beta$ PDMA- <i>b</i> -PDPA micelles/PSS films at pH 7.5 and 37°C .....	51
<b>Figure 23.</b> Evolution of film thickness after multilayers were immersed into BSA solution at pH 7.5 and 37°C .....	53
<b>Figure 24.</b> Adsorption of Lysozyme (Lys) onto $\beta$ PDMA- <i>b</i> -PDPA micelles/HA, $\beta$ PDMA- <i>b</i> -PDPA micelles/TA and $\beta$ PDMA- <i>b</i> -PDPA micelles/PSS films at pH 7.5 and 37°C.....	53
<b>Figure 25.</b> Evolution of film thickness after 3-layer films were immersed into Lysozyme (A), Casein (B), Ferritin (C) and BSA (D) solutions .....	54
<b>Figure 26.</b> Hydrophobicity plots of Ferritin, BSA, Casein, and Lysozyme.....	56
<b>Figure 27.</b> Evolution of film thickness after immersion of control (rhombus), 3-layer $\beta$ PDMA- <i>b</i> -PDPA micelles/HA (square), 3-layer $\beta$ PDMA- <i>b</i> -PDPA micelles/TA	

(circle) and 3-layer $\beta$ PDMA- <i>b</i> -PDPA micelles/PSS (triangle) into 25 mg/mL BSA solution at pH 7.5 and 37°C for 24 hours.....	57
<b>Figure 28.</b> Plasmid map of pSB1C3 showing presence of the GFP gene .....	58
<b>Figure 29.</b> Green fluorescence images of blank glass slide (control) and 1-, 3-, 5-layer $\beta$ PDMA- <i>b</i> -PDPA micelles/HA, $\beta$ PDMA- <i>b</i> -PDPA micelles/TA and $\beta$ PDMA- <i>b</i> -PDPA micelles/PSS coated glass slides .....	59
<b>Figure 30.</b> Quantitative representation of the fluorescent GFP signals from the bacteria adhering to different surfaces as determined by Image J .....	60
<b>Figure 31.</b> Images of crystal-violet stained blank or coated substrates incubated with <i>Staphylococcus aureus</i> ATCC 29213 and <i>Escherichia coli</i> ATCC 8739 before (A) and after (B) decolorization process.....	61
<b>Figure 32.</b> Normalized absorbance of the crystal violet staining solution obtained after decolorization of <i>E.coli</i> (A) and <i>S. aureus</i> (B) adhered to control glass slides or glass slides coated with 1-, 3-, 5- layer $\beta$ PDMA- <i>b</i> -PDPA micelles/HA, $\beta$ PDMA- <i>b</i> -PDPA micelles/TA and $\beta$ PDMA- <i>b</i> -PDPA micelles/PSS after 1 hour of incubation.	62
<b>Figure 33.</b> Viable bacterial count obtained by agar plating method with blank glass slide (control) and 1-, 3-, 5- layer $\beta$ PDMA- <i>b</i> -PDPA micelles/HA, $\beta$ PDMA- <i>b</i> -PDPA micelles/TA and $\beta$ PDMA- <i>b</i> -PDPA micelles/PSS coated glass slides after 1 hour incubation with <i>E.coli</i> (A) and <i>S.aureus</i> (B) .....	63
<b>Figure 34.</b> Long term (24 hour) bacterial adhesion.....	64
<b>Figure 35.</b> Long term (24 hour) bacterial adhesion. Quantitative representation of the fluorescent GFP signals.....	65
<b>Figure 36.</b> Kirby-Bauer tests from 5- layer Triclosan loaded $\beta$ PDMA- <i>b</i> -PDPA micelles/HA, $\beta$ PDMA- <i>b</i> -PDPA micelles/TA and Triclosan loaded $\beta$ PDMA- <i>b</i> -PDPA micelles/PSS films. 5-layer films of unloaded $\beta$ PDMA- <i>b</i> -PDPA micelles at pH 7.5 and pH 5.5 were used as control .....	67
<b>Figure 37.</b> Diameter of clear zones for Triclosan loaded 5-layer $\beta$ PDMA- <i>b</i> -PDPA micelles/HA, Triclosan loaded $\beta$ PDMA- <i>b</i> -PDPA micelles/TA and $\beta$ PDMA- <i>b</i> -PDPA micelles/PSS films at pH 7.5 and pH 5.5 .....	68
<b>Figure 38.</b> Fluorescence images of substrates after 1 hour incubation with SaOS-2 cells.....	70

## LIST OF ABBREVIATIONS

$\beta$ PDMA- <i>b</i> -PDPA	Poly[3-dimethyl (methacryloyloxyethyl) ammonium propane sulfonate- <i>block</i> -2-(diisopropylamino)ethyl methacrylate]
ZBCM	Zwitterionic block copolymer micelle
LbL	Layer-by-Layer
HA	Hyaluronic Acid
TA	Tannic Acid
PSS	Poly(sodium 4-styrene sulfonate)
BSA	Bovine Serum Albumin
MDR	Multi-drug resistant
LPS	Lipopolysaccharide
Bap1	Biofilm-associated protein 1
RbmC	Rugosity and biofilm structure modulator C
PHEMA	Poly(2-hydroxyethyl methacrylate)
PEG	Polyethylene glycol
OEG	Oligoethylene glycol
PEGMA	Poly(ethylene glycol) methacrylate
PAOXs	Poly(2-alkyl-2-oxazoline)s
PDMS	Poly(dimethylsiloxane)
<i>S. aureus</i>	<i>Staphylococcus aureus</i>
<i>E. coli</i>	<i>Escherichia coli</i>
PSPE	Poly [N-(3-sulphopropyl)-N-methacryloyloxyethyl-N,N-dimethyl ammonium betaine]
UCST	Upper critical solution temperature
LCST	Lower critical solution temperature
T <sub>g</sub>	Glass transition temperature
ILs	Ionic liquids
PCB	Polycarboxybetaine

PCBAA	Poly(carboxybetaineacrylamide)
PCBMA	Poly(carboxybetaine methacrylate)
PSB	Polysulfobetaines
PSBMA	Poly(sulfobetainemethacrylate)
PPB	Polyphosphobetaine
MPC	2-methacryloyloxyethyl phosphorylcholine
PC	Phosphorylcholine
PMPC	Poly(methacryloyloxyethyl phosphorylcholine)
PAA	Poly(acrylic acid)
PEI	Poly(ethylene imine)
PAH	Poly(allylamine hydrochloride)
MET	Metronidazole
MXF	Moxifloxacin hydrochloride
CHX	Chlorhexidine diacetate monohydrate
DIC	Diclofenac sodium salt
ALG	Sodium alginate
PLL	Polylysine hydrobromide
CHI	Chitosan
PPO	Polypropylene oxide
PEO	Poly(ethylene oxide)
TMC	N-Trimethyl chitosan
HP	Heparin
PMETAC	Poly[(trimethylamino) ethyl methacrylate chloride]
PTA	Poly[2-(tert-butylamino)ethyl methacrylate]
PDVBAPS	Poly[(3-(dimethyl(4-vinylbenzyl) ammonio) propyl sulfonate)]
2D	2-Dimensional
3D	3-Dimensional
DNA	Deoxyribonucleic acid
RNA	Ribonucleic acid
PVPON	Poly(vinylpyrrolidone)

PMAA	Poly (methacrylic acid)
PS	Polystyrene
PS- <i>b</i> -PAA	Poly(styrene- <i>block</i> -acrylic acid)
PDDA	Poly(diallyl-dimethylammonium chloride)
P4VP	Poly(4-vinylpyridine)
PS- <i>b</i> -P4VP	Poly(styrene- <i>block</i> -4-vinylpyridine)
PDMA	Poly(2-(dimethylamino)ethyl methacrylate)
PNIPAM	Poly-(N-isopropylacrylamide)
PDMA- <i>b</i> -PNIPAM	Poly(2-(dimethylamino)ethyl methacrylate)- <i>block</i> -poly-(N-isopropylacrylamide)
PAAm	Poly(acrylamide)
PAN	Poly(acrylonitrile)
P(AAm- <i>co</i> -AN)- <i>b</i> -PVP	Poly(acrylamide- <i>co</i> -acrylonitrile)- <i>block</i> -polyvinylpyrrolidone
OQAS	3-(trimethoxysilyl)propyl]octadecyl-dimethylammonium chloride
BAI	Biomaterial-associated infection
PLL	Poly-L-lysine
PLL- <i>g</i> -PEG	Poly-L-lysine-grafted polyethylene glycol
RGD	Arginine–glycine–aspartic acid peptide motif
KRSR	Lysine–arginine–serine–arginine peptide motif
VEGF	Vascular endothelial growth factor
bFGF	Basic fibroblast growth factor
TGF- $\beta$	Transforming growth factor- $\beta$
BMP-2	Bone morphogenic protein-2
PLGA	Poly (lactide- <i>co</i> -glycolide)
AMP	Antimicrobial peptides
MH broth	Mueller-Hinton broth
LB broth	Luria-Bertani broth
PBS	Phosphate Buffered Saline
SP-DiOC <sub>18</sub> (3)	3,3'-Dioctadecyl-5,5'-di(4-sulfophenyl) oxacarbocyanine

	sodium salt
DMEM	Dulbecco's Modified Eagle's medium
FBS	Fetal Bovine Serum
EDTA	Ethylenediaminetetraacetic acid
DI water	Deionized water
GFP	Green fluorescent protein
DLS	Dynamic light scattering
TEM	Transmission electron microscopy
AFM	Atomic force microscopy
DMSO	Dimethyl sulfoxide
CFU	Colony forming unit
OD	Optical density
NMR	Nuclear Magnetic Resonance
UV	Ultra Violet
Lys	Lysozyme

## CHAPTER 1

### INTRODUCTION

#### 1.1. The Importance of Anti-adhesiveness on Biomaterial Surfaces

Biomaterials can be used to facilitate the wound healing process or as implants to restore functionality in the body. Biocompatibility, biosafety and the interactions between the implant surface and cells in the environment play an important role in the design of biomaterials. In addition, bacterial attachment/growth on the biomaterial surface followed by biofilm formation is a major concern in the preparation of biomaterials. Biofilm is defined as multilayers of bacteria together with extracellular matrix components. Thus, antibiotics are not effective in removing biofilms due to poor drug diffusion into the biofilm [1]. Importantly, weak response to antibiotic treatment results in the development of resistance against multiple drugs; so called multi-drug resistant (MDR) bacteria [2]. Biofilm formation on biomaterials may lead to the rejection of the implanted biomaterial as well as severe infections that could either bring further complications or be fatal. Therefore, a biomaterial that can delay or eliminate biofilm development is highly desirable. Biofilm formation mechanism can be divided into three major stages: i) attachment, ii) maturation and iii) dispersion. The first stage in biofilm formation is the attachment stage which can be further subdivided as initial reversible attachment and irreversible attachment. In the initial reversible attachment flagella and type IV pili are important. Flagella enable bacteria and surface interactions whereas type IV pili-mediated motilities enable bacteria to aggregate and form microcolonies. Once the first layer of the biofilm established, the maturation stage is initiated. In the maturation stage cells of the same species or different species gather to form a bulk

fluid containing extracellular polymeric substances i.e. exopolysaccharides, proteins, enzymes and nucleic acids secreted from bacteria. At this stage biofilm fluid has its own channels allowing the passage of water, air and nutrients. In addition, each bacterium in the biofilm takes a specialized function and arrangement in communication with each other according to their metabolism and aero-tolerance. After maturation step, dispersion stage is initiated. The dispersion stage is important for the life-cycle of the biofilm. When the nutrients deplete or the population inside the biofilm exceeds, because of the competition and outgrown population, dispersion occurs. Dispersion can occur as a whole or a part of the biofilm and the release of planktonic bacteria, bacteria float or swim as a single cell, promotes the initiation of new biofilms at other sites [3]. Figure 1 shows the stages of a biofilm formation.

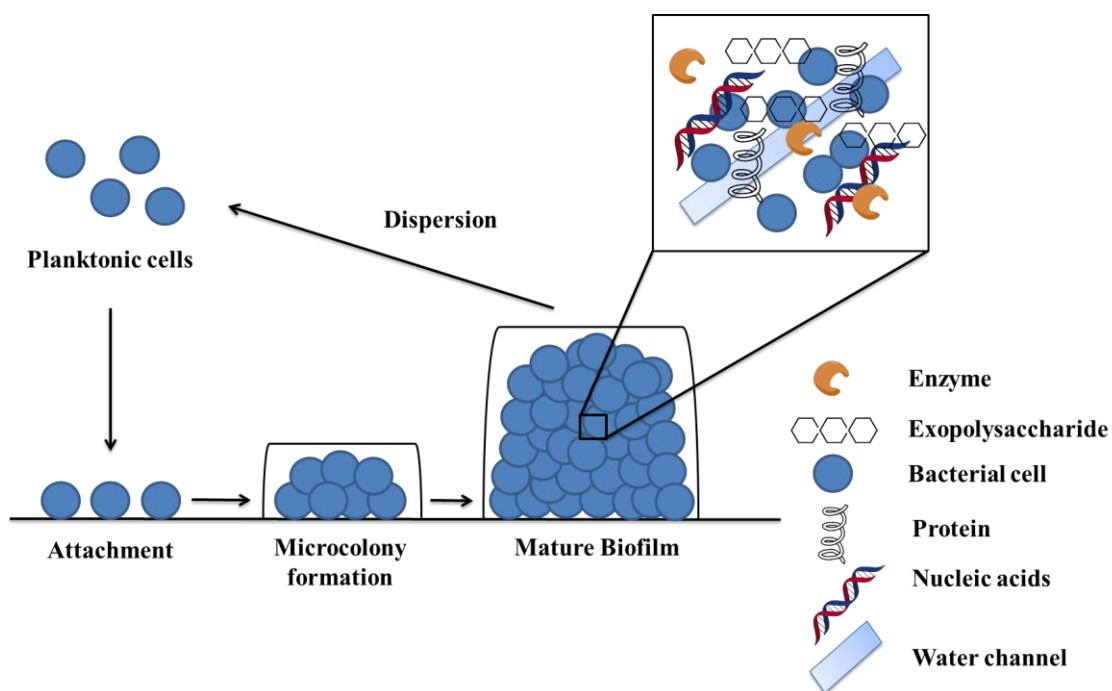


**Figure 1.** The process of biofilm formation and components of a mature biofilm. Modified from Sintim et. al. (2015) [3].

According to the Vroman effect, the first tissue response upon implantation of a biomaterial is the non-specific adsorption of high mobility proteins such as albumin that is later replaced by high affinity but less abundant proteins such as globulin and

fibrinogen; eventually the latter are replaced by the high molecular weight proteins, i.e. kininogen [4,5]. Bacterial interactions with a target cell surface starts with calcium binding proteins of the outer membrane such as LPS or pili. These cell surface proteins also provide for the motility of bacteria on the surface, mediating surface colonization [6–9]. Biofilm-associated protein 1 (Bap1) and Rugosity and biofilm structure modulator C (RbmC) are important for stable biofilm formation on the surface [10]. Therefore, inhibition of protein adsorption on the biomaterial surface is critical to prevent biofilm formation and implant/device failure.

## **1.2. Surface Modification of Biomaterials using Polymers**

Surface modification of biomaterials is a commonly applied method to improve biocompatibility, surface-body interactions of the biomaterial and to delay or eliminate biofilm development. Polymers have been extensively investigated to modify biomaterial surfaces due to relatively low cost of synthesis and easy manipulation of the physical and chemical properties. There are three major ways to functionalize biomaterial surfaces using polymers: i) coating the biomaterial surface using anti-adhesive polymers to prevent the first contact of microorganisms with the surface, so called "low-fouling polymers"; ii) releasing antimicrobial agents from polymer coatings; iii) physical/chemical immobilization of antimicrobial agents into the polymer coating to kill the bacteria upon contact.

### **1.2.1. Coating of the Biomaterial Surfaces using Anti-adhesive Polymers**

Previous studies have shown that hydrophilic, and highly hydrated polymers can prevent the adhesion of proteins and bacteria by forming a network of water molecules on top of the coating, which can act as a barrier for proteins and bacteria that are attracted to the biomaterial surface [11–16]. The anti-adhesive or anti-fouling polymers can be classified into five major types [17,18];

- i) Poly(2-hydroxyethyl methacrylate) (PHEMA) based polymers,

- ii) Polyethylene glycol (PEG), oligoethylene glycol (OEG) and Poly(ethylene glycol) methacrylate (PEGMA) based polymers,
- iii) Poly(2-alkyl-2-oxazoline)s (PAOXs) and
- iv) Polyzwitterions

In 1960s, use of HEMA based polymers as anti-fouling polymers has gained popularity. One example to HEMA based polymers is poly(2-hydroxyethyl methacrylate) (PHEMA), which is a neutral and hydroxyl rich material. Because of their hydroxyl-rich structures, they can make hydrogen bonds with water and can create well-hydrated surfaces that can show resistance to biomolecule adsorption or cell adhesion [19,20]. One disadvantage of PHEMA is its poor antifouling performance in undiluted human blood serum and plasma possibly because of its complex interactions between blood and serum proteins with the surface [21,22]. As a result the need for other anti-fouling polymers was emerged. Figure 2 shows the chemical structure of poly(2-hydroxyethyl methacrylate) (PHEMA), a commonly used HEMA based polymer for anti-fouling applications.

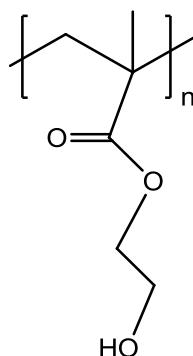


**Figure 2.** The chemical structure of HEMA. Modified from Chang et. al. (2014) [17].

In 1970s, the use of PEG or polymers with OEG moieties has gained attention because of their steric exclusion effect and water attracting properties to create a hydration layer providing them anti-adhesiveness [23,24]. For example, Ober et al. contrasted anti-fouling performance of PEG-based hydrophilic polymer coatings and hydrophobic surfaces functionalized either with poly(dimethylsiloxane) (PDMS) or

fluoropolymers in terms of their resistance to protein adsorption and cell adhesion. Their findings showed that hydrophilic PEG coatings resisted protein adsorption and cell spreading whereas hydrophobic PDMS or fluoropolymer modified surfaces were not resistant to protein adsorption, but are non-adhesive to cells and organisms due to their non-polar nature [18]. One drawback of PEG-based polymers as anti-fouling materials is their low chemical stability [25–28]. Therefore, investigations for alternative anti-fouling materials have been continued. Figure 3 shows the chemical structure of PEG or OEG and PEGMA.

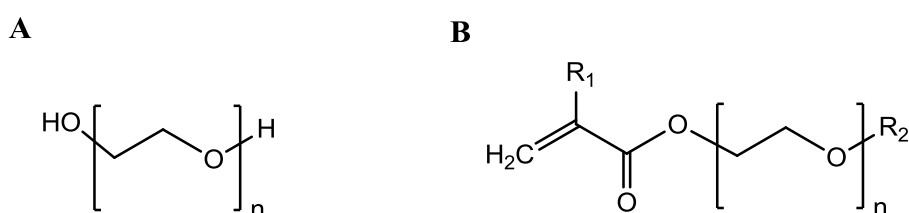


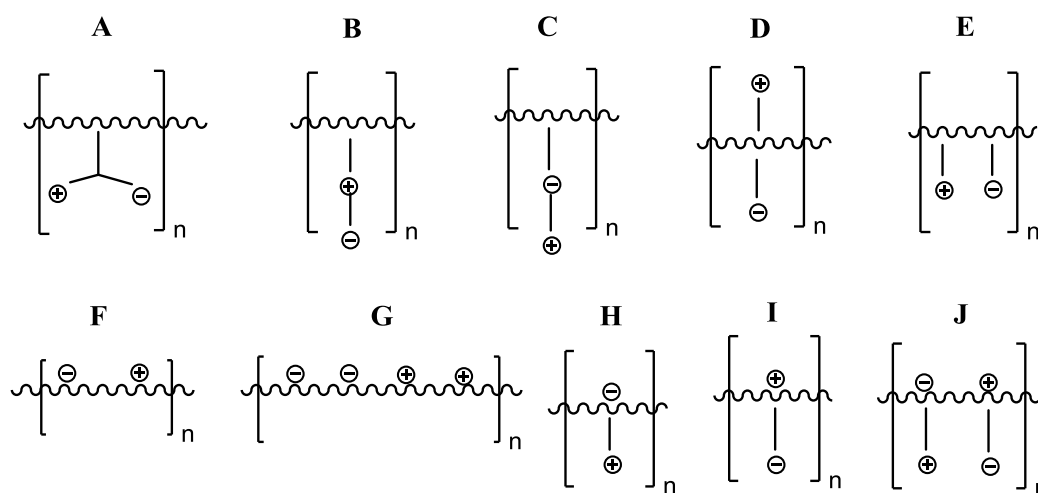
**Figure 3.** The chemical structures of PEG or OEG (A) and PEGMA (B). Modified from Chang et. al. (2014) [17].

PAOXs are well-known polymers since 1960s. Due to their relatively non-toxic property, they have been used for biological applications such as drug or gene delivery studies [29]. Towards the end of 1990s, the use of PAOXs as an anti-adhesive polymer has gained attention due to greater stability of PAOXs than PEG [30,31]. Among PAOXs, poly(2-methyl-2-oxazoline) and poly(2-ethyl-2-oxazoline) are examples of highly hydrophilic polymers that were reported to exhibit antifouling properties [12,18,32,33]. Figure 4 shows the chemical structure of PAOX, where R<sub>3</sub> represents an alkyl group.



**Figure 4.** The chemical structure of PAOX. Modified from Chang et. al. (2014) [17].

Polyzwitterions, are polymers that contain same number of cationic and anionic groups in their repeating units [34,35]. As scheme 1 demonstrates, the cationic or anionic moieties can be either on the polymer backbone (as in the F and G) or on the side chains (as in A, B, C, D and E) as well as one of them can be in backbone or the other one can be on the side chain (as in H, I and J) [36]. Among them, types B and C are more commonly studied in the literature [37,38,47–54,39–46].



**Scheme 1.** Possible repeating unit architectures for polyzwitterions. Modified from Laschewsky (2014) [36].

The major difference between polyzwitterions and polyampholytes is that, in polyampholytes the positive and negative charges can be scattered randomly throughout the chain of polymer resulting in mostly charged molecules; either positively charged or negatively charged. Therefore, polyampholytes typically behave either as polycations or as polyanions differing from polyzwitterions which show overall charge neutrality and behave as non-ionic polymers [36,44,55]. Unlike polyelectrolytes, solubility of polyzwitterions in aqueous solution decrease with increasing salt concentration, so called "anti-polyelectrolyte behaviour" [56].

Zwitterionic polymers, because of bearing equal amount of cationic and anionic groups on their backbone or on their side chains, are highly hydrophilic and show good anti-fouling properties against protein adsorption [16], bacterial adhesion and

prevent biofilm formation [57–59] even as a single layer coating [60–62]. In 2014, Erel et.al. reported the use of poly[3-dimethyl (methacryloyloxyethyl) ammonium propane sulfonate-*b*-2-(diisopropylamino)ethyl methacrylate] ( $\beta$ PDMA-*b*-PDPA) micelle monolayers as a potential anti-adhesive surface against *Staphylococcus aureus* [63]. Similar to ionically neutral hydrophilic polymers, zwitterionic polymers owe their antiadhesive behavior to the hydration layer formed through hydrogen bonding interactions and ionic solvation between the water molecules and the zwitterionic coating [64–67]. Therefore, they can be used in many application areas such as; antifouling coatings for biomedical devices [68], for marine coatings [69–71], biosensors [72] and blood contacted sensors [17,69]. In addition, because of their cellular membrane mimicking chemistry, they can be used as model membrane systems [73,74]. They can also be used as lubricating agents in aqueous media for coating of biomaterials used as synthetic human synovial joints [75,76] or separation membranes for water cleaning [77] and blood purification [78]. Polyzwitterions also find use in environmental engineering or food processing applications [79]. Furthermore, by modulating the charge on them by an internal or an external stimuli, these polymers can be made stimuli responsive smart polymers which can also be used in drug delivery applications [80–83].

#### **1.2.1.1. History of Polyzwitterions**

Polyzwitterions, although known since 1950s, did not attract attention for long time. In 1957, Ladenheim and Morawetz published a study describing a method for the synthesis of a poly (4-vinyl-pyridine betaine), a polymer with cationic and anionic functional groups on the side chains. The cationic group was a quaternized nitrogen atom in pyridine ring and the anionic group was a carboxylate moiety on each monomer [37]. Later, in 1958, Hart and Timmerman published a study for the synthesis of another zwitterionic polymer, poly-(4-vinyl-pyridine N-butyl sulfobetaine) with quaternized nitrogen atom in pyridine for cationic and sulfonate group for anionic functionality on the side chain of the polymer [38].

In 1986, Garner et al. showed the phase behavior and aqueous solution properties of a polyzwitterion, poly [N-(3-sulphopropyl)-N-methacryloxyethyl-N,N-dimethyl ammonium betaine] (PSPE). They reported that PSPE showed both upper critical solution temperature (UCST) and lower critical solution temperature (LCST) behaviors [39].

In 1988, Bazuin et al. showed the synthesis and mechanical properties for atactic random copolymers of ethyl acrylate and diethyl-(2-methylacryloxyethoxy-2-ethyl) - 1- (3-sulphopropyl) ammonium betaine. They studied the glass transition temperature ( $T_g$ ) and factors affecting the  $T_g$  of this copolymer [40].

In 1996, Laschewsky et al. studied polyzwitterions and their interactions with molten inorganic and organic salts with cationic and anionic moieties such as; azo dyes, triphenylmethanes, oxazines and hemicyanines. They prepared polyzwitterion/salt blends and reported that, homogeneous blends could be obtained when they used equimolar amounts of salt and polybetaines, suggesting strong interactions between the polybetaines and charged salts [41].

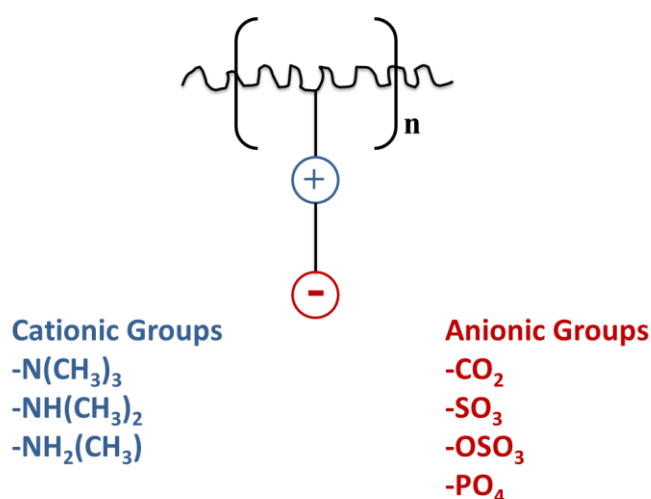
In 2010, Long et al. reported a similar study to Laschewsky. They reported the synthesis of two copolymers, i.e. polysulfobetaine methacrylate-*co*-butyl acrylate and polysulfobetaine methacrylamide-*co*-butyl acrylate. They incorporated molten salts (below 100°C) which they called as ionic liquids (ILs) into these polyzwitterions. By this way, they improved the electrical conductivity, chemical and physical stability of the polymer/salt blends which can be used in conductive membrane mimicking applications in electronic devices [35].

The deep interest in polyzwitterions started since late 1980s, after their biologically important analogues like hormones, vitamins, phospholipids and zwitterionic polypeptides have been realized.

### 1.2.1.2. Types of Polybetaines Based on Functional Groups

Zwitterionic polymers are called polybetaines when the source of positive charge is a quaternized nitrogen atom [66].

Polybetaines are classified into three major subgroups: Polycarboxybetaines, polyphosphobetaines and polysulfobetaines which are considered as mimetics of fouling-resistant materials because of their strong electrostatic interactions with water [34]. Scheme 2 shows commonly used cationic and anionic moieties for the design of polybetaines.



**Scheme 2.** Widely used cationic and anionic moieties for zwitterionic polybetaines. Modified from Liu et. al. [34].

- **Polycarboxybetaines (PCBs)**

PCBs are polybetaines where anionic charge sources from a carboxylic acid (-COOH) moiety. Figure 5 shows examples of polycarboxybetaines commonly used for biological applications. PCBs show pH-responsive behaviour due carboxylic acid units. PCBs have been shown to exert good antifouling properties against protein adhesion [84]. The unique property of polycarboxybetaines is that, because of the carboxylic acid group on each repeating unit, molecules which bear amino groups

such as antibodies can be coupled to PCBs. This is advantageous for surface functionalization of PCB-based drug carrier nanoparticles, surface coatings or tissue scaffolds and for bio-recognition purposes such as protein microarrays [85–87]. Another advantage of polycarboxybetaines is the easy conversion of a carboxylic acid group to an ester group. In this way PCB can also be used for gene or drug delivery purposes from ester functionalized side chains upon hydrolysis [87].

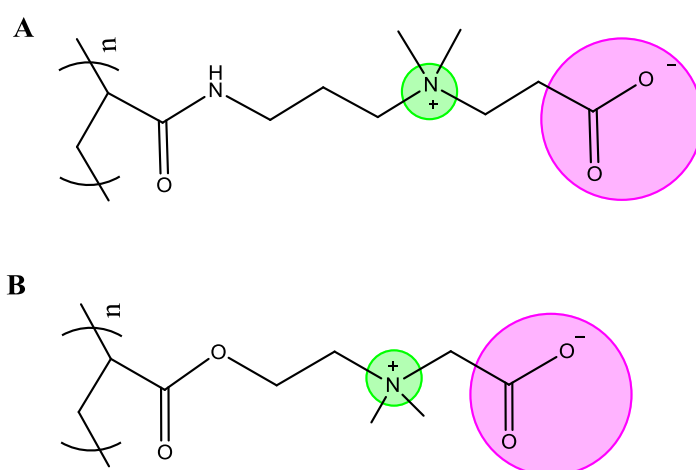


**Figure 5.** Examples for polycarboxybetaines; poly(carboxybetaineacrylamide) (PCBAA) (A), poly(carboxybetaine methacrylate) (PCBMA) (B). Modified from Chang et. al. (2014) [17].

- **Polysulfobetaines (PSBs)**

PSBs are polybetaines in which the negative charge sources from sulfonate ( $-\text{SO}_3^-$ ) groups. Figure 6 shows an example of a polysulfobetaine. Because of the existence of very abundant derivatives in the nature, such as taurine, an organic compound found in animal tissues, PSBs are assumed to be very promising in biological applications. Besides being biological mimetics, PSBs are shown to be biocompatible and non-cytotoxic for *in vivo* implantation [68]. PSBs also have good anti-fouling properties because of their strong hydration ability [64]. Although both PSBs and PCBs show strong hydration ability, they differ in terms of their interactions with water. As compared to PCB, PSB moieties make more coordination

with water i.e. PSBs interact with more water molecules. However, the interactions between PCB-water is stronger than that of PSB-water [88]. In addition, because of more favourable self-association ability of PSBs than PCBs, PSBs are preferred for drug carrier applications [88]. This interplay between PSB and PCB can be important for the purpose of application.

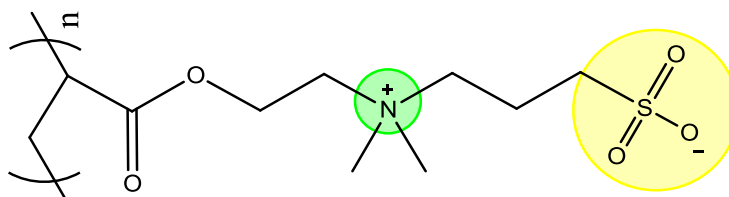


**Figure 6.** An example for a polysulfobetaine, poly(sulfobetainemethacrylate) (PSBMA). Modified from Chang et. al. (2014) [17].

- **Polyphosphobetaines (PPBs)**

PPBs are polybetaines where the anionic unit is a phosphate ( $-\text{PO}_4$ ) group. Due to being phospholipid analogues, PPBs are widely used in cellular membrane mimicking studies as lipid bilayer biomembranes or lipid based drug carriers to enable easy passage through cell membranes [42,89–93]. In 1978, Kadome et al. reported the synthesis of a polyphosphobetaine, which could induce electrostatic interactions with the water molecules unlike from other non-fouling polymer architectures [94]. Later in 1990, Ishihara et al. reported the synthesis of a polyphosphobetaine, using 2-methacryloyloxyethyl phosphorylcholine (MPC) as the monomer (as shown in figure 7). Upon polymerization of MPC, they prepared hydrogels showing blood biocompatibility which can be used as biomaterials [95]. In 1997, Zwaal et al. reported that the inner membranes of red blood cells caused thrombogenic response, while the outer membrane did not. This observation supports that lipid components at the outside surface containing zwitterionic phospholipids, like phosphorylcholine (PC), could be the reason for anti-fouling property of PPBs [96]. In 2002, O'Brien and Müller demonstrated several synthetic amphiphilic molecules. They used phospholipid like molecules having hydrophobic tail groups,

and incorporated different polar head groups having styryl, diacetylenyl, dienoyl, sorbyl, acryloyl, methacryloyl or lipoyl moieties. Upon polymerization of these monomers, they obtained synthetic bilayers and they compared their cell membrane mimicking properties in terms of elasticity and integrity [97]. In 2003, Lloyd et al. designed PC-based polymers to be used in a variety of biomedical device preparation applications to improve biocompatibility [98]. In 2009, Saavedra, Joubert and Zhang [55] and in 2011, Blumenthal and Puri [42] reviewed the application of photo-sensitive phospholipid like polyzwitterions as a drug carrier nanocapsules or as platforms to incorporate transmembrane proteins. They also reported the use of polyzwitterions as diagnostic tools for disease and pathogen detection, nano-imaging and biosensors. Although PPBs show good hydrophilicity and anti-adhesiveness, PSBs and PCBs are preferred more for application purposes [17] because of the difficulty in the synthesis of PPBs.

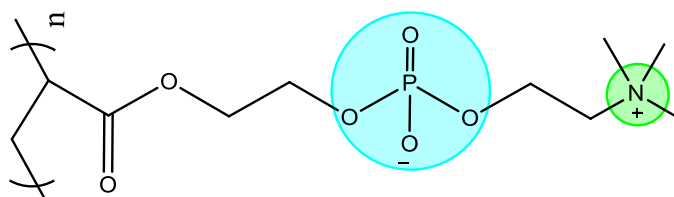


**Figure 7.** An example for a polyphosphobetaine, poly(methacryloyloxyethyl phosphorylcholine) (PMPC). Modified from Chang et. al. (2014) [17].

### 1.2.2. Releasing Anti-microbial Agents from Polymer Coatings

Releasing anti-microbial agents from polymer coatings, is another strategy to modify biomaterial surfaces. In 2014, Hammond and co-workers, reported preparation of a wide-spectrum antibiotic, Vancomycin releasing polymer coatings. In this study, they constructed multilayer films of poly( $\beta$ -aminoester), Vancomycin and one of the following biopolymers: i.e. alginate, dextran sulfate or chondroitin sulfate. Such a coating was shown to inhibit the growth of *S.aureus* via Vancomycin release [99]. In 2014, Rahaman and co-workers, reported LbL construction of multilayer films using poly(acrylic acid) (PAA) and poly(ethylene imine) (PEI) functionalized with biocidal

silver nanoparticles, (Ag-PEI). As a control, they used non-functionalized PEI as well and reported the antibacterial efficiency of both surfaces using *Esheria coli* as model organism [100]. In 2015, Gentile and co-workers, reported the construction of surfaces modified via LbL self-assembly using poly(sodium4-styrenesulfonate) (PSS) and poly(allylamine hydrochloride) (PAH). The antibacterial activity against *Porphyromonas gingivalis* was provided by metronidazole (MET) release from the PAH/PSS multilayers [101]. In 2018, Saramago et. al. reported the release of three ophthalmic drugs; moxifloxacin hydrochloride (MXF), chlorhexidine diacetate monohydrate (CHX), and diclofenac sodium salt (DIC) from the soft contact lense material which was LbL modified with i) sodium alginate (ALG)/ polylysine hydrobromide (PLL); ii) sodium hyaluronate (HA)/ chitosan (CHI); iii) HA/PLL. They reported the antibacterial properties of the multilayers against *Pseudomonas aeruginosa* and *Staphylococcus aureus* as model organisms [102].

### **1.2.3. Physical/Chemical Immobilization of Antimicrobial Agents into the Polymer Coatings to Kill the Bacteria upon Contact**

Direct killing of bacteria upon contact by immobilization of antimicrobial agents into polymer coatings is another way to functionalize biomaterial surfaces using polymers. The antimicrobial agents can be immobilized either during the coating or after the coating through both physical and chemical means. In 2005, Ji et al reported the multilayer construction using antibacterial agent Chitosan and anti-adhesive agent Heparin for prevention of bacteria adhesion as well as direct killing upon contact. They reported that only 3-8% of the *E.Coli* were viable on their multilayers after 24 h [103]. In 2011, Mei et. al. reported conjugation of Lysozyme onto a synthetic triblock copolymer with a central polypropylene oxide (PPO) block and two poly(ethylene oxide) (PEO) terminal blocks. This Lysozyme conjugated PEO-*b*-PPO-*b*-PEO was used for surface modification in which Lysozyme functioned as an antimicrobial agent by disrupting the cell wall of bacteria upon contact [104]. Similarly, in 2012, Muniz et. al prepared anti-adhesive and contact killing polymer multilayer coatings using N-Trimethyl chitosan (TMC), as an antibacterial agent, and heparin (HP), as an antiadhesive biopolymer [105]. In 2018, Yang et. al. reported the

construction of two polymeric brushes poly[(trimethylamino) ethyl methacrylate chloride] (PMETAC) or poly[2-(tert-butylamino)ethyl methacrylate] (PTA) onto a background layer of polyzwitterionic brush poly[(3-(dimethyl(4-vinylbenzyl) ammonio) propyl sulfonate] (PDVBAPS) through surface initiated atom transfer radical polymerization. Such a polymer coating was reported to show contact killing and salt-responsive antibacterial agent releasing properties [106].

In summary, the efficacy of coatings that release anti-microbial agents decrease once the anti-microbial agents deplete. On the other hand, it was also reported that microorganisms might gain resistance against immobilized antimicrobial agents on contact-killing coatings [107]. Therefore, although low fouling polymers undergo proteolytic degradation which reduces their stability for long term applications, these polymers are still more promising to delay or prevent biofilm development compared to other types of coatings [108–110].

### **1.3. Layer-by-Layer Self-assembly Technique**

Layer-by-layer (LbL) self-assembly is a simple, environmentally friendly and economical method to modify surfaces with polymers via various interactions such as electrostatic, hydrogen bonding, charge-transfer interactions or coordination bonding [111]. LbL technique was first discovered by Iler in 1966 to deposit positively and negatively charged silica nanoparticles on a glass surface [112]. Later, in 1992 Decher and Hong adopted this technique to polyelectrolytes [113]. LbL assembled films are used in many applications due to easy control of film thickness and multilayered structure, providing a simple approach to design and construct complicated surface modifications [114–121]. Figure 8 shows the schematic representations for LbL self-assembly process.

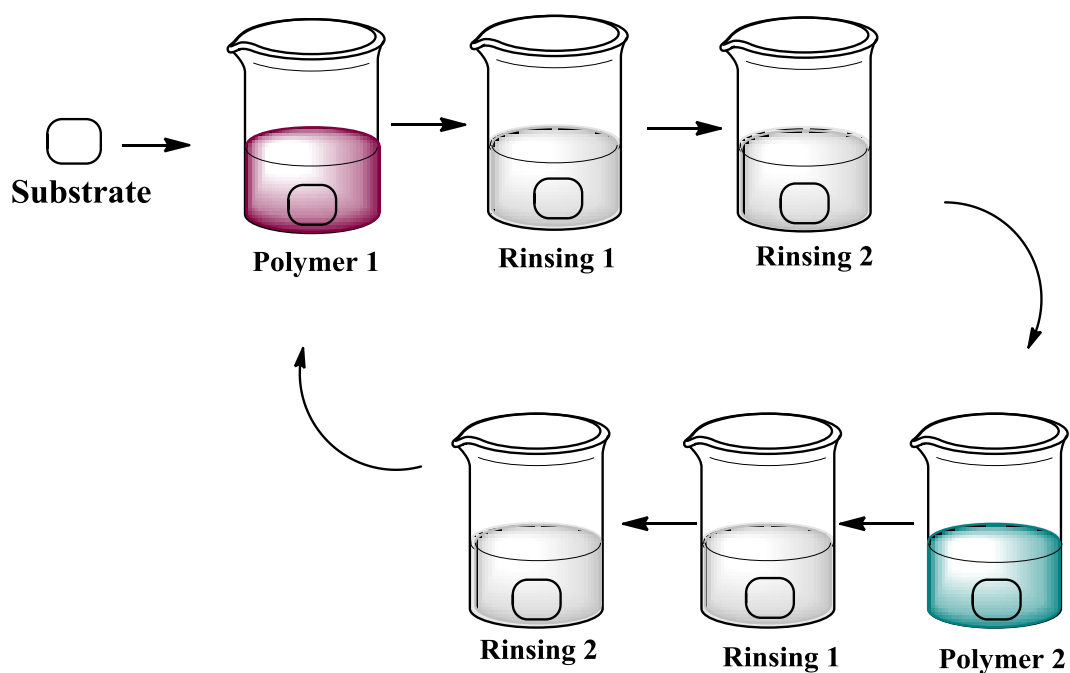


**Figure 8.** The schematic representation of LbL self-assembly process. Modified from Yang et. al. [122].

Figure 9 shows the interactions between the multilayers when the driving force for the construction is hydrogen bonding (A) or electrostatic interaction between charged groups (B).

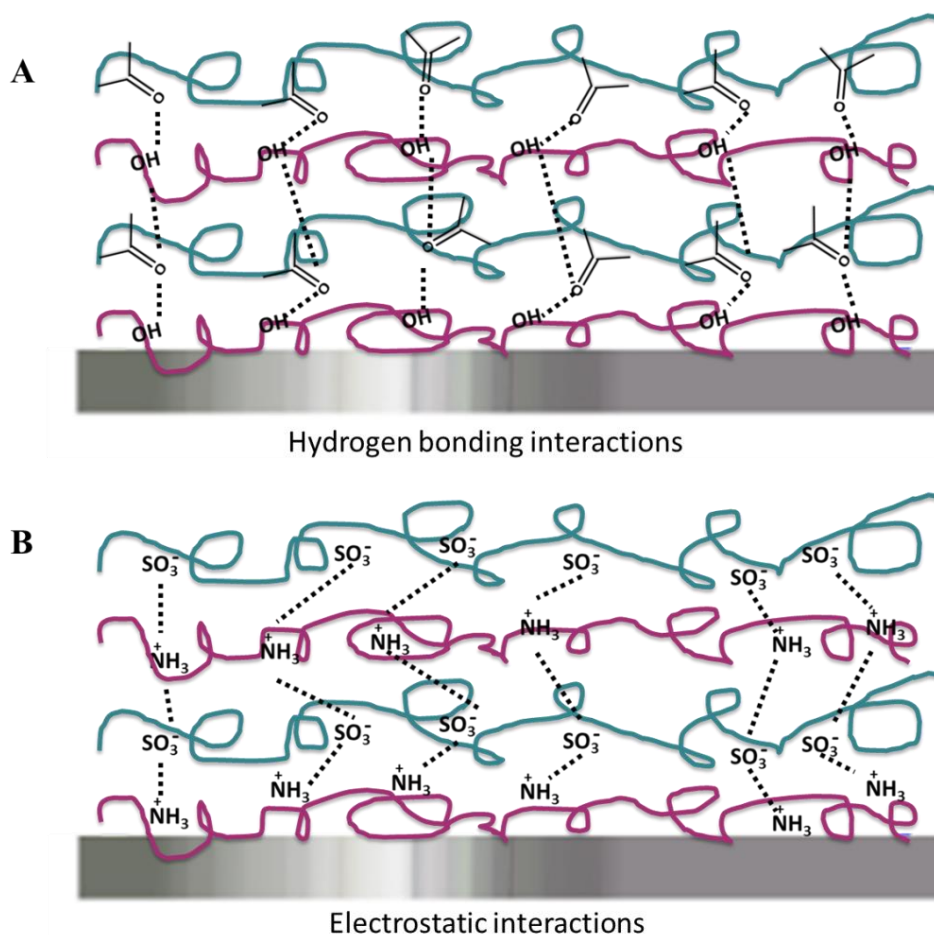


**Figure 9.** Schematic representation of the interactions between the layers when the driving force for the construction is hydrogen bonding (**A**) or electrostatic interactions (**B**). Modified from Yang et. al. [122].

There are many advantages of LbL self-assembly technique. It allows using aqueous polymer solutions and there is no limitation of size or shape for the substrate [123]. Substrates can be 2D shaped glass, quartz, silicon wafer or mica [124] as well as 3D shaped capsules, nanotubes [80]. LbL technique can also be used to incorporate drug, DNA, RNA, dye, magnetic nanoparticles within the multilayers [125]. With the use of stimuli responsive polymers, LbL constructed multilayer films can be made responsive to changes in the conditions like, pH, temperature, ionic strength, magnetic field, light, different solvent in the form of change in solubility, volume, conformation and phase of the polymer. This feature makes LbL technique promising for controlled drug release applications [80,122–126]. In LbL technique,

the film thickness can be controlled easily and layer properties can be altered during LbL assembly [127] as well as post assembly [80,128–130]. For example, Rubner and co-workers reported that, when PAA and PAH were constructed at pH 7, thin and flat layers were obtained. On the other hand, when the same polymer layers were deposited at pH 5, thick and loopy layers were obtained [127]. Figure 10 shows schematic representation of PAA/PAH multilayers constructed at pH 7 and pH 5.

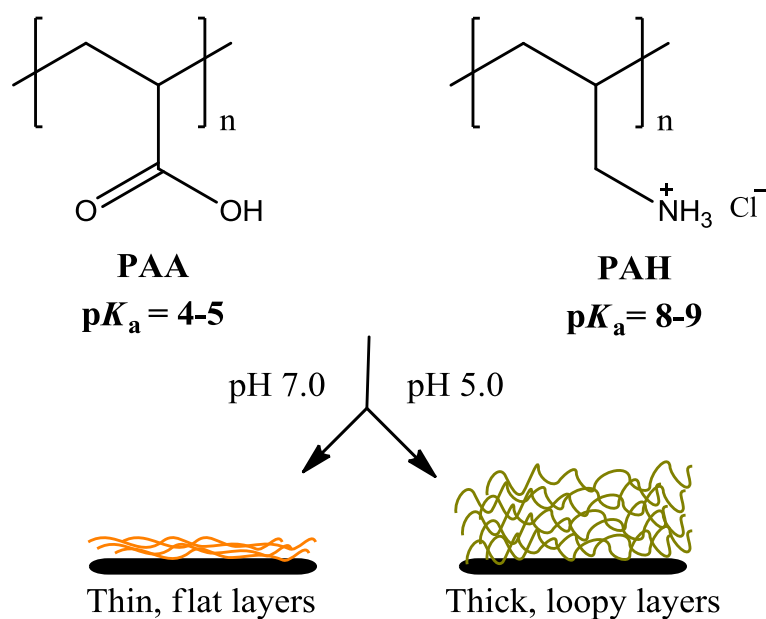
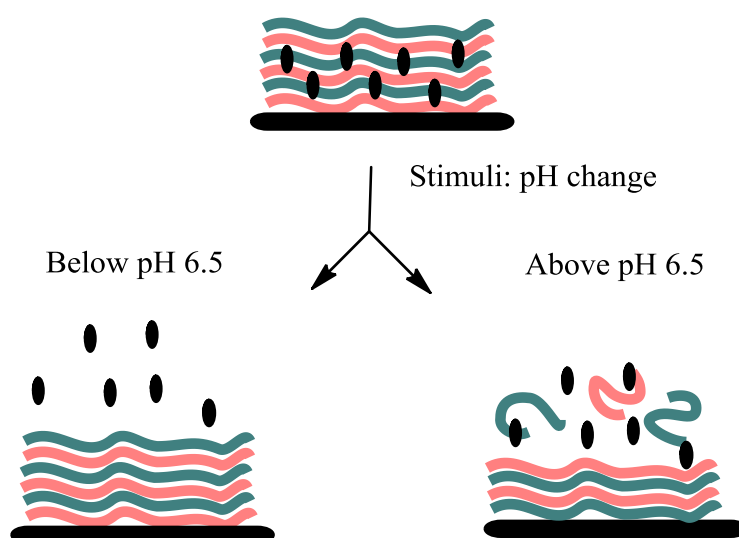


**Figure 10.** Controlling film thickness through film deposition pH during LbL self-assembly. Adapted from Rubner et. al. [127].

It is also possible to control the film properties at the post-assembly step. For example, multilayers of poly(vinylpyrrolidone) (PVPON) and PEO with various polyacids such as PAA and poly (methacrylic acid) (PMAA) were reported to exhibit pH dependent conformational change resulting in rhodamine 6G release either by destructive or non-destructive manner (Figure 11). In this study, above pH 6.5, multilayers were not stable and destructively released rhodamine 6G whereas below pH 6.5 multilayers were stable and non-destructive drug release was observed [130].



Controlled release of components by either non-destructive or destructive manner

**Figure 11.** Controlling film properties at the post-assembly step. Adapted from Granick et. al. [130].

### 1.3.1. Layer-by-Layer Self-assembly of Polybetaines

Incorporation of polybetaines into LbL films is challenging. In the traditional LbL films, there is formation of polyelectrolyte complexes between polyanions and polycations at the surface. However, in case of LbL assembly of polybetaines, polyelectrolyte-polybetaine complexes, because of being not electrically neutral, show tendency towards desorption from the surface during film deposition, leading to inhibition of LbL growth [131]. One of the first successful multilayer film deposition of polybetaines was reported by Laschewsky and co-workers. They coupled small and charged molecules with polybetaines to chemically activate them. After chemical activation, polybetaines became permanently charged polymers and thus could be used for traditional LbL construction [132,133]. In 2003 and in 2007 the studies for LbL deposition using PSB and PCB were reported by Schlenoff [134] and Sukhishvili [135]. Schlenoff and Sukhishvili followed two strategies: i) self-assembly of PSB and PCB with a polyanion under strongly acidic conditions when polybetaines carried net positive charge, ii) self-assembly of PSB and PCB with a

polyanion and a polycation at neutral pH values in an alternating manner forming hybrid films [134,135]

Erel-Goktepe and co-workers previously reported strategies to incorporate electrically neutral polyzwitterions into LbL films. They obtained block copolymer micelles with zwitterionic coronae via pH-induced self-assembly. Later they made a charge screening between negatively charged units of the zwitterionic micellar coronae and a polycation PAH and obtained positively charged zwitterionic micelle/PAH complexes. Multilayers were then constructed via LbL deposition of positively charged micellar complexes and PSS [66].

### **1.3.2. Block Copolymer Micelle Containing LbL Films**

Amphiphilic block copolymers can self-organize into micellar structures under specific conditions forming water-insoluble core and water-soluble coronae. The advantage of the hydrophobic core can be loading of water-insoluble molecules, thus increasing their solubility in aqueous environment. In 2005, Ma et. al. reported LbL construction of multilayers of poly(styrene-*b*-acrylic acid) (PS-*b*-PAA) micelles with hydrophobic PS-core and negatively charged PAA-coronae using poly(diallyldimethylammonium chloride) (PDDA). They reported release of pyrene from the hydrophobic cores, upon increase in the ionic strength due to the structural changes in the micelle structure i.e. shrinkage of the corona [136]. In 2006, Cho and co-workers, reported micelle/micelle multilayers using Nile-red loaded poly(styrene-*b*-4-vinylpyridine) (PS-*b*-P4VP) micelles with cationic P4VP-corona and pyrene loaded poly(styrene-*b*-acrylic acid) (PS-*b*-PAA) micelles with anionic PAA-coronae [137]. In 2007, Zhang et. al. reported LbL deposition of pyrene loaded (PS-*b*-PAA) micelles with PAA-coronae and PDDA [123]. In 2011, Sukhishvili and co-workers, reported preparation of pH and temperature responsive micellar multilayers. The multilayers were constructed using pH and temperature responsive cationic block copolymer micelles of poly(2-(dimethylamino)ethyl methacrylate)-*b*-poly-(N-isopropylacrylamide) (PDMA-*b*-PNIPAM) and a polyanion PSS. They reported controlled release of pyrene from the micelles in response to changes in pH and temperature [138]. In 2018, Palanisamy and Sukhishvili reported the multilayers of

temperature responsive poly(acrylamide-*co*-acrylonitrile)-*b*-polyvinylpyrrolidone (P(AAm-*co*-AN)-*b*-PVP) micelles and TA. They studied the reversible changes in the micellar size and film swelling in response to changes in the temperature. At temperatures above the UCST of the micelles, they observed water uptake within multilayers whereas at temperatures below the UCST of the micelles, they observed release of water from the micellar cores [139].

### 1.3.3. Anti-Adhesive and Antibacterial LbL Films

LbL coatings of zwitterionic polymers for anti-fouling applications to prepare surfaces that are anti-adhesive to proteins and bacteria [33,140,141] together with anti-bacterial properties [142–145] were reported.

In 2006, Rubner et.al. reported contact killing behaviour of a polymer having quaternized amino group, 3-(trimethoxysilyl)propyl]octadecyl-dimethylammonium chloride (OQAS), which resulted in the leakage of cytoplasm of bacteria due to the interactions between positively charged polymer and negatively charged cell wall of bacteria [146].

In 2012, Ji et. al. reported construction of multilayers composed of PEI-Ag<sup>+</sup> complex and PAA on a Teflon substrate. They reported that upon de-attachment from the surface, they obtained free-standing films with two different behaviors from the two sides of the films. One side of the films was superhydrophilic and capable of releasing silver that kills bacteria and the other side was superhydrophobic, capable of preventing bacteria adhesion [147].

In 2013, Hammond and co-workers, reported preparation of Gentamicin releasing multilayers. They constructed tetralayer films of hydrolyzable poly( $\beta$ -amino ester), CHI, PAA and PDDA via spray coating. They studied the anti-bacterial property of the multilayers using *Staphylococcus aureus* as model organism. Multilayers released Gentamicin upon hydrolysis of poly( $\beta$ -amino ester) at neutral pH conditions [148].

The disadvantage of anti-bacterial multilayers is that when the bioactive agent is diminished, they become less effective. Therefore, designing LbL films using bio-inert or low-fouling polymers becomes more important.

Recently, Erel-Goktepe and co-workers showed preparation of dual responsive surfaces, i.e. anti-adhesive and antibacterial using block copolymer micelles with zwitterionic corona- and pH-responsive core. In this study, micellar core blocks were used to load and release antibacterial agents [67].

#### **1.3.4. Surface Coatings Promoting Osteoblast Adhesion**

Biomaterial-associated infection (BAI) is one the most commonly seen hospital-acquired infections [149,150]. It is assumed that; up to 50% of all hospital-acquired infections are implant-related [151]. Therefore, inhibiting bacterial adhesion to reduce or prevent biomaterial-related infections is very important. However, the general methods for preventing bacterial adherence often prevent the desired eukaryotic cell adherence which inhibits biomaterial-host tissue integration and results in the rejection of the biomaterial. To this purpose, surfaces that promote the attachment and proliferation of eukaryotic cells while inhibiting bacterial adherence and colonization are needed [149]. The initial strategy was to use cell adhesive surfaces to promote both bacteria and eukaryotic cell adhesion together with antimicrobial agents [152]. However, this approach was found to be non-effective after the depletion of the antimicrobial agents. Therefore, anti-adhesive surfaces for both bacteria and eukaryotic cells together with eukaryotic cell adhesive motifs gained popularity. While anti-adhesiveness prevents adhesion of cells, eukaryotic cell adhesive motifs promote selective adhesion of eukaryotic cells. In 2011, Boyan and co-workers, reported the use of poly-L-lysine-grafted polyethylene glycol (PLL-g-PEG) coated Titanium surfaces. In this study the coated surfaces were functionalized with a peptide motif arginine–glycine–aspartic acid (RGD) that is found in extracellular matrix and was shown to increase osteoblast attachment. Another peptide motif, lysine–arginine–serine–arginine (KRSR), known to inhibit osteoblast attachment, was used as a negative control [153]. In 2012, Kim et. al. reported the use of heparin-dopamine coated Titanium surfaces to promote

eukaryotic cell adhesion mechanism. Heparin promotes eukaryotic cell adhesion due to its high binding affinities to vascular endothelial growth factor (VEGF), basic fibroblast growth factor (bFGF), and transforming growth factor- $\beta$  (TGF- $\beta$ ). In addition these authors functionalized these surfaces using Gentamicin, an anti-bacterial agent to prevent bacteria adhesion and bone morphogenic protein-2 (BMP-2) to promote osteoblast adhesion [154]. In 2014, Herrmann and co-workers, reported the preparation of anti-adhesive surfaces using block copolymer poly (lactide-*co*-glycolide) (PLGA) functionalized with antimicrobial peptides (AMP). The surfaces were able to kill bacteria on contact, and arginine– glycine–aspartate (RGD) peptides to promote the adhesion and spreading of host tissue cells [155]. Recently, Miura and co-workers, reported the effect of phosphate-enriched surfaces on osteoblast adhesion. The authors generated surfaces modified with PEGMA-Phosmer which behaved as anti-fouling purposes for bacteria as well as surfaces promoted osteoblast adhesion. They concluded that phosphate groups on the Phosmer, caused Calcium ion attraction and therefore promote osteoblast adhesion [156].

#### **1.4. Aim of the Thesis**

The aim of this thesis was to obtain LbL modified surfaces which show anti-adhesiveness against bacteria and proteins but at the same time allow adhesion of mammalian cells. In addition, this thesis aimed to understand the effect of chemical nature and the functional chemical groups of the polyanions, layer number and surface morphology of the films on the anti-adhesive properties. In this respect,  $\beta$ PDMA-*b*-PDPA micelles with zwitterionic  $\beta$ PDMA-corona and pH-responsive PDPA-core were LbL deposited at the surface using three different polyanions, i.e. HA, TA and PSS. Protein adhesion onto these three different types of multilayers was assessed through BSA, Casein, Lysozyme and Ferritin adsorption onto the coatings using ellipsometry and microBCA techniques. Bacterial adhesion was examined using Gram (-) bacteria *E.coli* and Gram (+) bacteria *S.aureus* as model bacterial cells using agar plating, crystal violet staining and fluorescent microscopy

techniques. Adhesion of osteoblast-like SaOS-2 cells as model mammalian cells onto multilayers was investigated through fluorescent microscopy.



## CHAPTER 2

### EXPERIMENTAL

#### 2.1. Materials

5-Chloro-2-(2,4-dichlorophenoxy)phenol (Triclosan), poly(sodium 4-styrene sulfonate) (PSS) ( $M_w$  70,000), Hyaluronic acid sodium salt from *Streptococcus equi* (HA;  $\sim 1.5\text{-}1.8 \times 10^6$  Da), Ferritin from equine spleen Type I, saline solution, Chloramphenicol, Casein from bovine milk, Gram Staining Kit for microscopy and formaldehyde solution were purchased from Sigma-Aldrich (USA). Tannic Acid (TA;  $M_w$  1701.20), Mueller-Hinton (MH) broth, Phosphate Buffered Saline (PBS), Sodium dihydrogenphosphate dehydrate and Luria Bertani (LB) broth (MILLER) were purchased from Merck Chemicals (Darmstadt, Germany). Bovine Serum Albumin (BSA) was purchased from VWR. Agar bacteriological (Agar No.1, Oxoid), MicroBCA protein assay kit and 3,3'-dioctadecyl-5,5'-di(4-sulfophenyl) oxacarbocyanine sodium salt (SP-DiOC<sub>18</sub>(3)) were purchased from Thermo Scientific (USA). Lysozyme *BioChemica* BC was purchased from AppliChem GmbH (Germany). Sterile PTFE syringe filters (0.22  $\mu\text{m}$  and 0.45  $\mu\text{m}$ ) were purchased from Sartorius AG (Goettingen, Germany). Dulbecco's Modified Eagle's medium (DMEM), Fetal Bovine Serum (FBS), Dulbecco's Phosphate Buffered Saline and trypsin-EDTA solution were purchased from Biological Industries (Kibbutz Beit Haemek, Israel). Cell culture plates and T25 flasks were purchased from Sarstedt (Nibracht, Germany). The deionized (DI) H<sub>2</sub>O was purified by passage through a Milli-Q system (Millipore). *Staphylococcus aureus* ATCC 29213 strain and *Escherichia coli* ATCC 8739 were kindly provided by Dr. Emel Uzunoğlu (Microbiology Laboratory, Giresun Medical Faculty) and Prof. Dr. Ayşegül Çetin

Gözen (Department of Biology, Middle East Technical University), respectively. *Escherichia coli* K12 ATCC 700926 was kindly provided by Prof. Dr. Hüseyin Avni Öktem (Department of Biology, Middle East Technical University). To generate fluorescently labeled bacteria, the *E. coli* K12 strain was transformed with a pSB1C3 (obtained from iGEM open sourceware <http://parts.igem.org/Part:pSB1C3>), a high copy number plasmid that expresses green fluorescent protein (GFP). Colonies were selected using chloramphenicol. PDMA<sub>0.72</sub>-*b*-PDPA<sub>0.28</sub> diblock copolymer was provided by Prof. Dr. Vural Bütün's Research Laboratory (Department of Chemistry, Eskişehir Osmangazi Üniversitesi).

## 2.2. Preparation and characterization of $\beta$ PDMA-*b*-PDPA micelles

0.1 mg/mL  $\beta$ PDMA-*b*-PDPA solution was prepared at pH 3 using 0.001 M phosphate buffer. pH of  $\beta$ PDMA-*b*-PDPA solution was gradually increased using 0.1 M NaOH solution and  $\beta$ PDMA-*b*-PDPA micelles were obtained at pH 7.5. The micellar solution was filtered through 0.22  $\mu$ m syringe filter prior to use. For preparation of Triclosan loaded  $\beta$ PDMA-*b*-PDPA micelles, first 2.5 mg/mL Triclosan solution was prepared in ethanol (> 99.8 %). 1 mL of Triclosan solution in ethanol was added dropwise into 200 mL of 0.001 M phosphate buffer. The final concentration of Triclosan was 0.0125 mg/mL. 0.1 mg/mL  $\beta$ PDMA-*b*-PDPA solution was prepared using Triclosan containing 0.001 M phosphate buffer solution. pH of the solution was increased to pH 7.5 for micellization.  $\beta$ PDMA-*b*-PDPA micellar solution was stirred overnight at dark for efficient Triclosan loading into the micellar cores. The solution was filtered through 0.22  $\mu$ m syringe filter prior to use.

Dynamic light scattering and zeta-potential measurements of  $\beta$ PDMA-*b*-PDPA were performed using Zetasizer Nano-ZS equipment (Malvern Instruments Ltd., U.K.). Hydrodynamic sizes were obtained by cumulants analysis of the autocorrelation data. Zeta-potential values were obtained from electrophoretic mobility values using the Smoluchowski approximation. TEM image of  $\beta$ PDMA-*b*-PDPA micelles was obtained using an FEI Tecnai G2 Spirit Bio-Twin CTEM operating at an acceleration voltage of 20 – 120 kV. A drop of  $\beta$ PDMA-*b*-PDPA micellar solution at pH 7.5 was

placed on the surface of a copper grid coated with a carbon substrate with 3 mm diameter and air-dried.

### **2.3. Deposition and characterization of multilayers**

Silicon wafers or glass slides were immersed into concentrated sulfuric acid for 85 minutes. Substrates were rinsed with deionized (DI) water and dried under a flow of nitrogen. Then, the substrates were immersed into 0.25 M NaOH solution for 10 minutes, followed by thorough rinsing with DI water and drying under nitrogen flow. 1-, 3- and 5- layer films were prepared at pH 7.5. For 1-layer films, the substrates were immersed into 0.1 mg/mL  $\beta$ PDMA-*b*-PDPA micellar solution at pH 7.5 for 15 minutes. For 3- and 5- layer films, substrates were immersed alternately into 0.1 mg/mL  $\beta$ PDMA-*b*-PDPA micellar solution and 0.1 mg/mL HA or TA or PSS solutions at pH 7.5 for 15 minutes. Between each layer deposition, substrates were rinsed twice using 0.001 M phosphate buffer solution at pH 7.5. Importantly, TA solution was always prepared fresh prior to multilayer construction due to degradation of TA at neutral conditions. HA was dissolved at 4°C overnight. All films had the  $\beta$ PDMA-*b*-PDPA micellar layer as the outmost layer.

For the preparation of Triclosan containing  $\beta$ PDMA-*b*-PDPA micellar films, Triclosan loaded  $\beta$ PDMA-*b*-PDPA micelles were used in film assembly. Film growth and pH-stability were monitored by measuring the dry film thickness using a spectroscopic ellipsometer (Optosense, USA, OPT-S6000). For microbiology experiments, each side of the coated wafers or glass slides were UV-sterilized for 1 hour. Film deposition was carried out under sterile conditions in a Class II Biosafety Cabinet.

AFM imaging of the films was performed using an NT-MDT Solver P47 AFM in tapping mode using Si cantilevers. Roughness values were obtained from images with 2 x 2  $\mu$ m scan size. Multilayers were deposited onto 1.5 cm x 1.5 cm silicon wafers as described in section 2.3. Static contact angles were measured using Attension Theta Lite optical tensiometer. Approximately 2  $\mu$ L drop of deionized water was formed and deposited onto the substrates. Three water droplets were

deposited onto each coated substrate. For each droplet, 10 independent measurements were recorded with 16 milisecond frame intervals.

#### **2.4. Growth conditions for bacteria**

Luria Bertani (LB) broth and Mueller Hinton (MH) broth were prepared using deionized water, autoclaved and filtered through 0.45 $\mu$ m syringe filter. LB broth was used for overnight culture of *S. aureus* ATCC 29213 and *E. coli* ATCC 8739. MH broth was used in the experiments done for examination of antibacterial and anti-adhesive properties for both coated and uncoated slides. The pH of MH broth was adjusted to either 5.5 or 7.5. All experiments were carried out aseptically.

#### **2.5. Cell culture and imaging**

SaOS-2 cells (human bone osteosarcoma cell line) were cultivated in DMEM complete medium supplemented with 10% FBS, 2 mM L-glutamine, 100 U/mL penicillin, and 100  $\mu$ g/mL streptomycin. After thawing 5% DMSO containing stocks, cells were cultivated in T25 flasks for 2 days. All cell culture flasks and plates were maintained in a humidified atmosphere at 37°C in 95% air and 5% CO<sub>2</sub>. The cells were routinely checked for mycoplasma contamination. Plasmocin was used at a maintenance dose to prevent any mycoplasma growth during the experiments. To harvest cells from the flasks, 0.5 mg/mL porcine trypsin with 0.2 mg/mL 4X Na-EDTA solution was used.

1-, 3-, 5-layer  $\beta$ PDMA-*b*-PDPA micelles/HA,  $\beta$ PDMA-*b*-PDPA micelles/TA and  $\beta$ PDMA-*b*-PDPA micelles/PSS coated substrates were placed inside 24-well tissue culture plate. 100,000 cells were seeded in each well incubated for 4 h. This duration was selected as it would allow the cells enough time to adhere, but not to proliferate since SaOS-2 cells have a doubling time of approximately 36-40 h. To assess the spreading of cells on the substrates, the plates were washed twice with sterile PBS and fixed in 10% paraformaldehyde for 1h. After rinsing the surfaces twice with PBS, the cells were permeabilized with 10 mM Tris-HCl containing 2 mM MgCl<sub>2</sub>

and 0.5% Triton X-100 in PBS for 1h and rinsed again 4 times with PBS. For better visualization the cells were treated with the lipid binding dye, 3,3'-dioctadecyl-5,5'-di(4-sulfophenyl) oxacarbocyanine sodium salt (SP-DiOC<sub>18</sub>(3)) at a final concentration of 5 µg/mL in PBS for 15 min in a cell culture incubator at 37°C and subsequently for 15 min on ice. The cells were observed under EVOS FLoid Cell Imaging microscope (Thermo Fisher Scientific) in the green channel. Images from 3 random sites for each substrate were recorded.

## **2.6. Transformation of *E. coli* K12 to stably express GFP**

Stable GFP expressing *E. coli* K12 ATCC 700926 was generated by transformation of 5 µg/mL pSB1C3 plasmid into competent cells using standard techniques. The transformed bacteria underwent antibiotic selection with 25 µg/mL chloramphenicol and the positive colonies were collected for fluorescent microscopy.

## **2.7. Light Microscopy**

25 µL of *S. aureus* ATCC 29213 or *E. coli* ATCC 8739 cultures (from a broth containing  $\sim 1.2 \times 10^7$  CFU.mL<sup>-1</sup>) were added onto blank glass slides (control) and 1-, 3-, 5-layer βPDMA-*b*-PDPA micelles/HA, βPDMA-*b*-PDPA micelles/TA and βPDMA-*b*-PDPA micelles/PSS coated slides, which were immersed into 1 mL MH broth in a 24-well cell culture plate. Samples were incubated for 1 hour at 37°C. All substrates were then washed three times with PBS. Control and coated substrates were examined under a 40X inverted light microscope (Leica, USA) and the bacteria were counted from the images for a quantitative analysis.

## **2.8. Fluorescent Microscopy**

25 µL of the *E. coli* K12 cells expressing GFP (from a broth supplemented with 25 µg/mL of chloramphenicol, containing  $\sim 2.5 \times 10^7$  CFU.mL<sup>-1</sup>) were added onto blank glass slides (control) and 1-, 3-, 5-layer βPDMA-*b*-PDPA micelles/HA, βPDMA-*b*-PDPA micelles/TA and βPDMA-*b*-PDPA micelles/PSS coated substrates which

were immersed into 1 mL MH broth in a 24-well cell culture plate. Samples were incubated for 1 hour at 37°C. The glass slides were then washed three times with PBS. All slides were examined under EVOS FLoid Cell Imaging microscopy using Green and White light channels, Thermo Fisher Scientific. Fluorescence intensities were quantified using Image J (<https://imagej.nih.gov/ij/index.html>).

## **2.9. Kirby-Bauer Test**

Agar plates containing MH broth at pH 7.5 or 5.5 were prepared. 80  $\mu$ L of *E. coli* ATCC 8739 cultures (grown in LB medium up to  $OD_{600} = 0.20$ ) was spread-plated on MH agar. Triclosan loaded 1-, 3-, and 5-layer  $\beta$ PDMA-b-PDPA micelles/HA,  $\beta$ PDMA-b-PDPA micelles/TA and  $\beta$ PDMA-b-PDPA micelles/PSS coated glass substrates were placed onto MH agar such that the uncoated sides of the substrates touched the MH agar. The plates were incubated overnight at 37°C and clear zones were measured. Two independent biological replicates were carried out.

## **2.10. Protein Adsorption Tests**

### **2.10.1. Determination of protein adsorption by measuring protein amount via microBCA assay**

Bovine Serum Albumin and Lysozyme adsorption on coated and blank (control) glass slides were evaluated by the microBCA assay. 1 cm x 1 cm glass slides were cut and cleaned as described in Section 2.3. 1-, 3-, and 5-layer films were deposited onto cleaned and sterilized 1 cm x 1 cm glass slides. Each substrate was placed in each well of a 24-well containing 1 mL of BSA solution (50 mg/mL prepared in PBS) or Lysozyme (25 mg/mL prepared in PBS). After 1 hour of incubation at 37°C, the substrates were washed three times with PBS, placed in 300  $\mu$ L of PBS containing 0.5 M NaCl and 1% SDS and vortexed for 1 minute each to remove proteins from the substrate surface. Lastly, microBCA assay was carried out according to the manufacturer's instructions. UV-Vis absorption spectra of these solutions were recorded at 562 nm using Multiscan Go Microplate

Spectrophotometer (Thermo, USA). The amount of BSA was determined using a calibration curve.

### **2.10.2. Determination of protein adsorption by ellipsometry**

1-, 3-, and 5-layer  $\beta$ PDMA-*b*-PDPA micelles/HA,  $\beta$ PDMA-*b*-PDPA micelles/TA and  $\beta$ PDMA-*b*-PDPA micelles/PSS films on silicon wafers were immersed into i) 25 mg/mL Casein; ii) 25 mg/mL Ferritin; iii) 25 mg/mL Lysozyme and iv) 25 mg/mL or 50 mg/mL BSA solutions for 1 hour at 37°C and rinsed three times using PBS. The substrates were dried and ellipsometric thickness values were recorded. All protein solutions were prepared using PBS at pH 7.5.

Long-term protein adhesion tests were performed using ellipsometry. Blank silicon wafer, and silicon wafers coated with 3-layer  $\beta$ PDMA-*b*-PDPA micelles/HA,  $\beta$ PDMA-*b*-PDPA micelles/TA and  $\beta$ PDMA-*b*-PDPA micelles/PSS films were immersed into BSA solution (25 mg/mL prepared in PBS at pH 7.5) for 24 hours at 37°C and rinsed three times using PBS. The substrates were dried and ellipsometric thickness values were recorded.

### **2.11. Counting of viable surface-adherent bacteria**

Cultures of *S. aureus* ATCC 29213 and *E. coli* ATCC 8739 in LB broth were adjusted to OD<sub>600</sub>=0.2 which corresponds to  $\sim 1.2 \times 10^7$  CFU.mL<sup>-1</sup> of bacteria. 1 cm x 1 cm glass slides, either blank (control) or coated with 1-, 3-, and 5-layer  $\beta$ PDMA-*b*-PDPA micelles/HA,  $\beta$ PDMA-*b*-PDPA micelles/TA and  $\beta$ PDMA-*b*-PDPA micelles/PSS coated substrates were immersed into 1 mL MH Broth containing 25  $\mu$ L of the bacterial cultures mentioned above in a 24-well cell culture plate and incubated at 37°C for 1 hour. Each substrate was washed three times by immersing into 1 mL sterile PBS (0.01 M phosphate buffer salts, 0.0027 M KCl, 0.137 M NaCl at pH 7.5) followed by immersing into 5 mL of PBS (pH 7.5). The slides were vortexed at 2000 rpm for 1 min, sonicated in a bath sonicator for 5 min, and vortexed at 2000 rpm for another 1 min. 100  $\mu$ L of the sample was 100x diluted in PBS (pH 7.5). 80  $\mu$ L of this diluted solution was spread-plated on LB agar. After an overnight

incubation at 37°C, colonies of viable bacteria were counted and normalized to the control in each replicated experiments.

### **2.12. Crystal violet staining assay**

Blank glass slides (control) or substrates coated with 1-, 3-, and 5-layer  $\beta$ PDMA-*b*-PDPA micelles/HA,  $\beta$ PDMA-*b*-PDPA micelles/TA and  $\beta$ PDMA-*b*-PDPA micelles/PSS films were placed in each well of a 24-well plate containing 1 mL of MH broth including 25  $\mu$ L of *S. aureus* ATCC 29213 or *E. coli* ATCC 8739 cultures (from a broth of  $1.2 \times 10^7$  CFU.mL<sup>-1</sup>) and incubated at 37°C for 1 h. Each substrate was washed three times with 1 mL PBS (pH 7.5) and then placed into 1 mL of 1% crystal violet solution and incubated at room temperature for 1 h. Each substrate was washed twice with 1 mL of PBS (pH 7.5) and then immersed into 400  $\mu$ L of a decolorizer solution containing ethanol and acetone for 5 min. This duration was enough to decolorize both Gram positive and Gram negative bacteria. 300  $\mu$ L from the decolorization solution was taken as 3 technical replicates (100  $\mu$ L each) and this solution was transferred into individual wells of a 96-well plate and the absorbance of each sample at 590 nm was immediately recorded in a Multiscan Go Microplate Spectrophotometer (Thermo, USA). The absorbance for the control was assumed as 100 % and data were normalized accordingly. To eliminate the contribution of the coatings to absorbance readings, coated substrates that were not incubated in bacteria-containing growth media were dipped into 1% crystal violet solution for 1 h and the absorbance values were subtracted from that of the coated substrates that were incubated in bacteria-containing media.

### **2.13. Hydrophobicity Plots**

Hydrophobicity plots were generated using ExPASyProtScale (<http://web.expasy.org/protscale/>). The accession numbers (AC) were found from UniProtKB and protein sequences were determined. Hydrophobicity plots were generated using Kyte & Doolittle parameters.

#### **2.14. Statistical analysis**

Film thickness measurements were expressed as the means of three different measurements obtained from different regions on a substrate and the standard deviation (SD) of means. Where indicated, statistical difference between samples were determined by either t-test or ANOVA. Holm-Sidak's test was also performed as a multiple comparisons test following ANOVA. p value  $\leq 0.05$  was considered to be significant.



## CHAPTER 3

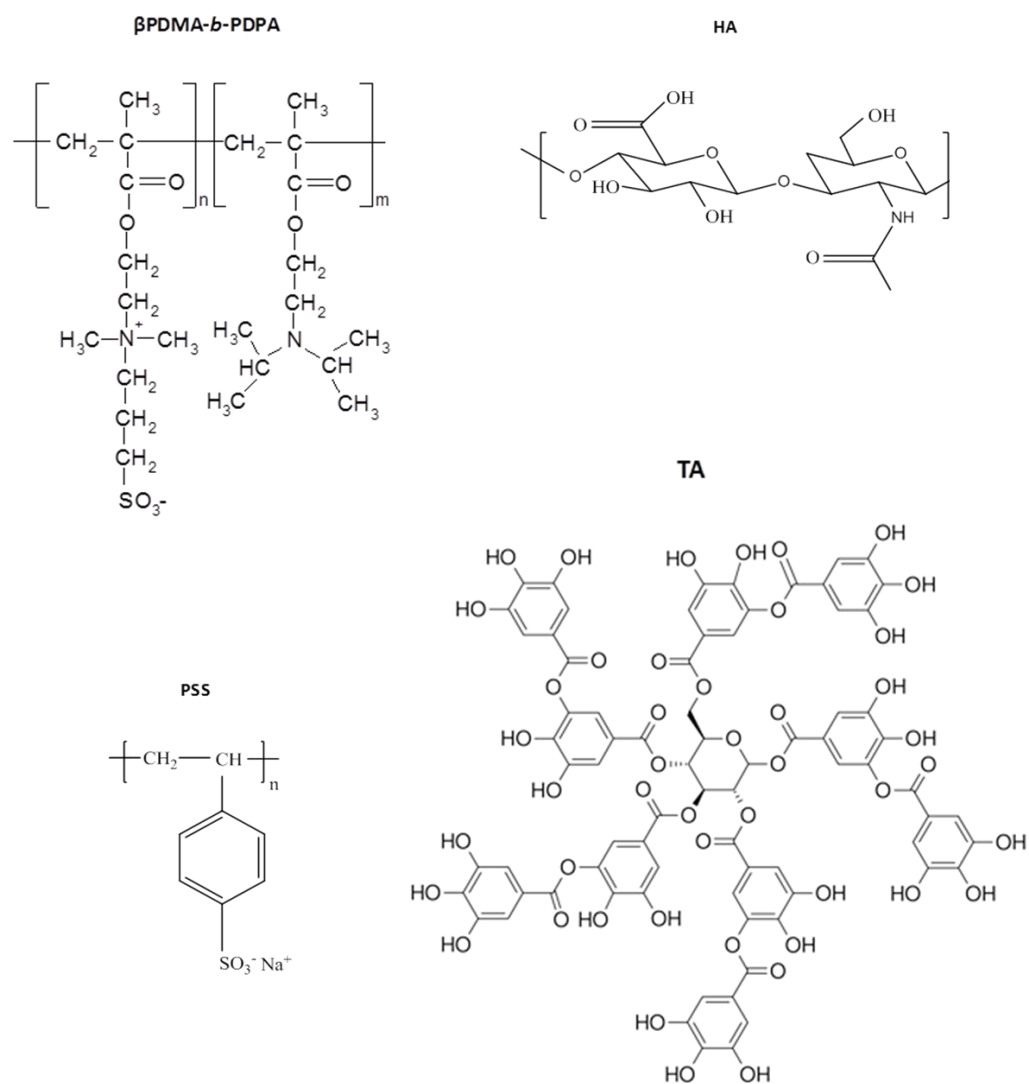
### RESULTS & DISCUSSION

#### 3.1. Preparation and Characterization of Multilayers

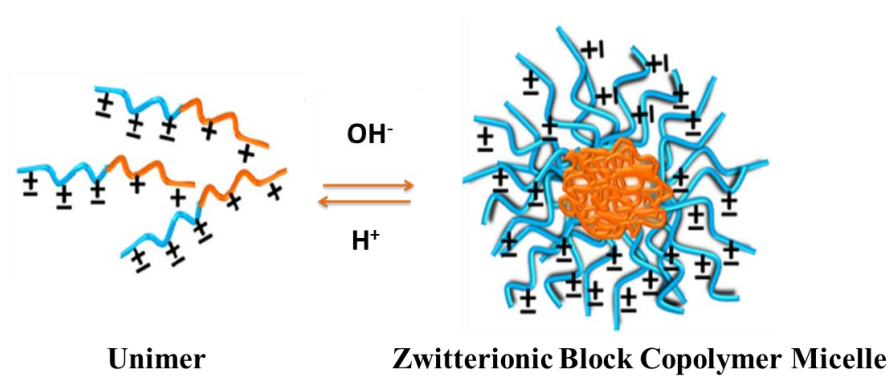
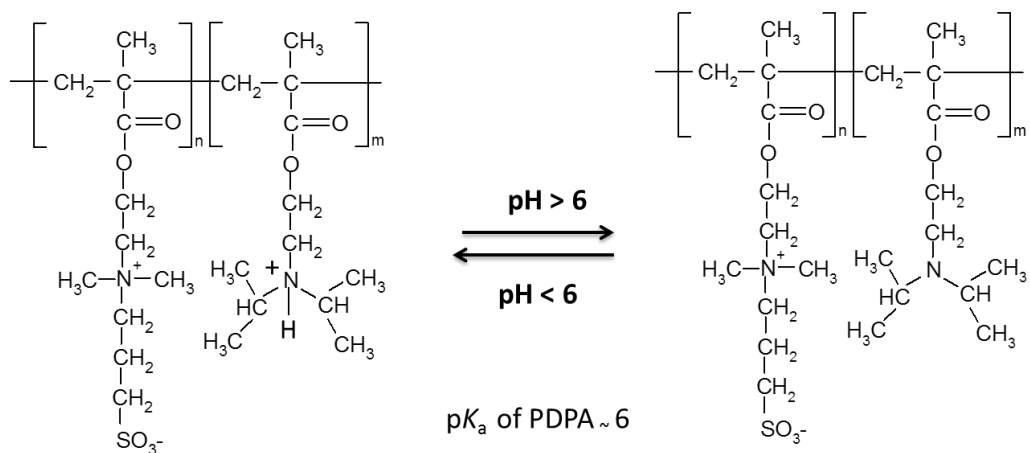
$\beta$ PDMA-*b*-PDPA micelles were prepared at pH 7.5 by gradually increasing the pH of  $\beta$ PDMA-*b*-PDPA solution from pH 3 to pH 7.5. The unprotonation of the amino groups of PDPA-core blocks above the  $pK_a$  of PDPA ( $\sim 6$ ) [157] followed by self-aggregation of PDPA blocks was the driving force for the pH-induced self-assembly of  $\beta$ PDMA-*b*-PDPA and formation of micellar aggregates. Scheme 3 shows the chemical structures for LbL assembly used for this study.  $\beta$ PDMA-*b*-PDPA micelles with  $\sim 18.1 \pm 0.5$  nm size were used as building blocks to construct the multilayers at pH 7.5. Scheme 4 shows the pH dependent micellization of  $\beta$ PDMA-*b*-PDPA. Figure 12A and 12B show the shift in the number average hydrodynamic size distribution of  $\beta$ PDMA-*b*-PDPA upon micellization and TEM image of  $\beta$ PDMA-*b*-PDPA micelles at pH 7.5, respectively. Note that micellization of  $\beta$ PDMA-*b*-PDPA at pH 11 has been reported before and the average size of the micelles was  $\sim 22$  nm [158]. Despite the electrically neutral zwitterionic corona,  $\beta$ PDMA-*b*-PDPA micelles had average zeta-potential of  $\sim 4.9 \pm 0.3$  mV at pH 7.5 due to either several unbetainized tertiary amino groups which could not be detected by  $^1\text{H}$  NMR Spectroscopy or some slight positive charge remaining on the surface of PDPA-core. Figure 12C shows the zeta potential distribution curve for  $\beta$ PDMA-*b*-PDPA micelles at pH 7.5.

$\beta$ PDMA-*b*-PDPA micelles were LbL deposited at the surface using three different polyanions, i.e. Hyaluronic Acid (HA), Tannic Acid (TA) and poly(styrene sulfonate) sodium salt (PSS) at pH 7.5. Figure 13A, 13B and 13C show the LbL

growth of  $\beta$ PDMA-*b*-PDPA micelles/HA,  $\beta$ PDMA-*b*-PDPA micelles/TA and  $\beta$ PDMA-*b*-PDPA micelles/PSS, respectively at pH 7.5.



**Scheme 3.** Chemical Structures of  $\beta$ PDMA-*b*-PDPA, HA, TA, and PSS.



**Scheme 4.** pH dependent micellization of  $\beta$ PDMA-*b*-PDPA.

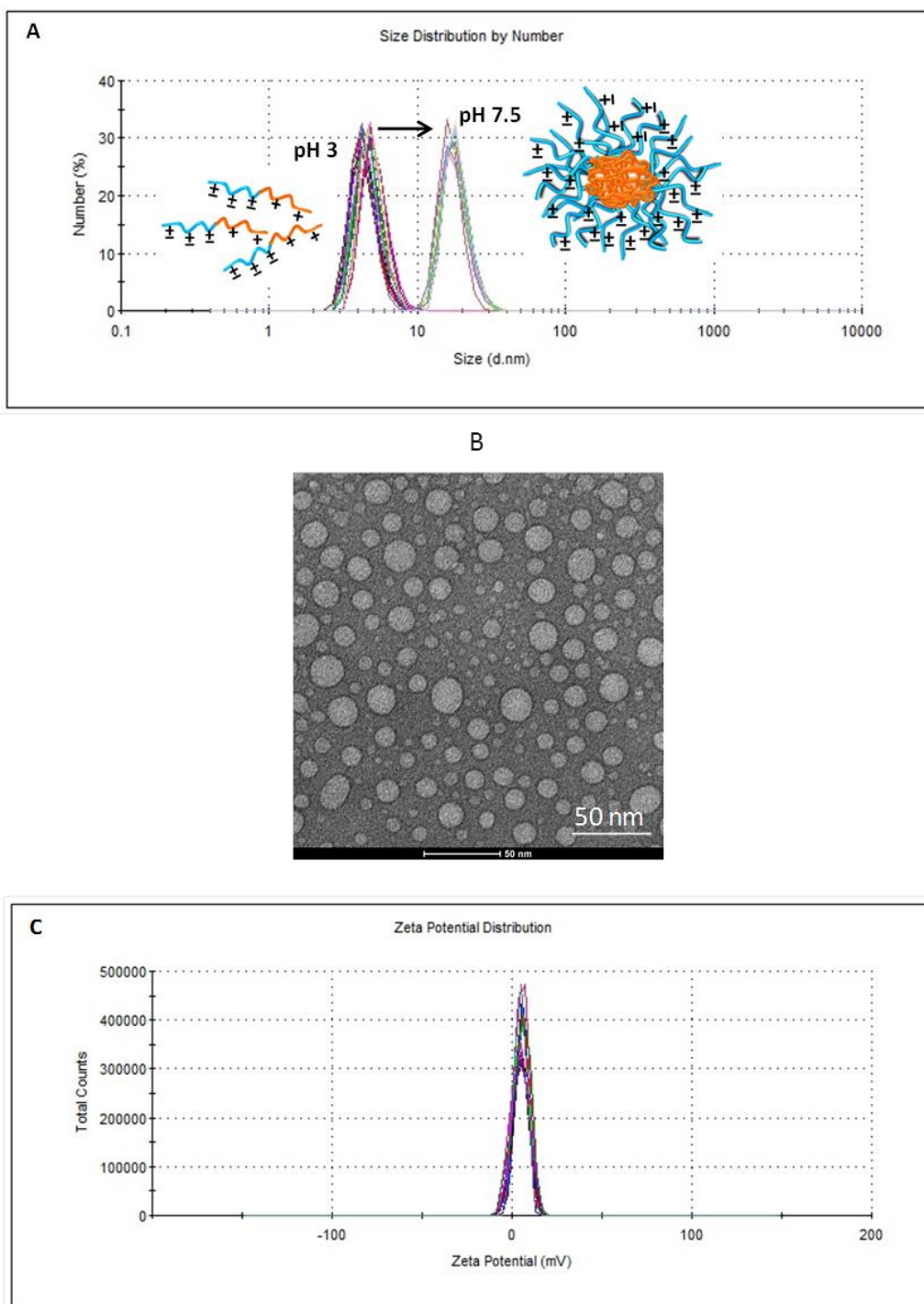


**Figure 12.** (A) Number-average hydrodynamic size distribution of  $\beta$ PDMA-*b*-PDPA at pH 3 and pH 7.5. Right direction arrow denotes the shift in size distribution to higher values. (B) TEM image of  $\beta$ PDMA-*b*-PDPA micelles at pH 7.5. (C) Zeta potential distribution of  $\beta$ PDMA-*b*-PDPA micelles at pH 7.5. Size and zeta potential

distribution curves obtained from several individual measurements of the same sample are represented with different colors.

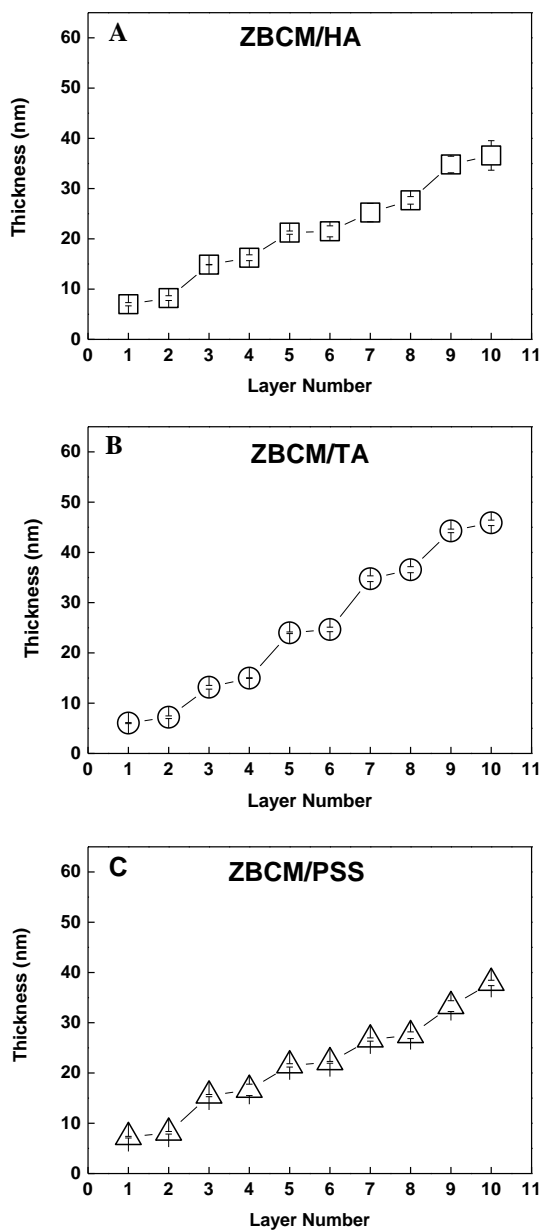


**Figure 13.** LbL growth of  $\beta$ PDMA-*b*-PDPA micelles with HA (A), TA (B) and PSS (C) at pH 7.5.

It is observed that, LbL deposition of  $\beta$ PDMA-*b*-PDPA micelles and PSS could not be formed at pH 8.5 [66]. To understand the driving force behind multilayer

formation at pH 7.5, LbL deposition at pH 7.5, pH 8 and pH 8.5 were compared. Figure 14 compares the LbL growth profile of  $\beta$ PDMA-*b*-PDPA micelles with HA (A), TA (B) and PSS (C) at pH 7.5, 8 and 8.5.

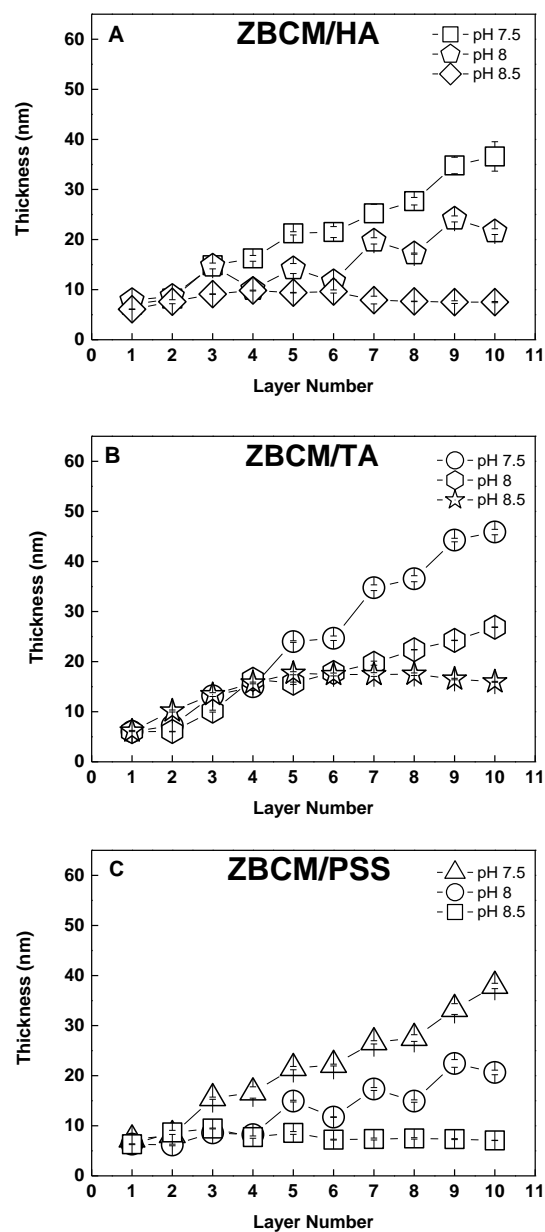


**Figure 14.** Comparison of layer-by-layer growth of  $\beta$ PDMA-*b*-PDPA micelles/HA (A);  $\beta$ PDMA-*b*-PDPA micelles/TA (B) and  $\beta$ PDMA-*b*-PDPA micelles/PSS (C) at pH 7.5, pH 8 and pH 8.5.

It is observed that multilayers could be grown at pH 7.5 and pH 8 but not at pH 8.5. The inhibition of LbL growth at pH 8.5 can be explained by the formation of electrically non-neutral  $\beta$ PDMA-*b*-PDPA micelles-polyanion complexes at the surface resulting in desorption during the self-assembly procedure. Therefore, successful LbL growth at pH 7.5 and pH 8 suggested that the interactions among the layers was more than the electrostatic association among quaternized amino groups of  $\beta$ PDMA-coronae and sulfonate/phenolate/carboxylate groups of the polyanions at pH 7.5 and pH 8. These results suggested two possible scenarios as the driving force for LbL growth:

- i) Zeta potential measurements showed that  $\beta$ PDMA-*b*-PDPA micelles had positive zeta potential at pH 7.5 and pH 8 ( $\sim 4.9 \pm 0.3$  mV and  $\sim 0.98 \pm 1.1$  mV at pH 7.5 and pH 8, respectively) possibly arising from either several unbetainized amino groups remained on the  $\beta$ PDMA-coronae which could not be detected by  $^1\text{H}$  NMR analysis and/or few protonated amino groups of PDPA remained at the core-corona interface. In general, the result obtained from the calculation of  $^1\text{H}$  NMR spectrum based on such conversion may contain 1-2 % error. These residues might be the source of positive zeta potential at pH 7.5 and pH 8. This additional association among the polyanions and tertiary amino groups on  $\beta$ PDMA-*b*-PDPA micelles might have contributed to LbL assembly which was not possible when the layers associated solely through the quaternized amino groups of  $\beta$ PDMA-coronae and sulfonate/phenolate/carboxylate groups of the polyanions. Indeed, the lower thickness values obtained at pH 8 also supports this possibility. As the film deposition pH increased from 7.5 to 8, the percent ionization of free tertiary amino groups on  $\beta$ PDMA-*b*-PDPA micelles decreased resulting in lower extent of association at the surface and lower thickness values at pH 8. However, at pH 8.5, when the tertiary amino groups got further deprotonated and the layers interacted solely through quaternized amino groups of  $\beta$ PDMA-coronae and sulfonate/phenolate/carboxylate groups of the polyanions, LbL growth was inhibited. Of note,  $\beta$ PDMA-*b*-PDPA micelles carried no more positive zeta potential beyond pH 8.

- ii) Contribution of hydrogen bonding interactions to LbL growth which was disrupted as the film deposition pH increased and polyacids got further deprotonated. This is likely to be true for  $\beta$ PDMA-*b*-PDPA micelles/HA and  $\beta$ PDMA-*b*-PDPA micelles/TA films which possibly interacted also through hydrogen bonding interactions among sulfonate groups of  $\beta$ PDMA-coronae and hydroxyl groups of TA or HA. However, the fact that PSS and  $\beta$ PDMA-*b*-PDPA micellar layers, which were not expected to associate through hydrogen bonding interactions due to lack of hydrogen donating groups in PSS, also showed similar LbL growth trend at pH 7.5, pH 8 and pH 8.5 strengthens the first scenario. However, it is worth mentioning that hydrogen bonding interactions among  $\beta$ PDMA-*b*-PDPA micelles and TA or HA and dipole-dipole interactions among  $\beta$ PDMA-*b*-PDPA micelles and PSS possibly contributed to LbL growth.

In all films, the thickness increment after every micellar layer was greater than that of a polyanion layer. The highest thickness was obtained for  $\beta$ PDMA-*b*-PDPA micelles and TA films. TA is a polyphenol composed of five digalloyl ester groups bound to a central glucose core. It has twenty five hydroxyl groups per molecule. The  $pK_a$  of TA varies with the source that it is extracted [159]. The  $pK_{a,1}$  and  $pK_{a,2}$  of TA which was used in this study were estimated as 6.5 and 8, respectively in one of our recent studies [160]. Therefore, TA was partially charged at the deposition pH of 7.5. On the other hand, HA has a  $pK_a$  of 2.87 for COOH groups [161] and PSS is a strong polyanion. The lower thickness of  $\beta$ PDMA-*b*-PDPA micelles/HA and  $\beta$ PDMA-*b*-PDPA micelles/PSS films was correlated with the adsorption of fully charged HA and PSS on the layer of  $\beta$ PDMA-*b*-PDPA micelles in the extended form. An earlier study on LbL assembly of TA has shown that the thickness value of a layer of TA was greater than the molecular dimensions of TA [162] and this was explained by the self-association of polyphenols [163]. Therefore, the greater thickness of  $\beta$ PDMA-*b*-PDPA micelles/TA films was correlated with the self-association of TA molecules.

The surface morphology of the multilayers was also examined via AFM imaging. Figure 15 and 16 contrasts the AFM height images and roughness values of 3-layers

of  $\beta$ PDMA-*b*-PDPA micelles/HA,  $\beta$ PDMA-*b*-PDPA micelles/TA and  $\beta$ PDMA-*b*-PDPA micelles/PSS films from different z-scales and same z-scales, respectively.

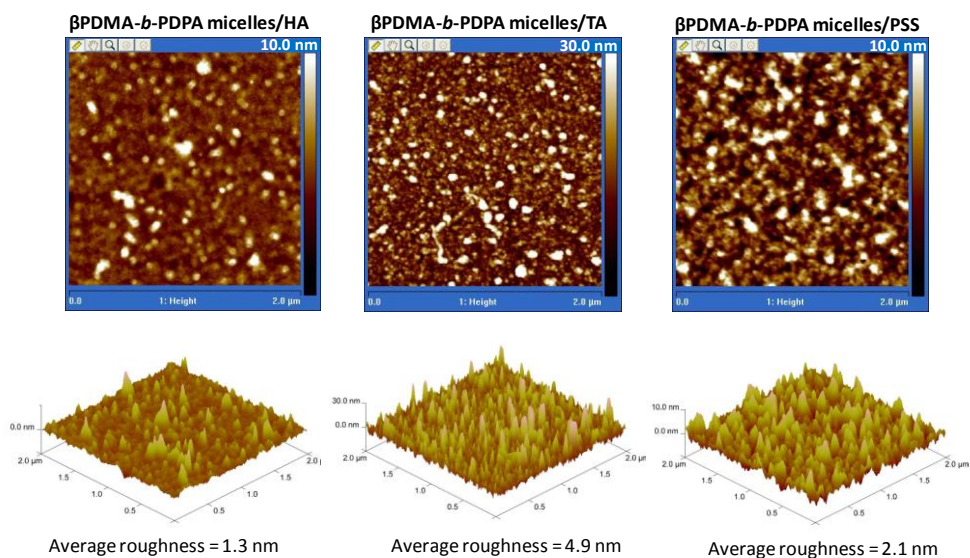


**Figure 15.** AFM height images and roughness values of 3-layer  $\beta$ PDMA-*b*-PDPA micelles/HA,  $\beta$ PDMA-*b*-PDPA micelles/TA and  $\beta$ PDMA-*b*-PDPA micelles/PSS films. The average surface roughness values were estimated over  $2\ \mu\text{m} \times 2\ \mu\text{m}$  areas on three different randomly selected places of the sample surface.

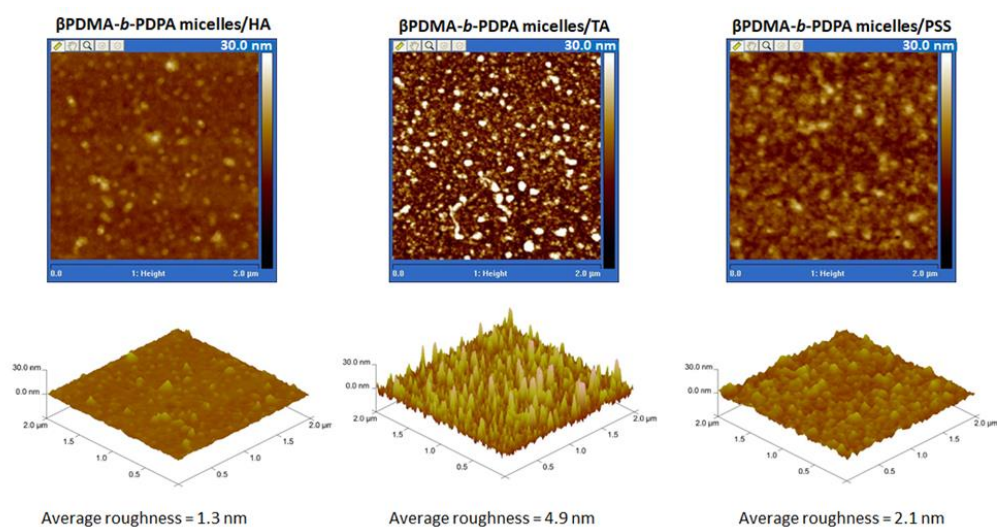


**Figure 16.** AFM height images (same z-scales) and roughness values of 3-layers  $\beta$ PDMA-*b*-PDPA micelles/HA,  $\beta$ PDMA-*b*-PDPA micelles/TA and  $\beta$ PDMA-*b*-

PDPA micelles/PSS films. The average surface roughness values were estimated over 2  $\mu\text{m}$  x 2  $\mu\text{m}$  areas on three different randomly selected places of the sample surface.

The surface of  $\beta\text{PDMA-}b\text{-PDPA}$  micelles/TA film was rougher (roughness  $\sim 4.9$  nm) than the surfaces of both  $\beta\text{PDMA-}b\text{-PDPA}$  micelles/HA and  $\beta\text{PDMA-}b\text{-PDPA}$  micelles/PSS films with roughness values of  $\sim 1.3$  nm and  $\sim 2.1$  nm, respectively. The greater roughness of  $\beta\text{PDMA-}b\text{-PDPA}$  micelles/TA films could be correlated with self-association of TA in solution leading to adsorption of TA in the aggregated form. The lateral size values of the surface features on all types of 3-layer films varied between 40-75 nm which were greater than the size of  $\beta\text{PDMA-}b\text{-PDPA}$  micelles obtained by DLS. As a control experiment, the lateral size of surface objects on 1-layer of  $\beta\text{PDMA-}b\text{-PDPA}$  micelles was measured. It was found that 1-layer  $\beta\text{PDMA-}b\text{-PDPA}$  micellar film was incomplete and irregularly packed and the size of surface features varied between 28 nm and 60 nm. We suggest that in case of 3-layer films, when TA, HA or PSS coated surfaces (2-layer films) interacted with  $\beta\text{PDMA-}b\text{-PDPA}$  micellar solution (deposition of the third layer),  $\beta\text{PDMA-}b\text{-PDPA}$  micelles possibly adsorbed onto higher parts of the surface rather than in the holes and the surface features were not solely  $\beta\text{PDMA-}b\text{-PDPA}$  micelles deposited as the outmost layer but a combination of the micelles and the underlying surface features. It is worth to note that the size of the objects at the surface of 1-layer film was still higher than  $\beta\text{PDMA-}b\text{-PDPA}$  micellar size obtained by DLS. This could be due to spreading of  $\beta\text{PDMA-}b\text{-PDPA}$  micelles as well as association of  $\beta\text{PDMA-}b\text{-PDPA}$  micelles with each other at the surface through zwitterionic coronal chains.

The wettability of the films was also examined. The wettability of multilayer films was reported to be determined by the outermost layer [59]. Besides, chemical composition, surface roughness and degree of interpenetration was found to play a role in wettability [164]. Figure 17 shows the evolution of contact angle as a function of layer number. For all films, the contact angles varied between  $20.2^\circ$ - $27.1^\circ$  when the outmost layer was  $\beta\text{PDMA-}b\text{-PDPA}$  micelles. However, the contact angle increased in the order of  $\beta\text{PDMA-}b\text{-PDPA}$  micelles/TA,  $\beta\text{PDMA-}b\text{-PDPA}$

micelles/PSS and  $\beta$ PDMA-*b*-PDPA micelles/HA when the outermost layer was the polyanion. A study by Wenzel reported that for surfaces with contact angle smaller than 90°, increasing surface roughness enhanced the surface wettability [165]. The results are in good agreement with this report since the lowest contact angle was recorded for  $\beta$ PDMA-*b*-PDPA micelles/TA films, which exhibited the highest surface roughness.

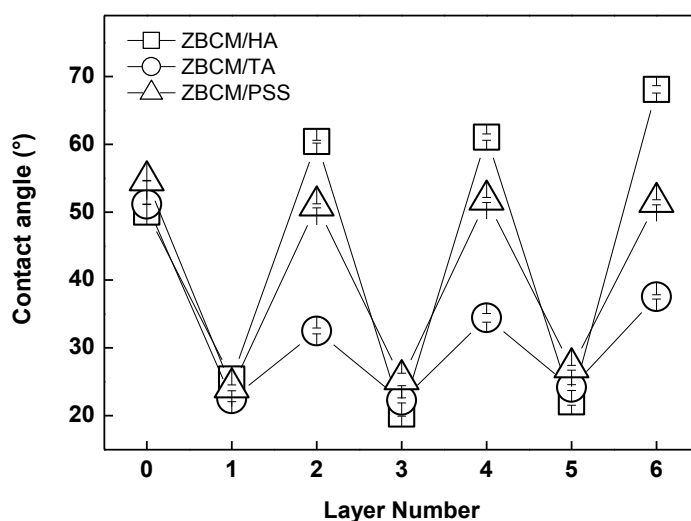


**Figure 17.** Static contact angles of  $\beta$ PDMA-*b*-PDPA micelles/HA (square),  $\beta$ PDMA-*b*-PDPA micelles/TA (circle) and  $\beta$ PDMA-*b*-PDPA micelles/PSS (triangle) films.

### 3.2. Stability of Multilayers

Prior to determining the anti-adhesive and anti-bacterial properties of the films, the stability of the multilayers was examined. To mimic a biological environment, multilayers were immersed into PBS at 37°C. The amount of material retained on the surface was determined at pH 7.5 as well as pH 5.5 as a representation of the acidic environment at an infectious site. Figure 18 shows the fraction retained at the surface of  $\beta$ PDMA-*b*-PDPA micelles/HA,  $\beta$ PDMA-*b*-PDPA micelles/TA and  $\beta$ PDMA-*b*-PDPA micelles/PSS at pH 7.5 (A) and pH 5.5 (B) at 37°C in PBS solution.

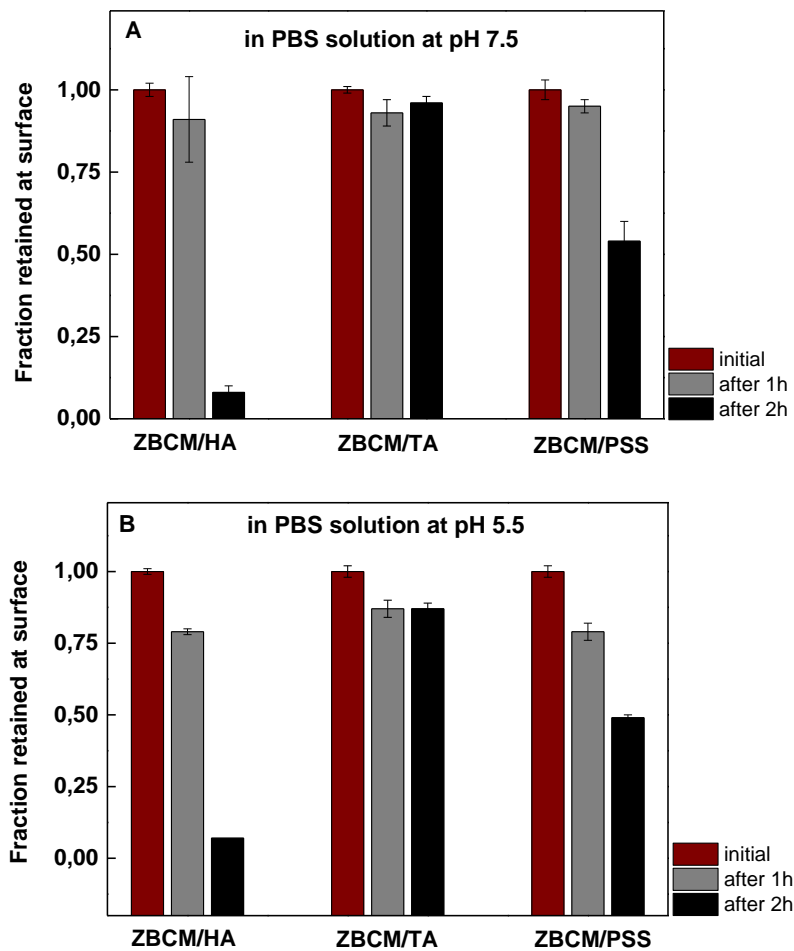


**Figure 18.** Fraction retained at the surface of  $\beta$ PDMA-*b*-PDPA micelles/HA,  $\beta$ PDMA-*b*-PDPA micelles/TA and  $\beta$ PDMA-*b*-PDPA micelles/PSS films after immersion into PBS at pH 7.5 (A); pH 5.5 (B) at 37°C. In all figures, the red columns correspond to fractions before immersion, the gray columns correspond to the fractions of the films retained at the surface after being immersed into PBS for 1 hour at 37°C and the black columns correspond to the fractions of the films retained at the surface after being immersed into PBS for 2 hours at 37°C. ZBCM refers to  $\beta$ PDMA-*b*-PDPA micelles.

The stability of the films in bacterial culture medium (LB broth) was also examined. Similar to stability experiments performed in PBS, 3-layer  $\beta$ PDMA-*b*-PDPA micelles/HA,  $\beta$ PDMA-*b*-PDPA micelles/TA and  $\beta$ PDMA-*b*-PDPA micelles/PSS films were immersed into bacterial culture medium at 37°C and at pH 7.5 and pH

5.5. Fractions retained at the surface after immersion into bacterial culture medium (Figure 19A and 19B) were similar to those obtained upon immersion into PBS (Figure 18A and 18B) for 1- and 2-hour periods.

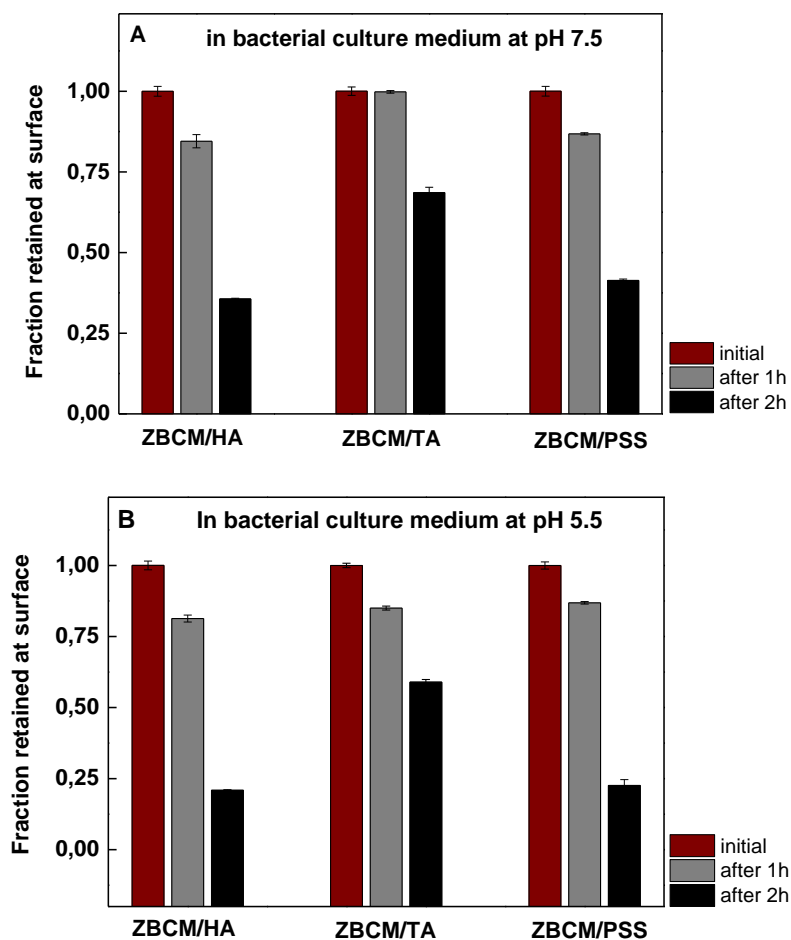


**Figure 19.** Fraction retained at the surface of  $\beta$ PDMA-*b*-PDPA micelles/HA,  $\beta$ PDMA-*b*-PDPA micelles/TA and  $\beta$ PDMA-*b*-PDPA micelles/PSS films after immersion into bacterial culture medium at pH 7.5 (A) and pH 5.5 (B) at 37°C. In all figures, the red columns correspond to fractions before immersion, the gray columns correspond to the fractions of the films retained at the surface after being immersed into bacterial culture medium for 1 hour at 37°C and the black columns correspond to the fractions of the films retained at the surface after being immersed into bacterial culture medium for 2 hours at 37°C. ZBCM refers to  $\beta$ PDMA-*b*-PDPA micelles.

No significant difference in stability between pH 7.5 and pH 5.5 was observed for the three films. Importantly, although all multilayers were deposited at pH 7.5, different extent of erosion from the surface was recorded upon immersion of the films in PBS even at pH 7.5. This may be correlated with the high salt content of PBS. PBS is a mixture composed of 0.002 M NaH<sub>2</sub>PO<sub>4</sub>, 0.008 M Na<sub>2</sub>HPO<sub>4</sub>, 0.0027 M KCl and 0.137 M NaCl. The salt content of PBS is significantly greater than that of 0.001 M phosphate buffer solution which was used for the preparation of deposition and rinsing solutions. The salt ions penetrating from PBS into the multilayers have possibly resulted in disruption of polymer ionic pairs within the multilayers and induced release of polymer chains from the surface. Among the three film systems,  $\beta$ PDMA-*b*-PDPA micelles/TA films showed the greatest stability. This was correlated with the dendrimer-like structure of TA enhancing the association among the layers. In addition, hydrogen bonding interactions between the phenolic hydroxyl groups of TA and sulfonate groups of  $\beta$ PDMA-coronae possibly provided additional stability to  $\beta$ PDMA-*b*-PDPA micelles/TA films. Indeed, the stability of  $\beta$ PDMA-*b*-PDPA micelles/TA films at pH 5.5 can be an indication of the contribution of hydrogen bonding interactions to the stability of multilayers despite the protonation of TA with decreasing pH and disruption of electrostatic association among  $\beta$ PDMA-*b*-PDPA micelles and TA ( $pK_{a,1} = \sim 6.5$  and  $pK_{a,2} = \sim 8$  for TA [160]).  $\beta$ PDMA-*b*-PDPA micelles and HA films, which could also potentially form hydrogen bonding interactions among the layers, did not present such a stability in PBS. It is possible that dendrimer-like structure of TA was highly critical for multilayer stability. Wan and Xu reported that the stability of poly(sulfobetaine methacrylate) (PSBMA)/TA films was greater than that of PSBMA/poly(acrylic acid) (PAA) films under identical conditions and mentioned the dendritic structure of TA as one of the causative factors [166,167].  $\beta$ PDMA-*b*-PDPA micelles/PSS films also showed greater stability in PBS compared to  $\beta$ PDMA-*b*-PDPA micelles/HA films. The greater molar concentration of the functional groups of PSS as well as greater hydrophobicity of PSS arising from the aromatic rings possibly rendered  $\beta$ PDMA-*b*-PDPA micelles/PSS films more stable than  $\beta$ PDMA-*b*-PDPA micelles/HA films. The effect of hydrophobicity on the stability of multilayer films has been reported earlier [168].

The stability of multilayers was also examined over long-term period. For that the multilayers were immersed into PBS and bacterial culture medium at pH 7.5 and 5.5 for 24 hour-period. However, in contrast to the stability of  $\beta$ PDMA-*b*-PDPA micelles/TA films in PBS for a 24-hour period (~ 82 % retained at pH 7.5 and ~ 72 % at pH 5.5), same multilayers were almost completely dissolved in bacterial culture medium within the same duration. Figure 20 shows the long-term stabilities of the multilayers in PBS solution at pH 7.5 (A) and pH 5.5 (B) and Figure 21 shows the long-term stabilities of the multilayers in bacterial culture medium at pH 7.5 (A) and pH 5.5 (B).

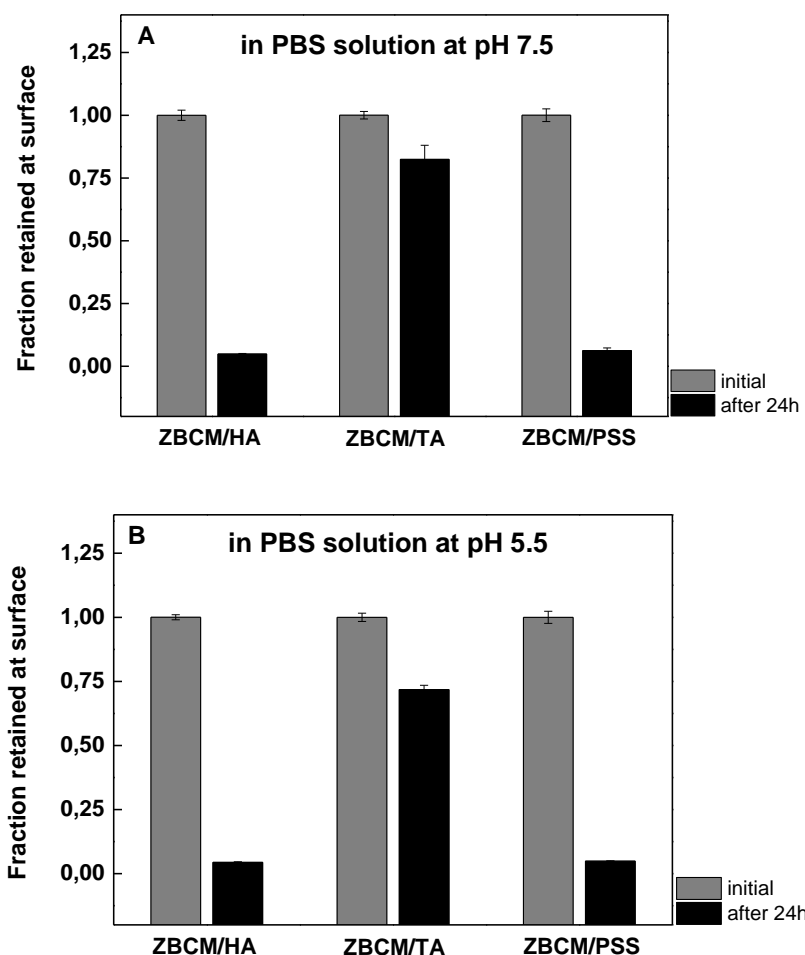


**Figure 20.** Fraction retained at the surface of  $\beta$ PDMA-*b*-PDPA micelles/HA,  $\beta$ PDMA-*b*-PDPA micelles/TA and  $\beta$ PDMA-*b*-PDPA micelles/PSS films after

immersion into PBS at pH 7.5 (A) and pH 5.5 (B) for 24 hours at 37°C. In all figures, the gray columns correspond to fractions before immersion, the black columns correspond to the fraction of the films retained at the surface after being immersed into PBS for 24 hours at 37°C. ZBCM refers to  $\beta$ PDMA-*b*-PDPA micelles.

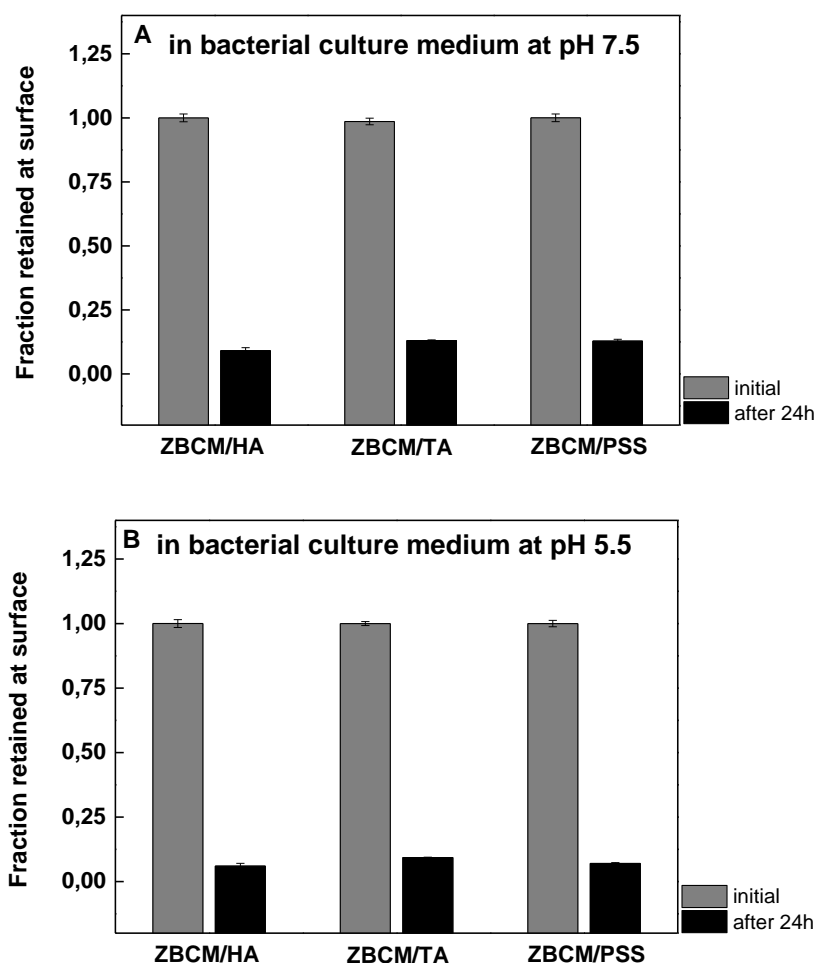


**Figure 21.** Fraction retained at the surface of  $\beta$ PDMA-*b*-PDPA micelles/HA,  $\beta$ PDMA-*b*-PDPA micelles/TA and  $\beta$ PDMA-*b*-PDPA micelles/PSS films after immersion into bacterial culture medium at pH 7.5 (A) and pH 5.5 (B) for 24 hours at 37°C. In all figures, the gray columns correspond to fractions before immersion, the black columns correspond to the fraction of the films retained at the surface after being immersed into bacterial culture medium for 24 hours at 37°C. ZBCM refers to  $\beta$ PDMA-*b*-PDPA micelles.

### 3.3. Protein Adsorption onto Multilayers

The adherence of BSA to 1-, 3-, and 5-layer films was analysed by immersing the substrates into PBS at pH 7.5 containing BSA at a concentration of 50 mg/mL. The UV absorbance values of three replicates of 1-, 3-, and 5-layer films of each system were recorded using the microBCA assay followed by a calculation of the BSA amount adsorbed at the surface using a calibration curve. As seen in Figure 22, 3-layer films showed the minimum amount of BSA adsorption in the  $\beta$ PDMA-*b*-PDPA micelles/HA and  $\beta$ PDMA-*b*-PDPA micelles/PSS systems.

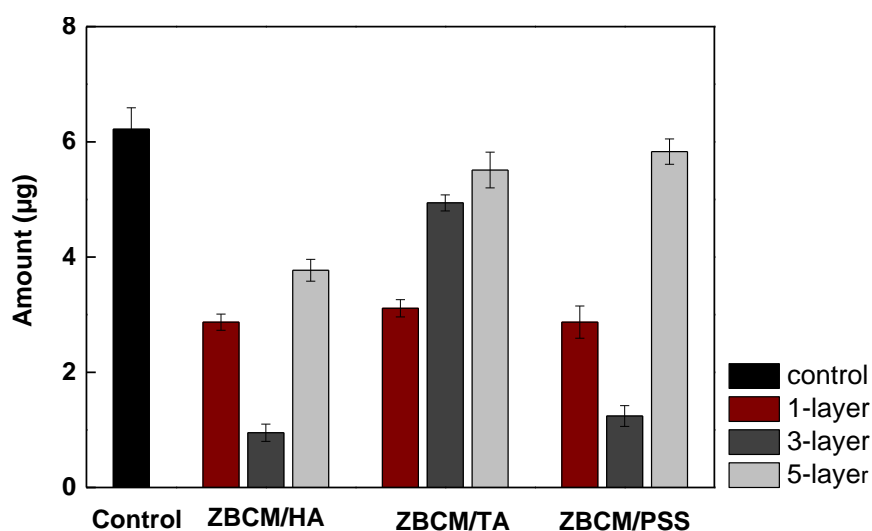


**Figure 22.** Protein adsorption onto modified or unmodified slides. Amount of BSA adsorbed onto  $\beta$ PDMA-*b*-PDPA micelles/HA,  $\beta$ PDMA-*b*-PDPA micelles/TA and  $\beta$ PDMA-*b*-PDPA micelles/PSS films at pH 7.5 and 37°C. For each film system, the first, second and third columns refer to the adsorption onto 1-, 3- and 5-layer films, respectively.

The lower BSA adsorption onto 3-layer  $\beta$ PDMA-*b*-PDPA micelles/HA and  $\beta$ PDMA-*b*-PDPA micelles/PSS films compared to 1-layer films can be explained with the higher surface coverage in 3-layer films. When a comparison is made between 3- and 5-layer films, the higher amount of BSA adsorption onto 5-layer films can be correlated with the decrease in the number of free zwitterionic units at the topmost layer due to higher interpenetration of the layers as they move away from the

substrate. Interestingly,  $\beta$ PDMA-*b*-PDPA micelles/TA demonstrated a different profile. The amount of BSA deposited at the surface increased with an increasing layer number of  $\beta$ PDMA-*b*-PDPA micelles/TA films. More importantly, the amount adsorbed onto 3-layer  $\beta$ PDMA-*b*-PDPA micelles/TA films were significantly higher than that adhered onto 3-layer  $\beta$ PDMA-*b*-PDPA micelles/HA or  $\beta$ PDMA-*b*-PDPA micelles/PSS films. This can result from the difference with the greater surface roughness of  $\beta$ PDMA-*b*-PDPA micelles/TA films, promoting BSA deposition at the surface due to increased surface area. Moreover, TA is partially ionized at pH 7.5, thus protonated phenolic hydroxyl groups could have also enhanced the adhesion of BSA on the surface. Hydroxyl groups have been reported to promote protein adsorption [167,169].

BSA adsorption at the surface of multilayers was also examined by ellipsometry. Figure 23 shows the evolution of film thickness before and after BSA adsorption onto 3-layer  $\beta$ PDMA-*b*-PDPA micelles/HA,  $\beta$ PDMA-*b*-PDPA micelles/TA and  $\beta$ PDMA-*b*-PDPA micelles/PSS films. The greatest change in thickness was observed for  $\beta$ PDMA-*b*-PDPA micelles/TA films upon immersion of the multilayers into 50 mg/mL BSA solution, which was slightly lower than the amount adsorbed onto the control substrate. 3-layer  $\beta$ PDMA-*b*-PDPA micelles/HA and 3-layer  $\beta$ PDMA-*b*-PDPA micelles/PSS films were similar in the changes of their thickness. The thickness change for  $\beta$ PDMA-*b*-PDPA micelles/HA was slightly lower than that for  $\beta$ PDMA-*b*-PDPA micelles/PSS. The results obtained from ellipsometry measurements were in good agreement with the results obtained from microBCA assay.

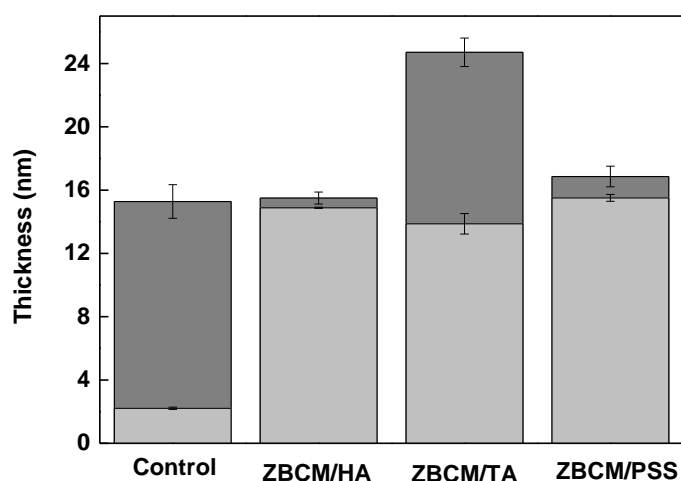


**Figure 23.** Evolution of film thickness after multilayers were immersed into BSA solution at pH 7.5 and 37°C. Light gray parts correspond to the initial thickness of the films. Dark gray parts correspond to the increment in film thickness upon BSA adsorption. Concentration of BSA solution was 50 mg/mL. ZBCM refers to  $\beta$ PDMA-*b*-PDPA micelles.

The anti-adhesive behaviour of 3-layer films against various proteins, i.e. Lysozyme, Casein and Ferritin were also evaluated using ellipsometry. Figure 24 shows the Lys (Lysozyme) adsorption profiles of 3-layer films of three different film systems again by the microBCA assay (A) and ellipsometry (B) techniques.

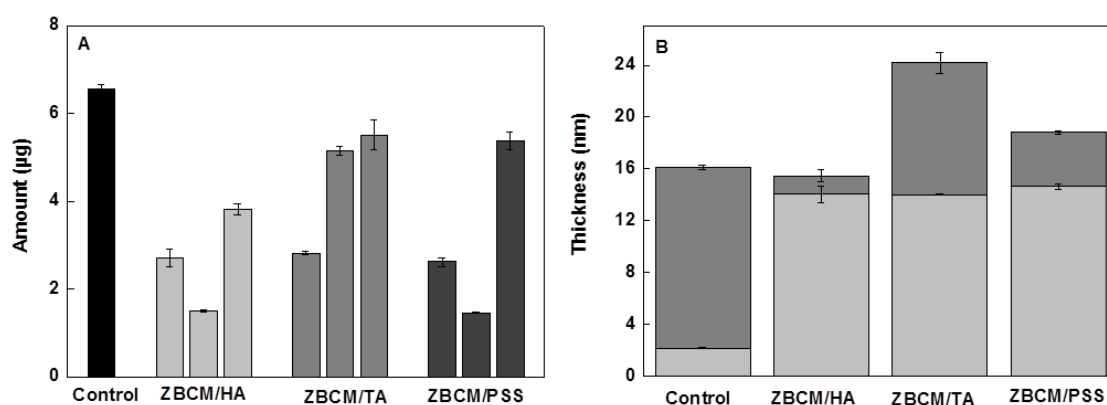


**Figure 24.** Adsorption of Lysozyme (Lys) onto  $\beta$ PDMA-*b*-PDPA micelles/HA,  $\beta$ PDMA-*b*-PDPA micelles/TA and  $\beta$ PDMA-*b*-PDPA micelles/PSS films at pH 7.5

and 37°C. Lys adsorption was determined by the microBCA assay. For each film system, the first, second and third columns refer to the adsorption onto 1-, 3- and 5-layer films, respectively (A). Ellipsometry analysis showing the evolution of film thickness after 3-layer films were immersed into Lys solution at pH 7.5 and 37°C. Light gray parts correspond to the initial thickness of the films. Dark gray parts correspond to the increment in film thickness upon BSA adsorption. Concentration of Lys solution was 25 mg/mL (B). ZBCM refers to  $\beta$ PDMA-*b*-PDPA micelles.

As with BSA adsorption onto various films, both techniques provided similar findings for Lys adsorption as well. Therefore, for the rest of the protein adhesion experiments, ellipsometry technique was used. Due to lower solubility Casein in PBS, for comparison, all data shown in Figure 25 were obtained by conducting the experiments using 25 mg/mL protein solutions prepared in PBS at pH 7.5.

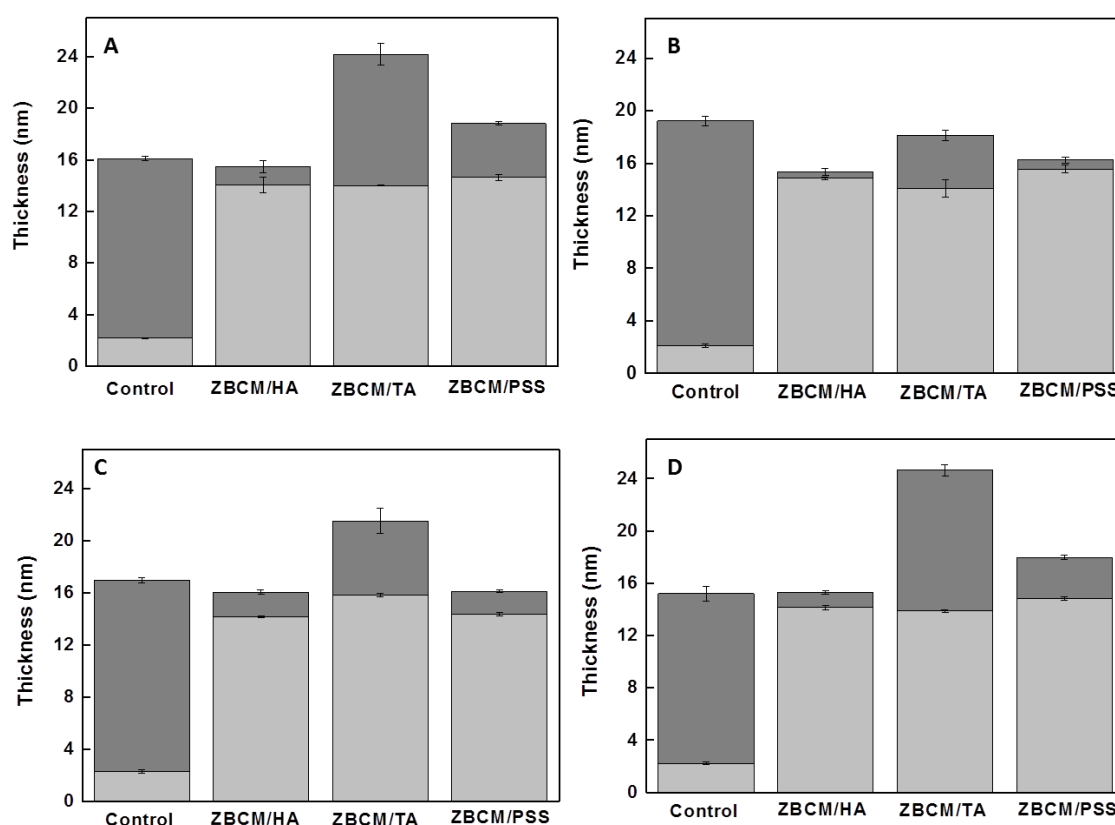


**Figure 25.** Evolution of film thickness after 3-layer films were immersed into Lysozyme (A), Casein (B), Ferritin (C) and BSA (D) solutions. Light gray parts

correspond to the initial thickness of the films. Dark gray parts correspond to the increment in film thickness upon protein adsorption. Concentrations of the protein solutions were all 25 mg/mL. ZBCM refers to  $\beta$ PDMA-*b*-PDPA micelles.

All types of films were anti-adhesive against the proteins compared to the controls. However, anti-adhesive behaviour of  $\beta$ PDMA-*b*-PDPA micelles/HA films was the most prominent possibly due to lower surface roughness and more hydrophilic nature of the multilayers. As discussed earlier,  $\beta$ PDMA-*b*-PDPA micelles/TA films attracted greater amount of protein to the surface. BSA and Lys adsorptions onto  $\beta$ PDMA-*b*-PDPA micelles/TA multilayers were greater than Ferritin and Casein. A comparison of the hydrophobicity plots of Ferritin, Casein, Lys and BSA (Figure 26) showed that Ferritin and Casein had more hydrophobic regions than Lys and BSA, which showed more hydrophilic regions. Therefore, Ferritin and Casein with more hydrophobic regions might have adhered less onto a hydrophilic surface. Protein adsorption onto surfaces is a complicated process. It depends on various factors, such as charge and chemical characteristic of the surface, electrostatic or physical interactions between the surface and protein, hydrophilic/hydrophobic nature of the surface as well as the protein [170]. The energy barrier for the displacement of water molecules from a hydrophilic surface is large. Therefore, in general, the driving force for the adsorption of proteins onto a hydrophilic surface is charge interactions among the surface and protein and surface-induced changes in protein conformation, providing the enough energy change to drive protein adsorption [171]. The zwitterionic outmost layer is neutral. However, the underlying polyanion layer could also contribute to interface chemistry, charge interactions, surface-induced changes in protein conformation and hydrophilic/hydrophobic regions of the protein and these properties may all be correlated with the greater adsorption of Lys and BSA onto multilayers. Understanding the differences in the amount of adsorption of various proteins onto the same surface requires more detailed studies.

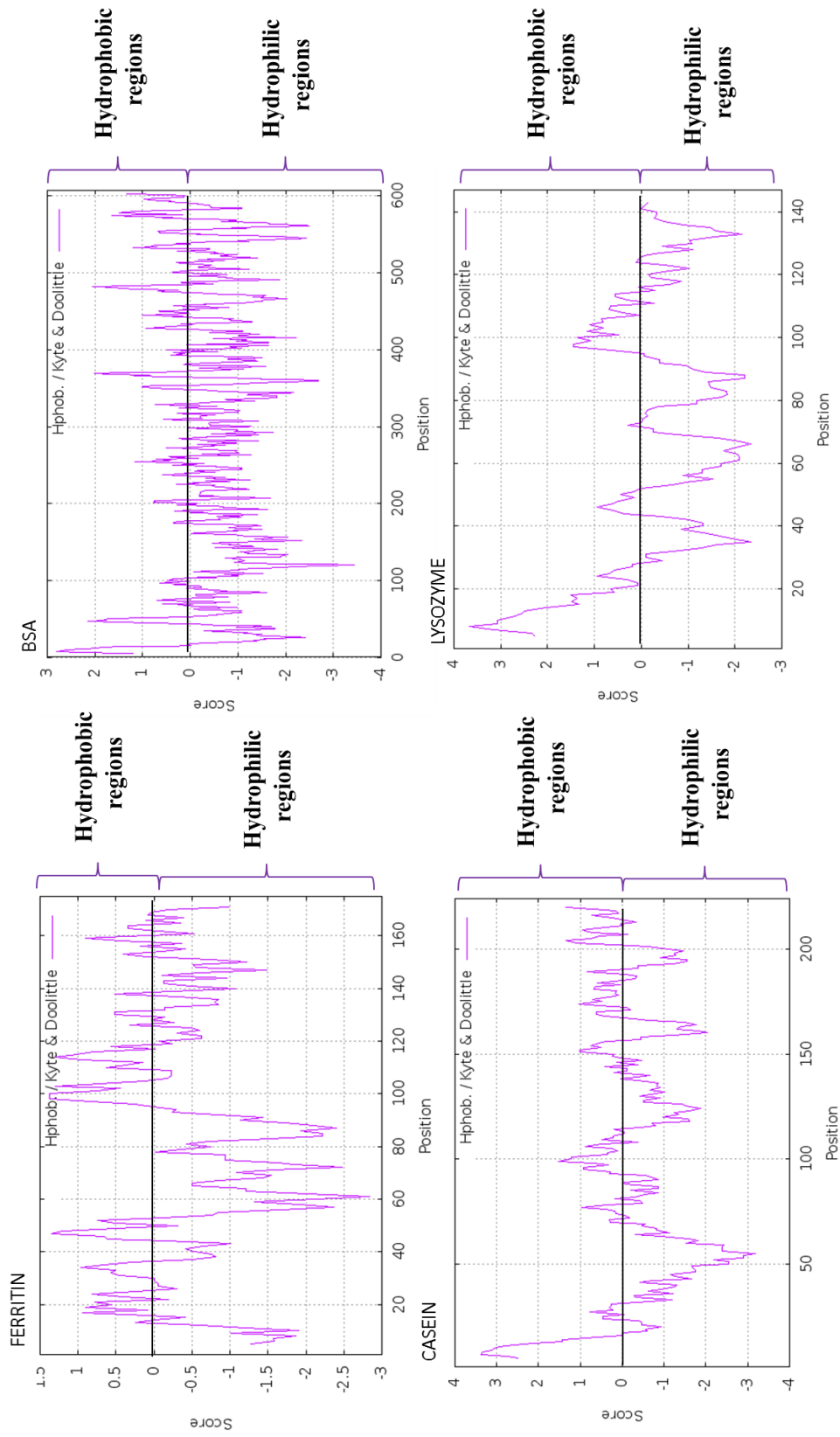


**Figure 26.** Hydrophobicity plots of Ferritin, BSA, Casein, and Lysozyme.

Figure 27 shows the effect of long term incubation of the multilayers in protein solution on protein adsorption. BSA was selected as a model protein. 3-layer films of all types were immersed into 25 mg/mL BSA solution (prepared in PBS) at 37°C for 24 hours.

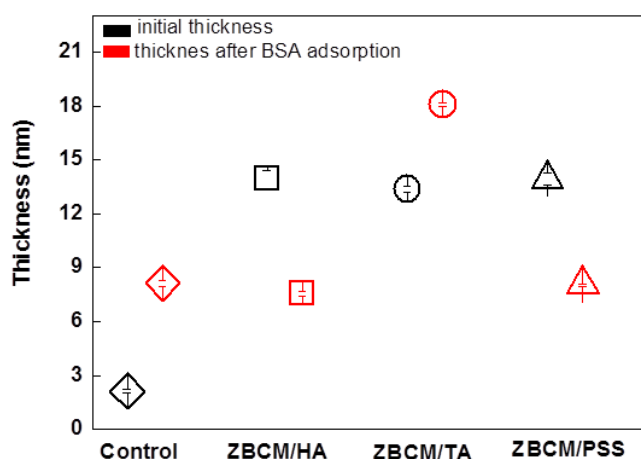


**Figure 27.** Evolution of film thickness after immersion of control (rhombus), 3-layer  $\beta$ PDMA-*b*-PDPA micelles/HA (square), 3-layer  $\beta$ PDMA-*b*-PDPA micelles/TA (circle) and 3-layer  $\beta$ PDMA-*b*-PDPA micelles/PSS (triangle) into 25 mg/mL BSA solution at pH 7.5 and 37°C for 24 hours. ZBCM refers to  $\beta$ PDMA-*b*-PDPA micelles.

$\beta$ PDMA-*b*-PDPA micelles/TA films had the greatest adsorption of BSA on the surface.  $\beta$ PDMA-*b*-PDPA micelles/HA and  $\beta$ PDMA-*b*-PDPA micelles/PSS films had thickness values similar to that of the control surface, pointing out dissolution of the multilayers, which possibly resulted in loss of the anti-adhesive behaviour of these surfaces. These results are in good agreement with the long-term (24 hours) stability data of the multilayers in PBS (Figure 20) where  $\beta$ PDMA-*b*-PDPA micelles/TA films were observed to be the most stable in PBS among the three film systems.

### 3.4. Anti-adhesive and Anti-bacterial Properties of the Multilayers

#### 3.4.1. Bacterial Anti-adhesive Properties of Multilayers

To determine the adherence of bacteria to the different films, an *E. coli* K-12 strain transformed with a GFP expressing plasmid was used (Figure 26).

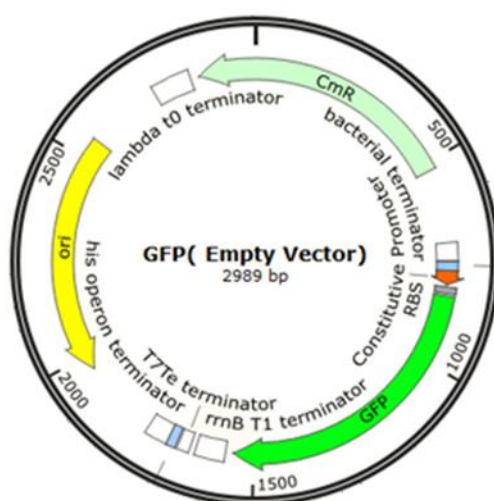


**Figure 28.** Plasmid map of pSB1C3 showing presence of the GFP gene. <http://parts.igem.org/Part:pSB1C3>.

It was observed that both  $\beta$ PDMA-*b*-PDPA micelles/HA and  $\beta$ PDMA-*b*-PDPA micelles/PSS systems allowed minimal adherence of bacteria as shown by the remarkably low GFP signal compared to the control uncoated sample (Figure 29). On the other hand, the  $\beta$ PDMA-*b*-PDPA micelles/TA films showed higher adherence to *E. coli* and this adherence increased as the number of layers in the sample increased. Figure 30 shows the quantification of fluorescence intensity of the images calculated. Quantitative representation of the fluorescent GFP signals from the bacteria adhering to different surfaces as determined by Image J.

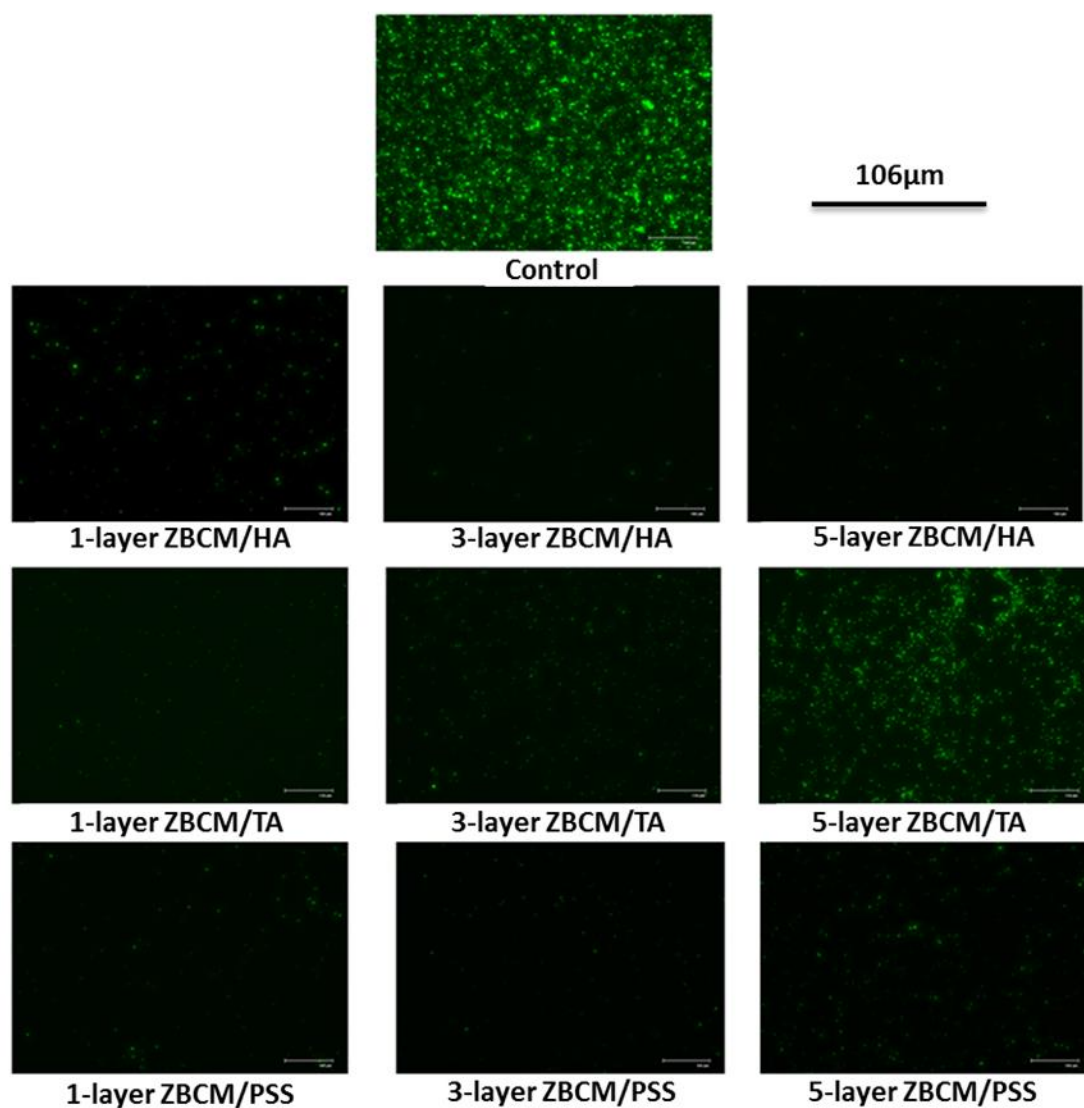


**Figure 29.** Green fluorescence images of blank glass slide (control) and 1-, 3-, 5-layer  $\beta$ PDMA-*b*-PDPA micelles/HA,  $\beta$ PDMA-*b*-PDPA micelles/TA and  $\beta$ PDMA-*b*-PDPA micelles/PSS coated glass slides after 1 hour incubation with *Escherichia coli* ATCC 700926. ZBCM refers to  $\beta$ PDMA-*b*-PDPA micelles.

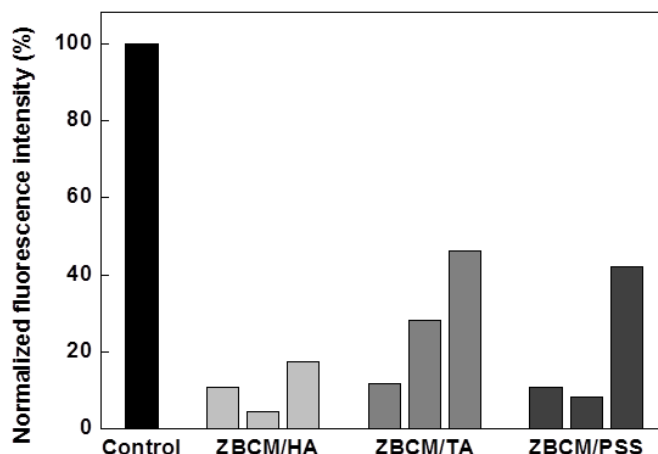
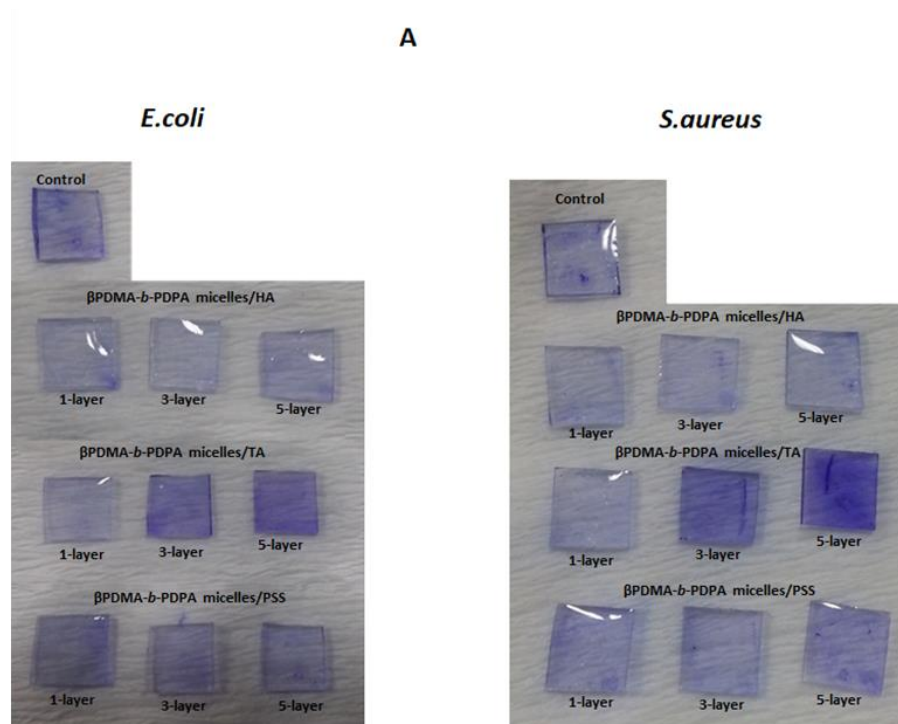
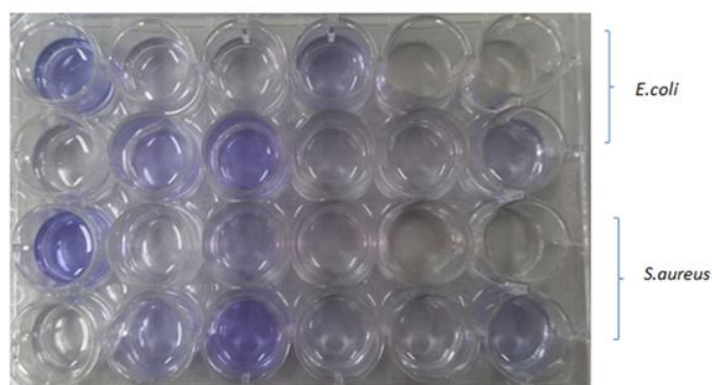


**Figure 30.** Quantitative representation of the fluorescent GFP signals from the bacteria adhering to different surfaces as determined by Image J. For each film system, the first, second and third columns refer to the fluorescence intensity obtained from microscopic images of 1-, 3- and 5-layer films, respectively.

Transformation of plasmids into *S. aureus* is technically challenging due to the presence of Restriction Modification systems that restrict entry of foreign DNA [172]. Therefore, crystal violet dye was used to stain adherent *S.aureus* as well as *E.coli* on the different surfaces ( $\beta$ PDMA-*b*-PDPA micelles/HA,  $\beta$ PDMA-*b*-PDPA micelles/TA and  $\beta$ PDMA-*b*-PDPA micelles/PSS) with a differing number of layers. Figure 31A shows the macroscopic images of the slides after crystal violet staining. To quantify the signal, we washed the bacteria with a decolorizing solution for over 5 min to remove the dye from both bacterial strains. Figure 31B shows the macroscopic images of the decolorization solution. The color was then quantified using a spectrophotometer at 590nm. Statistically significant reduction in adherence on all surfaces was observed; however, the anti-adhesive nature of  $\beta$ PDMA-*b*-PDPA micelles/TA films at 3 and 5 layers was weaker than the other surfaces. Figure 32 shows the normalized absorbance of the crystal violet staining solution after decolorization process for *E.coli* and *S.aureus*.



**B**



control	1-layer ZBCM/HA	3-layer ZBCM/HA	5-layer ZBCM/HA		
1-layer ZBCM/TA	3-layer ZBCM/TA	5-layer ZBCM/TA	1-layer ZBCM/PSS	3-layer ZBCM/PSS	5-layer ZBCM/PSS
control	1-layer ZBCM/HA	3-layer ZBCM/HA	5-layer ZBCM/HA		
1-layer ZBCM/TA	3-layer ZBCM/TA	5-layer ZBCM/TA	1-layer ZBCM/PSS	3-layer ZBCM/PSS	5-layer ZBCM/PSS

**Figure 31.** Images of crystal-violet stained blank or coated substrates incubated with *Staphylococcus aureus* ATCC 29213 and *Escherichia coli* ATCC 8739 before (A) and after (B) decolorization process. ZBCM refers to  $\beta$ PDMA-*b*-PDPA micelles.

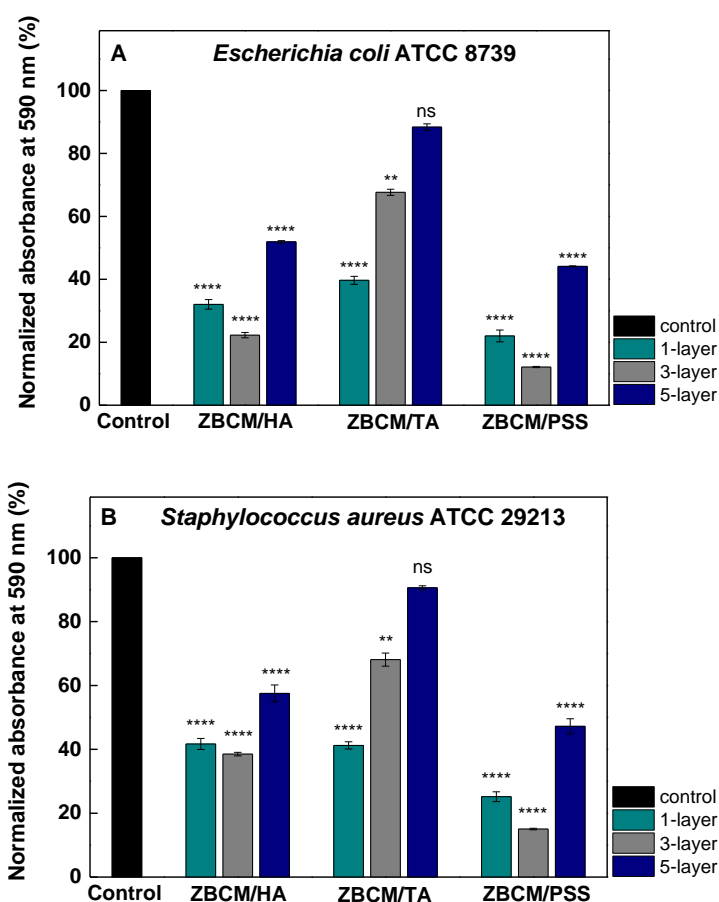


**Figure 32.** Normalized absorbance of the crystal violet staining solution obtained after decolorization of *E.coli* (A) and *S. aureus* (B) adhered to control glass slides or glass slides coated with 1-, 3-, 5- layer  $\beta$ PDMA-*b*-PDPA micelles/HA,  $\beta$ PDMA-*b*-PDPA micelles/TA and  $\beta$ PDMA-*b*-PDPA micelles/PSS after 1 hour of incubation. For each film system, the first, second and third columns refer to data obtained from 1-, 3- and 5-layered films, respectively. ZBCM refers to  $\beta$ PDMA-*b*-PDPA micelles.

To further support the bacterial adhesion data, an agar plating method was carried out with both *S.aureus* and *E. coli* on 1-, 3-, and 5-layer films of  $\beta$ PDMA-*b*-PDPA micelles/HA,  $\beta$ PDMA-*b*-PDPA micelles/TA and  $\beta$ PDMA-*b*-PDPA micelles/PSS. All films had zwitterionic  $\beta$ PDMA-*b*-PDPA micelles as the outmost layer. It was observed that the 5-layered films showed the least bacterial anti-adhesive property compared to 1-layer and 3-layered films, which showed moderate anti-adhesive properties (Figure 33).

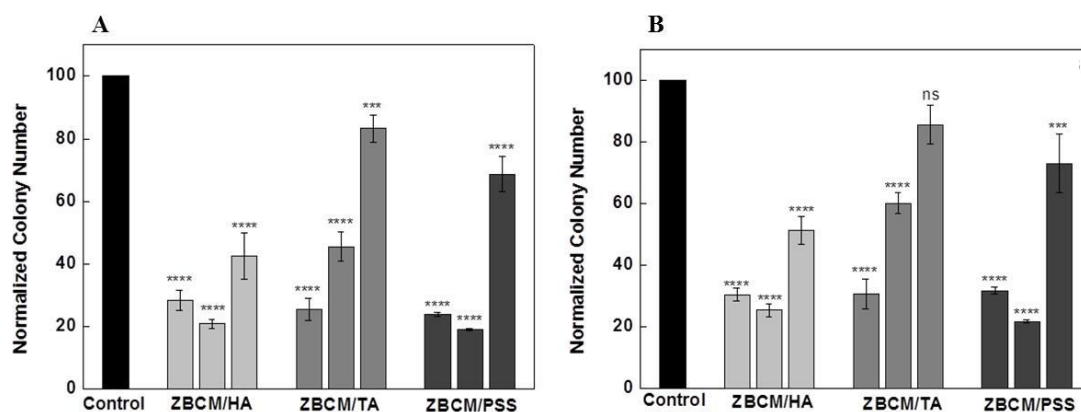


**Figure 33.** Viable bacterial count obtained by agar plating method with blank glass slide (control) and 1-, 3-, 5- layer  $\beta$ PDMA-*b*-PDPA micelles/HA,  $\beta$ PDMA-*b*-PDPA micelles/TA and  $\beta$ PDMA-*b*-PDPA micelles/PSS coated glass slides after 1 hour incubation with *E.coli* (A) and *S.aureus* (B). For each film system, the first, second and third columns refer to the 1-, 3- and 5-layer films, respectively. Colony numbers for each control group was considered as 100% and the data for the experimental groups were normalized to the value assumed for the control. Error bars represent standard error (SE) of mean. ZBCM refers to  $\beta$ PDMA-*b*-PDPA micelles.

This is in agreement with the data shown in Figure 29, where HA containing films showed the highest anti-adhesiveness while TA containing films showed the least. Importantly, bacterial anti-adhesive results were in complete agreement with the protein adhesion data (Figures 22-25), indicating that the interaction of surface molecules on the bacteria with the functional groups on the 1-layer/multilayered surfaces could be a mechanism of bacterial adherence [10,173,174]. Modification of the surface with the different substrates (HA, TA or PSS) could have interfered with this interaction [175–177]. The resistance to protein adherence and anti-adhesive properties of a surface modified with zwitterionic poly(sulfobetaine methacrylate) has been correlated before by Cheng et al. [60,178]. However, it has also been reported that a surface which showed anti-adhesive behaviour against proteins had not necessarily exhibited anti-adhesive characteristic against bacteria [179]. In this study, resistance to protein adhesion (at least for the proteins under investigation)

was in good agreement with the bacterial anti-adhesive behaviour of the surfaces against *E. coli* and *S.aureus*.

Figures 34 and 35 show the long-term bacterial adherence studies using GFP expressing *E.coli* K12. The results showed that the adhesiveness of all surfaces became similar after 24 hours of incubation at 37°C (between 53 and 60% with respect to the control as 100%). This means that the surfaces containing HA and PSS (that were highly anti-adhesive at 1 hour, see Figure 29) were unstable at 24 hours and therefore remarkably increased in their ability to adhere to bacteria. The TA containing films, on the other hand, were already highly adherent at 1 hour. However, since the surface was relatively more stable, the adhesiveness of bacteria remained the same even after 24 hours of incubation.

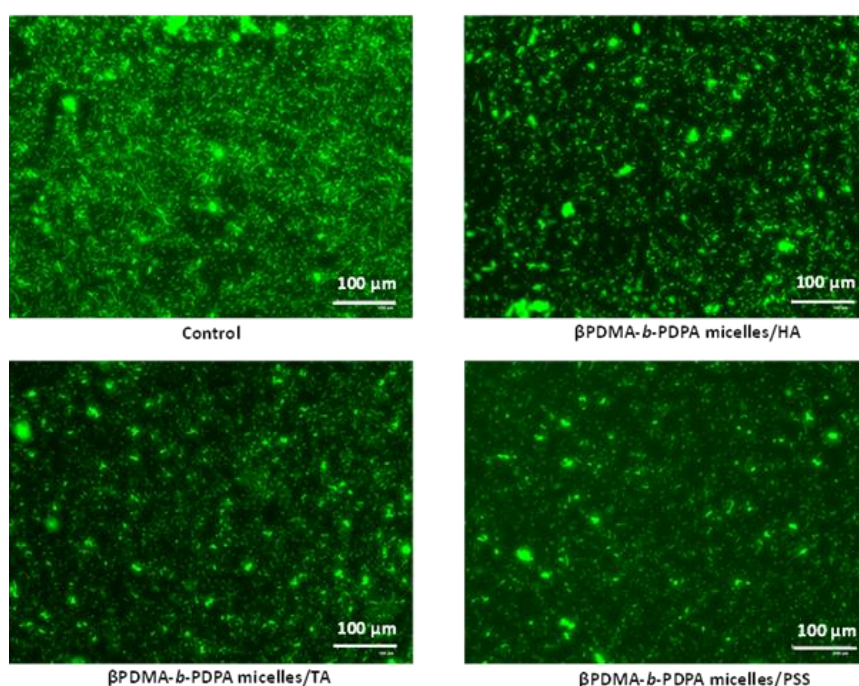


**Figure 34.** Long term (24 hour) bacterial adhesion. Adherence of GFP expressing *E.coli* K12 to glass slides (control) or glass slides coated with 3-layers of βPDMA-b-PDPA micelles/HA, βPDMA-b-PDPA micelles/TA and βPDMA-b-PDPA micelles/PSS.

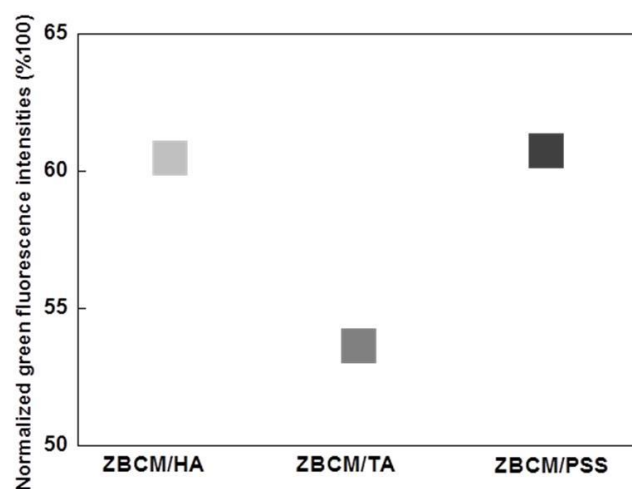


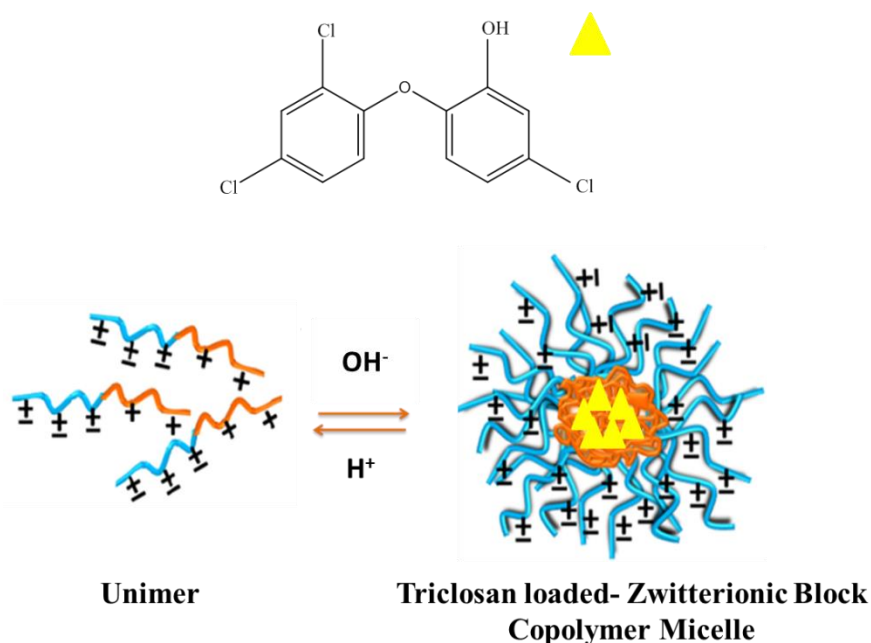
**Figure 35.** Long term (24 hour) bacterial adhesion. Quantitative representation of the fluorescent GFP signals from the bacteria adhering to 3-layer  $\beta$ PDMA-*b*-PDPA micelles/HA,  $\beta$ PDMA-*b*-PDPA micelles/TA and  $\beta$ PDMA-*b*-PDPA micelles/PSS coated substrates as determined by Image J. The control substrate (blank glass slide) was assumed as 100 % and the fluorescence intensities obtained from 3-layer films were normalized to the value assumed for the control. ZBCM refers to  $\beta$ PDMA-*b*-PDPA micelles.

These data are also in agreement with the long-term protein adsorption behaviour of the films (Figure 27).

### 3.4.2. Anti-bacterial activity of multilayers

Block copolymer micelles are ideal carriers for hydrophobic functional molecules due to their hydrophobic core regions. Block copolymer micelles with a polybasic core are of interest specifically for the delivery of hydrophobic molecules at moderately acidic conditions. Therefore, block copolymer micelles that have a polybasic core and dissolve at moderately acidic pH to release the cargo are important for anti-bacterial applications due to local pH drops in the body at an infectious site. To determine whether the block copolymer micelles used in the current study could be modified to show anti-bacterial function against *E. coli* ATCC 8739, the anti-bacterial agent Triclosan was loaded into the micellar cores and

multilayers were prepared using Triclosan embedded  $\beta$ PDMA-*b*-PDPA micelles as building blocks. The anti-bacterial activity of  $\beta$ PDMA-*b*-PDPA micelles/HA,  $\beta$ PDMA-*b*-PDPA micelles/TA and  $\beta$ PDMA-*b*-PDPA micelles/PSS multilayers was assessed at neutral and moderately acidic conditions using a modified version of Kirby-Bauer test. The amount of Triclosan released from the multilayers was deduced by comparing the diameters of the “zone of inhibition” around the substrates coated with 5-layer films placed on agar. As control substrates, multilayers composed of unloaded  $\beta$ PDMA-*b*-PDPA micelles were prepared. As seen in Figure 36, no clear zone of inhibition of bacterial growth was observed for the films of unloaded micelles. However, 5-layer films of all types of Triclosan loaded  $\beta$ PDMA-*b*-PDPA micelles showed a clear zone of inhibition of bacterial growth on MH agar at both pH 7.5 and pH 5.5, indicating an antibacterial effect on *E. coli* ATCC 8739. Scheme 5 shows the chemical structure of Triclosan, 5-chloro-2-(2,4-dichlorophenoxy) phenol and representation for Triclosan loaded  $\beta$ PDMA-*b*-PDPA micelles.



**Scheme 5.** Chemical structure of Triclosan and representation for Triclosan loaded  $\beta$ PDMA-*b*-PDPA micelles.

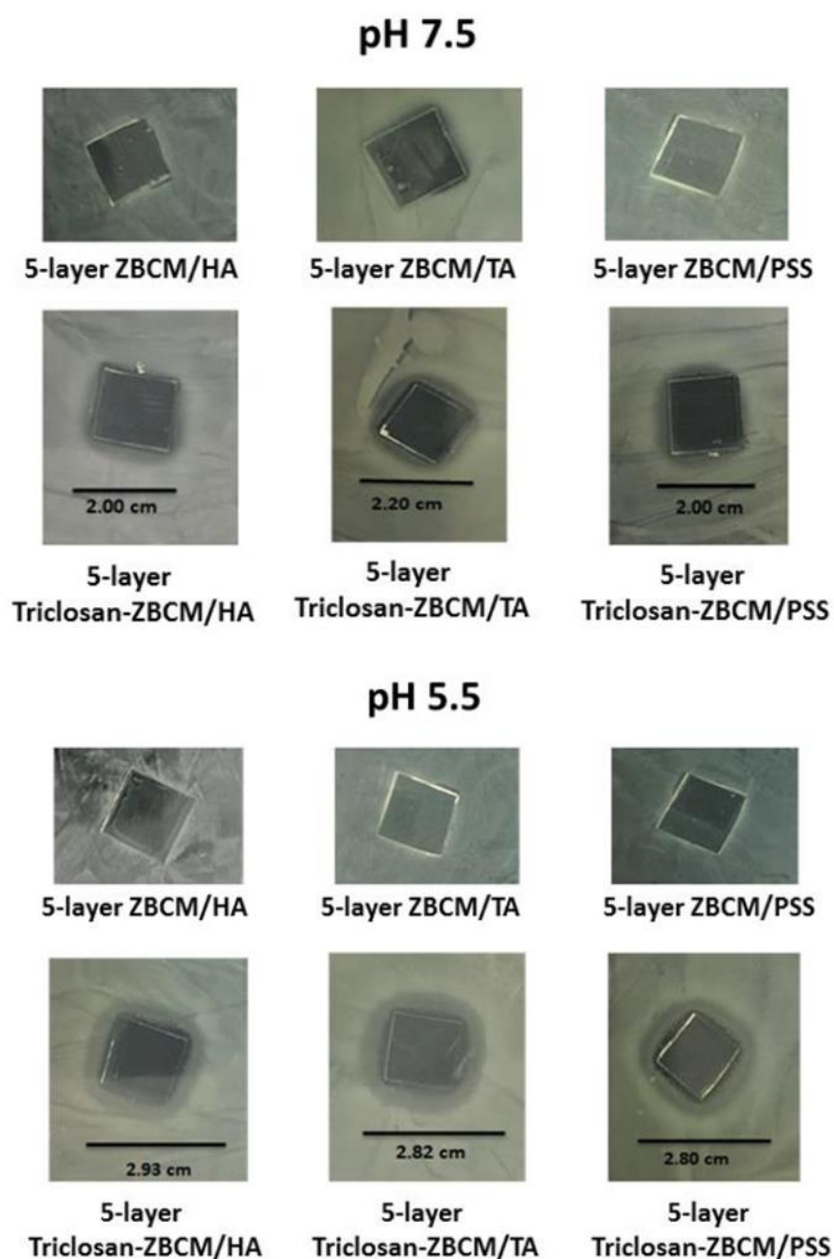


**Figure 36.** Kirby-Bauer tests from 5- layer Triclosan loaded  $\beta$ PDMA-*b*-PDPA micelles/HA,  $\beta$ PDMA-*b*-PDPA micelles/TA and Triclosan loaded  $\beta$ PDMA-*b*-PDPA micelles/PSS films. 5-layer films of unloaded  $\beta$ PDMA-*b*-PDPA micelles at pH 7.5 and pH 5.5 were used as control. ZBCM refers to  $\beta$ PDMA-*b*-PDPA micelles.

Preliminary experiments indicated that there was no difference in the growth rate of the bacteria in MH broth at pH 7.5 or at 5.5; additionally, treatment of *E. coli* with

50 $\mu$ g/ml Triclosan resulted in comparable cell death at both pH values. Importantly, a larger zone was observed at pH 5.5 due to protonation of the tertiary amino groups of PDPA-core blocks and pH-induced release of Triclosan. Figure 37 shows the diameter of the clear zones for Triclosan loaded 5-layer  $\beta$ PDMA-*b*-PDPA micelles/HA,  $\beta$ PDMA-*b*-PDPA micelles/TA and  $\beta$ PDMA-*b*-PDPA micelles/PSS films at pH 7.5 and pH 5.5. Of note, the zone of inhibition was larger for 5-layer films than that for 3-layer films specifically at pH 5.5 most likely due to higher number of Triclosan loaded  $\beta$ PDMA-*b*-PDPA micelles at the surface resulting in greater release of Triclosan (data not shown).

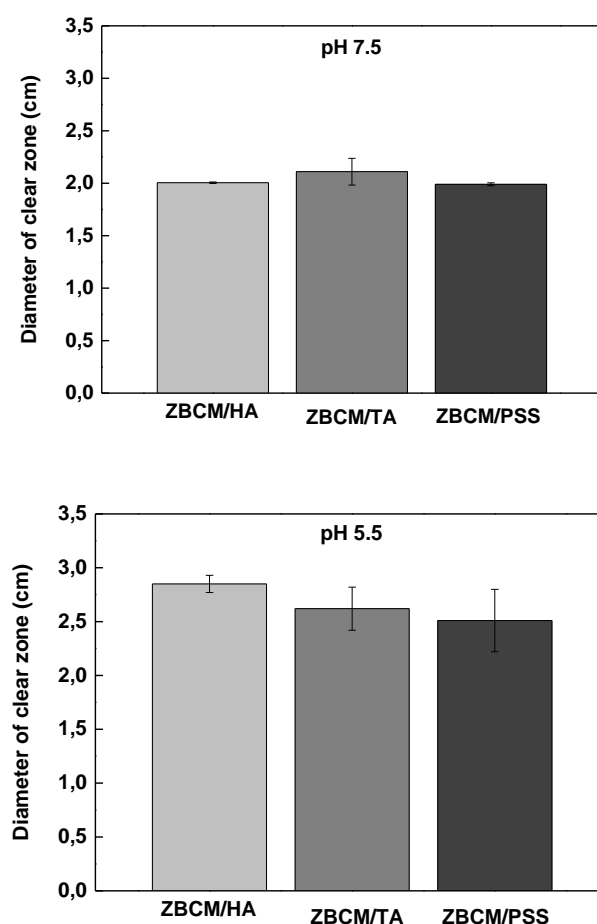


**Figure 37.** Diameter of clear zones for Triclosan loaded 5-layer  $\beta$ PDMA-*b*-PDPA micelles/HA, Triclosan loaded  $\beta$ PDMA-*b*-PDPA micelles/TA and  $\beta$ PDMA-*b*-PDPA micelles/PSS films at pH 7.5 and pH 5.5. ZBCM refers to  $\beta$ PDMA-*b*-PDPA micelles.

### 3.5. Osteoblast-like Cell (SaOS-2) Adhesion Properties of Multilayers

Anti-bacterial and anti-adhesive surface coatings for biomaterials are the most ideal coatings to prevent biofilm associated infections [180]. However, for an implant to be functional in the body, the required surface interactions between cells in the body fluid and implant surface should occur [181]. Therefore, surfaces that are anti-adhesive for bacteria and at the same time, adhesive for mammalian cells like fibroblasts or osteoblasts would be the ideal for biomaterial coating [182]. To understand whether bacterial anti-adhesive surfaces used in this study were adhesive for mammalian cells, the human osteoblast-like SaOS-2 cells were used. Osteoblast-like SaOS-2 cells were chosen, because of the usage of zwitterionic polymers for knee and bone replacement surgeries, due to their good lubrication properties. The 1-, 3- and 5- layer  $\beta$ PDMA-*b*-PDPA micelles/HA,  $\beta$ PDMA-*b*-PDPA micelles/TA and  $\beta$ PDMA-*b*-PDPA micelles/PSS multilayers were prepared on glass substrates and incubated with SaOS-2 cells for 4h as described. The uncoated glass was used as a control. To visualize the adherent cells on the different substrates, cells were incubated with the lipophilic dye, 3,3'-dioctadecyl-5,5'-di(4-sulfophenyl) oxacarbocyanine sodium salt (SP-DiOC<sub>18</sub>(3)) that can bind to the plasma membrane. Figure 38 shows the fluorescent microscopy images of the various surfaces incubated with SaOS-2 cells for 4h.

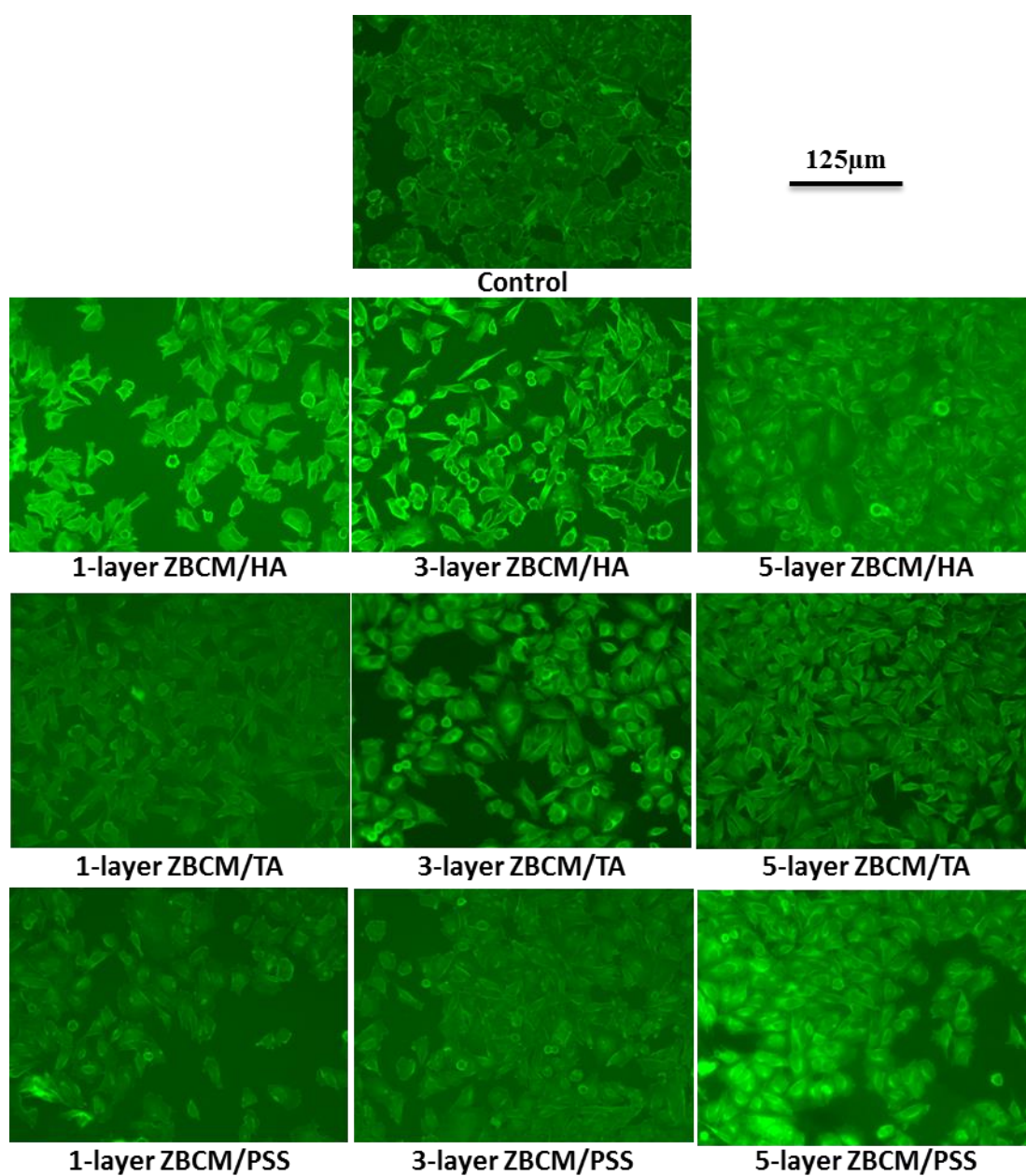


**Figure 38.** Fluorescence images of blank glass slide (control) and 1-, 3-, 5- layer  $\beta$ PDMA-*b*-PDPA micelles/HA,  $\beta$ PDMA-*b*-PDPA micelles/TA and  $\beta$ PDMA-*b*-PDPA micelles/PSS coated glass slides after 1 hour incubation with SaOS-2 cells. ZBCM refers to  $\beta$ PDMA-*b*-PDPA micelles.

It was observed that all surfaces allowed the adsorption and spreading of the cells after 4h of incubation. In fact the substrates allowed the SaOS-2 cells to remain adsorbed, survive and proliferate even after 24h of incubation (data not shown). The

fact that there was no significant difference between the adhesiveness of the cells indicated that, the difference of the surfaces in terms of their morphology or chemical functional groups may not be the major factor for mammalian cell adherence. This is in contrast to the bacteria adhesion where the functional groups and morphology of the surfaces were seen to play a major role. This result can be because of the differences in the mechanisms of bacterial and mammalian cell attachment and surface protein interactions [183]. Being the extracellular matrix component of HA, the high adhesiveness of  $\beta$ PDMA-*b*-PDPA micelles/HA multilayers towards SaOS-2 cells was expected [184]. However, the adhesiveness of  $\beta$ PDMA-*b*-PDPA micelles/TA and  $\beta$ PDMA-*b*-PDPA micelles/PSS multilayers, independent of the layer number, might indicate a different mechanism for adhesion. Although zwitterionic polymers are known to exert good anti-fouling behavior against bacteria as well as mammalian cells [183,185], the reported studies usually assumed to have complete charge neutrality within the polymer [185]. As shown in Figure 12C, the overall charge of the  $\beta$ PDMA-*b*-PDPA micelles in the solution were not exactly zero. In addition, as seen in the AFM analysis, the  $\beta$ PDMA-*b*-PDPA micelles underwent spreading and interpenetrating with the polyanion on the surface. These may result in the formation of free sulfonate groups on the surface which can be attractive to  $\text{Ca}^{2+}$  ions. Similar strategy for the adhesive behavior of phosphate groups on polyphosphobetaine was reported by Miura et al [156]. The importance of calcification in osteogenesis, bone formation, was reported in the studies of Liu and Xu [186]. Therefore, the effect of  $\text{Ca}^{2+}$  deposition on the surfaces may promote the adhesion of osteoblast cells, even in monolayer coated  $\beta$ PDMA-*b*-PDPA micelles. Although the exact mechanism behind the different anti-fouling profile of  $\beta$ PDMA-*b*-PDPA micelle multilayers remains to be established, the adhesive property of the substrates towards SaOS-2 cells is a highly desirable characteristic that will be necessary to promote tissue-implant interaction and implant acceptance [182].



## CHAPTER 4

### CONCLUSIONS

In this study block copolymer micelles were prepared through pH-induced self-assembly of  $\beta$ PDMA-*b*-PDPA in aqueous solution at pH 7.5 and 25°C. These micelles were then used as building blocks to modify the surface of substrates forming ultra-thin films composed of 1-, 3- and 5-layers. For the preparation of multilayers, HA, TA or PSS were used as the polyanion and layers were deposited in a LbL fashion for 3 or 5 layers to generate ultra-thin films. It is observed that 3-layer  $\beta$ PDMA-*b*-PDPA micelles/HA and  $\beta$ PDMA-*b*-PDPA micelles/PSS films were anti-adhesive against various proteins such as BSA, Lys, Ferritin and Casein. The anti-adhesiveness of 3-layer  $\beta$ PDMA-*b*-PDPA micelles/HA and  $\beta$ PDMA-*b*-PDPA micelles/PSS films was found to be greater than that of 1-layer films of the same polymer pairs due to higher surface coverage by  $\beta$ PDMA-*b*-PDPA micelles. Anti-adhesive behaviour of  $\beta$ PDMA-*b*-PDPA micelles/HA and  $\beta$ PDMA-*b*-PDPA micelles/PSS films diminished as the layer number increased from 3 to 5, possibly due to greater extent of interpenetration of the layers while moving away from the surface resulting in lower number of free zwitterionic units at the topmost layer. Interestingly, protein adsorption onto 1-, 3- and 5- layer  $\beta$ PDMA-*b*-PDPA micelles/TA films exhibited a different profile. The layers became more adhesive when the number of layers was increased and more importantly, the amount of protein adsorbed onto  $\beta$ PDMA-*b*-PDPA micelles/TA films was significantly greater than that adsorbed onto  $\beta$ PDMA-*b*-PDPA micelles/HA and  $\beta$ PDMA-*b*-PDPA micelles/PSS films. The difference was correlated with the greater surface roughness of  $\beta$ PDMA-*b*-PDPA micelles/TA films and hydroxyl groups of TA which possibly increased the protein adsorption at the surface. Bacterial anti-adhesive tests were performed against a model Gram-negative bacterium, *Escherichia coli* and a model

Gram-positive bacterium, *Staphylococcus aureus*. Results obtained for both bacteria were in excellent agreement with protein resistant behaviour of the films. Anti-adhesive behaviour was found to be lost when multilayers were exposed to protein solutions for long-term. However, we showed that by taking advantage of the hydrophobic micellar cores, these micelles could be loaded with an anti-bacterial agent Triclosan and multilayers constructed using Triclosan loaded  $\beta$ PDMA-*b*-PDPA micelles exhibited anti-bacterial activity in the long term. The anti-bacterial activity of the films was found to increase at moderately acidic pH due to protonation of the tertiary amino groups of PDPA and dissolution of the micellar cores. The adhesiveness of the multilayers was compared in terms of osteoblast-like cell line using SaOS-2. All multilayers were shown to exhibit fouling properties. In contrast to anti-adhesive behaviour, no significant difference in anti-bacterial activity and adhesiveness against SaOS-2 cells was recorded between the different types of films. The difference in the behavior of the adhesiveness of the surfaces was correlated to different adhesion mechanisms of bacterial and eukaryotic cells. The HA, due to being an extracellular matrix component, could be improved the adhesiveness of  $\beta$ PDMA-*b*-PDPA micelles/HA multilayers towards SaOS-2 cells.  $\beta$ PDMA-*b*-PDPA micelles/TA multilayers, which were already not showing anti-adhesiveness against bacteria, again were not anti-adhesive for SaOS-2 cells, could be because of greater surface roughness of  $\beta$ PDMA-*b*-PDPA micelles/TA films and hydroxyl groups of TA.  $\beta$ PDMA-*b*-PDPA micelles/PSS multilayers were adhesive for SaOS-2 cells could be explained by the increased electrostatic interactions promoting deposition of calcium ion and resulted in SaOS-2 adhesion.

## REFERENCES

- [1] N. Hadjesfandiari, K. Yu, Y. Mei, J.N. Kizhakkedathu, Polymer brush-based approaches for the development of infection-resistant surfaces, *J. Mater. Chem. B*. 2 (2014) 4968. doi:10.1039/C4TB00550C.
- [2] D. Davies, Understanding biofilm resistance to antibacterial agents, *Nat. Rev. Drug Discov*. 2 (2003) 114–122. doi:10.1038/nrd1008.
- [3] N. Rabin, Y. Zheng, C. Opoku-Temeng, Y. Du, E. Bonsu, H.O. Sintim, Biofilm formation mechanisms and targets for developing antibiofilm agents, *Future Med. Chem*. 7 (2015) 493–512. doi:10.4155/fmc.15.6.
- [4] O.J.G.M. Goor, J.E.P. Brouns, P.Y.W. Dankers, Introduction of anti-fouling coatings at the surface of supramolecular elastomeric materials via post-modification of reactive supramolecular additives, *Polym. Chem*. 8 (2017) 5228–5238. doi:10.1039/C7PY00801E.
- [5] E.F. Leonard, L. Vroman, Is the Vroman effect of importance in the interaction of blood with artificial materials?, *J. Biomater. Sci. Polym. Ed*. 3 (1991) 95–107. doi:10.1163/156856292X00105.
- [6] P.C. Bogino, M. de las M. Oliva, F.G. Sorroche, W. Giordano, The Role of Bacterial Biofilms and Surface Components in Plant-Bacterial Associations, *Int. J. Mol. Sci*. 14 (2013) 15838–15859. doi:10.3390/ijms140815838.
- [7] C. Berne, A. Ducret, G.G. Hardy, Y. V Brun, Adhesins Involved in Attachment to Abiotic Surfaces by Gram-Negative Bacteria, *Microbiol. Spectr*. 3 (2015) 1–45. doi:10.1128/microbiolspec.MB-0018-2015.
- [8] T.R. Garrett, M. Bhakoo, Z. Zhang, Bacterial adhesion and biofilms on surfaces, *Prog. Nat. Sci*. 18 (2008) 1049–1056. doi:10.1016/j.pnsc.2008.04.001.

- [9] J.J. Adams, G. Pal, Z. Jia, S.P. Smith, Mechanism of bacterial cell-surface attachment revealed by the structure of cellulosomal type II cohesin-dockerin complex, *Proc. Natl. Acad. Sci.* 103 (2006) 305–310. doi:10.1073/pnas.0507109103.
- [10] J.N.C. Fong, F.H. Yildiz, Biofilm Matrix Proteins, *Microbiol. Spectr.* 3 (2015) 1–27. doi:10.1128/microbiolspec.MB-0004-2014.
- [11] C.R. Kinnane, G.K. Such, G. Antequera-García, Y. Yan, S.J. Dodds, L.M. Liz-Marzan, F. Caruso, Low-Fouling Poly( N -vinyl pyrrolidone) Capsules with Engineered Degradable Properties, *Biomacromolecules.* 10 (2009) 2839–2846. doi:10.1021/bm900673m.
- [12] R. Konradi, C. Acikgoz, M. Textor, Polyoxazolines for Nonfouling Surface Coatings - A Direct Comparison to the Gold Standard PEG, *Macromol. Rapid Commun.* 33 (2012) 1663–1676. doi:10.1002/marc.201200422.
- [13] S. Pasche, S.M. De Paul, J. Vörös, N.D. Spencer, M. Textor, Poly( L-lysine)-graft -poly(ethylene glycol) Assembled Monolayers on Niobium Oxide Surfaces: A Quantitative Study of the Influence of Polymer Interfacial Architecture on Resistance to Protein Adsorption by ToF-SIMS and in Situ OWLS, *Langmuir.* 19 (2003) 9216–9225. doi:10.1021/la034111y.
- [14] G. Li, G. Cheng, H. Xue, S. Chen, F. Zhang, S. Jiang, Ultra low fouling zwitterionic polymers with a biomimetic adhesive group, *Biomaterials.* 29 (2008) 4592–4597. doi:10.1016/j.biomaterials.2008.08.021.
- [15] S.Y. Yang, J.D. Mendelsohn, M.F. Rubner, New Class of Ultrathin, Highly Cell-Adhesion-Resistant Polyelectrolyte Multilayers with Micropatterning Capabilities, *Biomacromolecules.* 4 (2003) 987–994. doi:10.1021/bm034035d.
- [16] Z. Zhang, H. Vaisocherová, G. Cheng, W. Yang, H. Xue, S. Jiang, Nonfouling Behavior of Polycarboxybetaine-Grafted Surfaces: Structural and Environmental Effects, *Biomacromolecules.* 9 (2008) 2686–2692. doi:10.1021/bm800407r.

- [17] M.C. Sin, S.H. Chen, Y. Chang, Hemocompatibility of zwitterionic interfaces and membranes, *Polym. J.* 46 (2014) 436–443. doi:10.1038/pj.2014.46.
- [18] S. Krishnan, C.J. Weinman, C.K. Ober, Advances in polymers for anti-biofouling surfaces, *J. Mater. Chem.* 18 (2008) 3405–3413. doi:10.1039/b801491d.
- [19] E.H. Leduc, S.J. Holt, Hydroxypropyl Methacrylate, A New Water-Miscible Embedding Medium for Electron Microscopy, *J. Cell Biol.* 26 (1965) 137–155. doi:10.1083/jcb.26.1.137.
- [20] A.L. Lewis, Z.L. Cumming, H.H. Goreish, L.C. Kirkwood, L.A. Tolhurst, P.W. Stratford, Crosslinkable coatings from phosphorylcholine-based polymers, *Biomaterials.* 22 (2001) 99–111. doi:10.1016/S0142-9612(00)00083-1.
- [21] B. Mrabet, M.N. Nguyen, A. Majbri, S. Mahouche, M. Turmine, A. Bakhrouf, M.M. Chehimi, Anti-fouling poly(2-hydroxyethyl methacrylate) surface coatings with specific bacteria recognition capabilities, *Surf. Sci.* 603 (2009) 2422–2429. doi:10.1016/j.susc.2009.05.020.
- [22] C. Yoshikawa, A. Goto, Y. Tsujii, T. Fukuda, T. Kimura, K. Yamamoto, A. Kishida, Protein Repellency of Well-Defined, Concentrated Poly(2-hydroxyethyl methacrylate) Brushes by the Size-Exclusion Effect, *Macromolecules.* 39 (2006) 2284–2290. doi:10.1021/ma0520242.
- [23] H. Ma, J. Hyun, P. Stiller, A. Chilkoti, “Non-Fouling” Oligo(ethylene glycol)-Functionalized Polymer Brushes Synthesized by Surface-Initiated Atom Transfer Radical Polymerization, *Adv. Mater.* 16 (2004) 338–341. doi:10.1002/adma.200305830.
- [24] J. Zheng, L. Li, H.-K. Tsao, Y.J. Sheng, S. Chen, S. Jiang, Strong Repulsive Forces between Protein and Oligo (Ethylene Glycol) Self-Assembled Monolayers: A Molecular Simulation Study, *Biophys. J.* 89 (2005) 158–166. doi:10.1529/biophysj.105.059428.

- [25] D. Leckband, S. Sheth, A. Halperin, Grafted poly(ethylene oxide) brushes as nonfouling surface coatings, *J. Biomater. Sci. Polym. Ed.* 10 (1999) 1125–1147. doi:10.1163/156856299X00720.
- [26] Y.Y. Luk, M. Kato, M. Mrksich, Self-Assembled Monolayers of Alkanethiolates Presenting Mannitol Groups Are Inert to Protein Adsorption and Cell Attachment, *Langmuir*. 16 (2000) 9604–9608. doi:10.1021/la0004653.
- [27] M. Shen, L. Martinson, M.S. Wagner, D.G. Castner, B.D. Ratner, T.A. Horbett, PEO-like plasma polymerized tetraglyme surface interactions with leukocytes and proteins: in vitro and in vivo studies, *J. Biomater. Sci. Polym. Ed.* 13 (2002) 367–390. doi:10.1163/156856202320253910.
- [28] E. Ostuni, R.G. Chapman, R.E. Holmlin, S. Takayama, G.M. Whitesides, A Survey of Structure–Property Relationships of Surfaces that Resist the Adsorption of Protein, *Langmuir*. 17 (2001) 5605–5620. doi:10.1021/la010384m.
- [29] N. Adams, U.S. Schubert, Poly(2-oxazolines) in biological and biomedical application contexts, *Adv. Drug Deliv. Rev.* 59 (2007) 1504–1520. doi:10.1016/j.addr.2007.08.018.
- [30] R. Konradi, B. Pidhatika, A. Mühlebach, M. Textor, Poly-2-methyl-2-oxazoline: A Peptide-like Polymer for Protein-Repellent Surfaces, *Langmuir*. 24 (2008) 613–616. doi:10.1021/la702917z.
- [31] K. Knop, R. Hoogenboom, D. Fischer, U.S. Schubert, Poly(ethylene glycol) in Drug Delivery: Pros and Cons as Well as Potential Alternatives, *Angew. Chemie Int. Ed.* 49 (2010) 6288–6308. doi:10.1002/anie.200902672.
- [32] A.A. Cavallaro, M.N. MacGregor-Ramiasa, K. Vasilev, Antibiofouling Properties of Plasma-Deposited Oxazoline-Based Thin Films, *ACS Appl. Mater. Interfaces*. 8 (2016) 6354–6362. doi:10.1021/acsami.6b00330.
- [33] B.K.D. Ngo, M.A. Grunlan, Protein Resistant Polymeric Biomaterials, *ACS*

- Macro Lett. 6 (2017) 992–1000. doi:10.1021/acsmacrolett.7b00448.
- [34] F. Xuan, J. Liu, Preparation, characterization and application of zwitterionic polymers and membranes: current developments and perspective, *Polym. Int.* 58 (2009) 1350–1361. doi:10.1002/pi.2679.
- [35] R.H. Brown, A.J. Duncan, J.-H. Choi, J.K. Park, T. Wu, D.J. Leo, K.I. Winey, R.B. Moore, T.E. Long, Effect of Ionic Liquid on Mechanical Properties and Morphology of Zwitterionic Copolymer Membranes, *Macromolecules.* 43 (2010) 790–796. doi:10.1021/ma902028u.
- [36] A. Laschewsky, Structures and Synthesis of Zwitterionic Polymers, *Polymers.* 6 (2014) 1544–1601. doi:10.3390/polym6051544.
- [37] H. Ladenheim, H. Morawetz, A new type of polyampholyte: Poly(4-vinyl pyridine betaine), *J. Polym. Sci.* 26 (1957) 251–254. doi:10.1002/pol.1957.1202611319.
- [38] R. Hart, D. Timmerman, New polyampholytes: The polysulfobetaines, *J. Polym. Sci.* 28 (1958) 638–640. doi:10.1002/pol.1958.1202811820.
- [39] D.N. Schulz, D.G. Peiffer, P.K. Agarwal, J. Larabee, J.J. Kaladas, L. Soni, B. Handwerker, R.T. Garner, Phase behaviour and solution properties of sulphobetaine polymers, *Polymer.* 27 (1986) 1734–1742. doi:10.1016/0032-3861(86)90269-7.
- [40] C.G. Bazuin, Y.L. Zheng, R. Muller, J.C. Galin, Random ethyl acrylate-sulphonatopropylbetaine copolymers: 2. Dynamic mechanical properties, *Polymer.* 30 (1989) 654–661. doi:10.1016/0032-3861(89)90150-X.
- [41] N. Bonte, A. Laschewsky, B. Mayer, V. Vermeylen, Homogeneous mixtures of polybetaines with low molecular weight salts, *Macromol. Symp.* 102 (1996) 273–280. doi:10.1002/masy.19961020133.
- [42] A. Puri, R. Blumenthal, Polymeric Lipid Assemblies as Novel Theranostic Tools, *Acc. Chem. Res.* 44 (2011) 1071–1079. doi:10.1021/ar2001843.

- [43] D.S. Johnston, S. Sanghera, M. Pons, D. Chapman, Phospholipid polymers—Synthesis and spectral characteristics, *Biochim. Biophys. Acta - Biomembr.* 602 (1980) 57–69. doi:10.1016/0005-2736(80)90289-8.
- [44] S. Kudaibergenov, W. Jaeger, A. Laschewsky, Polymeric Betaines: Synthesis, Characterization, and Application, in: *Chinese J. Radiol.*, 2006: pp. 157–224. doi:10.1007/12\_078.
- [45] H.-H. Hub, B. Hupfer, H. Koch, H. Ringsdorf, Polymerizable Phospholipid Analogues—New Stable Biomembrane and Cell Models, *Angew. Chemie Int. Ed. English.* 19 (1980) 938–940. doi:10.1002/anie.198009381.
- [46] K.M. Zurick, M. Bernards, Recent biomedical advances with polyampholyte polymers, *J. Appl. Polym. Sci.* 131 (2014) 1–9. doi:10.1002/app.40069.
- [47] M. Ahlers, W. Müller, A. Reichert, H. Ringsdorf, J. Venzmer, Specific Interactions of Proteins with Functional Lipid Monolayers—Ways of Simulating Biomembrane Processes, *Angew. Chemie Int. Ed. English.* 29 (1990) 1269–1285. doi:10.1002/anie.199012691.
- [48] W. Chaibi, A. Ziane, Z. Benzehaim, L. Bennabi, K. Guemra, Synthesis and Characterization of Cationic Poly(N-[3-Hexyldimethyl-Aminopropyl] Methacrylamide Bromide) Water-Soluble Polymer, *Mater. Sci. Appl. Chem.* 33 (2016) 40–44. doi:10.1515/msac-2016-0008.
- [49] D.F. O'Brien, T.H. Whitesides, R.T. Klingbiel, The photopolymerization of lipid-diacetylenes in bimolecular-layer membranes, *J. Polym. Sci. Polym. Lett. Ed.* 19 (1981) 95–101. doi:10.1002/pol.1981.130190302.
- [50] S.L. Regen, K. Yamaguchi, N.K.P. Samuel, M. Singh, Polymerized-depolymerized vesicles. A reversible phosphatidylcholine-based membrane, *J. Am. Chem. Soc.* 105 (1983) 6354–6355. doi:10.1021/ja00358a050.
- [51] N. Bonte, A. Laschewsky, V. Vermylen, Hybrid materials made from polymeric betaines and low molar mass salts, *Macromol. Symp.* 117 (1997) 195–206. doi:10.1002/masy.19971170123.

- [52] G.E. Perlmann, E. Katchalski, Conformation of Poly-L-methionine and Some of its Derivatives in Solution, *J. Am. Chem. Soc.* 84 (1962) 452–457. doi:10.1021/ja00862a026.
- [53] T. Wu, F.L. Beyer, R.H. Brown, R.B. Moore, T.E. Long, Influence of Zwitterions on Thermomechanical Properties and Morphology of Acrylic Copolymers: Implications for Electroactive Applications, *Macromolecules*. 44 (2011) 8056–8063. doi:10.1021/ma201211j.
- [54] C.-Z. Yang, K.K.S. Hwang, S.L. Cooper, Morphology and properties of polybutadiene - and polyether - polyurethane zwitterionomers, *Makromolekular Chem. Phys.* 184 (1983) 651–668. doi:10.1002/macp.1983.021840318.
- [55] H. Zhang, J.R. Joubert, S.S. Saavedra, Membranes from Polymerizable Lipids, in: *Chinese J. Radiol.*, 2010: pp. 1–42. doi:10.1007/12\_2009\_3.
- [56] M.. Ali, H.. Perzanowski, S.. Ali, Polymerization of functionalized diallyl quaternary ammonium salt to poly(ampholyte–electrolyte), *Polymer*. 41 (2000) 5591–5600. doi:10.1016/S0032-3861(99)00764-8.
- [57] Q. Shao, L. Mi, X. Han, T. Bai, S. Liu, Y. Li, S. Jiang, Differences in Cationic and Anionic Charge Densities Dictate Zwitterionic Associations and Stimuli Responses, *J. Phys. Chem. B.* 118 (2014) 6956–6962. doi:10.1021/jp503473u.
- [58] A.B. Lowe, C.L. McCormick, Synthesis and Solution Properties of Zwitterionic Polymers, *Chem. Rev.* 102 (2002) 4177–4190. doi:10.1021/cr020371t.
- [59] Z. Zhang, T. Chao, S. Chen, S. Jiang, Superlow Fouling Sulfobetaine and Carboxybetaine Polymers on Glass Slides, *Langmuir*. 22 (2006) 10072–10077. doi:10.1021/la062175d.
- [60] G. Cheng, Z. Zhang, S. Chen, J.D. Bryers, S. Jiang, Inhibition of bacterial adhesion and biofilm formation on zwitterionic surfaces, *Biomaterials*. 28 (2007) 4192–4199. doi:10.1016/j.biomaterials.2007.05.041.

- [61] P.-S. Liu, Q. Chen, S.-S. Wu, J. Shen, S.-C. Lin, Surface modification of cellulose membranes with zwitterionic polymers for resistance to protein adsorption and platelet adhesion, *J. Memb. Sci.* 350 (2010) 387–394. doi:10.1016/j.memsci.2010.01.015.
- [62] J.B. Schlenoff, Zwitterion: Coating Surfaces with Zwitterionic Functionality to Reduce Nonspecific Adsorption, *Langmuir*. 30 (2014) 9625–9636. doi:10.1021/la500057j.
- [63] C. Hippus, V. Bütün, I. Erel-Goktepe, Bacterial anti-adhesive properties of a monolayer of zwitterionic block copolymer micelles, *Mater. Sci. Eng. C*. 41 (2014) 354–362. doi:10.1016/j.msec.2014.04.023.
- [64] J. Wang, Z. Wang, Y. Liu, J. Wang, S. Wang, Surface modification of NF membrane with zwitterionic polymer to improve anti-biofouling property, *J. Memb. Sci.* 514 (2016) 407–417. doi:10.1016/j.memsci.2016.05.014.
- [65] G. Decher, Fuzzy Nanoassemblies: Toward Layered Polymeric Multicomposites, *Science* (80-. ). 277 (1997) 1232–1237. doi:10.1126/science.277.5330.1232.
- [66] P. Yusan, I. Tuncel, V. Bütün, A.L. Demirel, I. Erel-Goktepe, pH-responsive layer-by-layer films of zwitterionic block copolymer micelles, *Polym. Chem.* 5 (2014) 3777–3787. doi:10.1039/C4PY00040D.
- [67] B. Onat, V. Bütün, S. Banerjee, I. Erel-Goktepe, Bacterial anti-adhesive and pH-induced antibacterial agent releasing ultra-thin films of zwitterionic copolymer micelles, *Acta Biomater.* 40 (2016) 293–309. doi:10.1016/j.actbio.2016.04.033.
- [68] Z. Zhang, T. Chao, L. Liu, G. Cheng, B.D. Ratner, S. Jiang, Zwitterionic Hydrogels: an in Vivo Implantation Study, *J. Biomater. Sci. Polym. Ed.* 20 (2009) 1845–1859. doi:10.1163/156856208X386444.
- [69] L. Zheng, H.S. Sundaram, Z. Wei, C. Li, Z. Yuan, Applications of zwitterionic polymers, *React. Funct. Polym.* 118 (2017) 51–61.

doi:10.1016/j.reactfunctpolym.2017.07.006.

- [70] Z. Zhang, J.A. Finlay, L. Wang, Y. Gao, J.A. Callow, M.E. Callow, S. Jiang, Polysulfobetaine-Grafted Surfaces as Environmentally Benign Ultralow Fouling Marine Coatings, *Langmuir*. 25 (2009) 13516–13521. doi:10.1021/la901957k.
- [71] S. Dobretsov, M. Teplitski, V. Paul, Mini-review: quorum sensing in the marine environment and its relationship to biofouling, *Biofouling*. 25 (2009) 413–427. doi:10.1080/08927010902853516.
- [72] S. Joshi, P. Pellacani, T.A. van Beek, H. Zuilhof, M.W.F. Nielen, Surface characterization and antifouling properties of nanostructured gold chips for imaging surface plasmon resonance biosensing, *Sensors Actuators B Chem*. 209 (2015) 505–514. doi:10.1016/j.snb.2014.11.133.
- [73] Y.-H.M. Chan, S.G. Boxer, Model Membrane Systems and Their Applications State of the field, 11 (2008) 581–587. doi:10.1016/j.cbpa.2007.09.020.
- [74] A. Venault, Y. Chang, Designs of Zwitterionic Interfaces and Membranes, *Langmuir*. (2018) acs.langmuir.8b00562. doi:10.1021/acs.langmuir.8b00562.
- [75] M. Chen, W.H. Briscoe, S.P. Armes, H. Cohen, J. Klein, Polyzwitterionic brushes: Extreme lubrication by design, *Eur. Polym. J.* 47 (2011) 511–523. doi:10.1016/j.eurpolymj.2010.10.007.
- [76] M. Chen, W.H. Briscoe, S.P. Armes, J. Klein, Lubrication at Physiological Pressures by Polyzwitterionic Brushes, *Science (80-. )*. 323 (2009) 1698–1701. doi:10.1126/science.1169399.
- [77] N. Shahkaramipour, T.N. Tran, S. Ramanan, H. Lin, Membranes with surface-enhanced antifouling properties for water purification, *Membranes*. 7 (2017) 1–18. doi:10.3390/membranes7010013.
- [78] R. Wang, T. Xiang, W.-F. Zhao, C.-S. Zhao, A facile approach toward multifunctional polyurethane/polyethersulfone composite membranes for versatile

- applications, *Mater. Sci. Eng. C*. 59 (2016) 556–564.  
doi:10.1016/j.msec.2015.10.058.
- [79] M. Hadidi, A.L. Zydney, Fouling behavior of zwitterionic membranes: Impact of electrostatic and hydrophobic interactions, *J. Memb. Sci.* 452 (2014) 97–103. doi:10.1016/j.memsci.2013.09.062.
- [80] J.F. Quinn, A.P.R. Johnston, G.K. Such, A.N. Zelikin, F. Caruso, Next generation, sequentially assembled ultrathin films: beyond electrostatics, *Chem. Soc. Rev.* 36 (2007) 707. doi:10.1039/b610778h.
- [81] M. Lin, S. Meng, W. Zhong, Z. Li, Q. Du, P. Tomasik, Novel Biodegradable Blend Matrices for Controlled Drug Release, *J. Pharm. Sci.* 97 (2008) 4240–4248. doi:10.1002/jps.21297.
- [82] H. Priya James, R. John, A. Alex, K.R. Anoop, Smart polymers for the controlled delivery of drugs – a concise overview, *Acta Pharm. Sin. B*. 4 (2014) 120–127. doi:10.1016/j.apsb.2014.02.005.
- [83] S. Liu, R. Maheshwari, K.L. Kiick, Polymer-Based Therapeutics, *Macromolecules*. 42 (2009) 3–13. doi:10.1021/ma801782q.
- [84] J. Ladd, Z. Zhang, S. Chen, J.C. Hower, S. Jiang, Zwitterionic Polymers Exhibiting High Resistance to Nonspecific Protein Adsorption from Human Serum and Plasma, *Biomacromolecules*. 9 (2008) 1357–1361.  
doi:10.1021/bm701301s.
- [85] Z. Zhang, S. Chen, S. Jiang, Dual-Functional Biomimetic Materials: Nonfouling Poly(carboxybetaine) with Active Functional Groups for Protein Immobilization, *Biomacromolecules*. 7 (2006) 3311–3315.  
doi:10.1021/bm060750m.
- [86] H. Vaisocherová, W. Yang, Z. Zhang, Z. Cao, G. Cheng, M. Piliarik, J. Homola, S. Jiang, Ultralow Fouling and Functionalizable Surface Chemistry Based on a Zwitterionic Polymer Enabling Sensitive and Specific Protein Detection in Undiluted Blood Plasma, *Anal. Chem.* 80 (2008) 7894–7901.

doi:10.1021/ac8015888.

- [87] S. Jiang, Z. Cao, Ultralow-Fouling, Functionalizable, and Hydrolyzable Zwitterionic Materials and Their Derivatives for Biological Applications, *Adv. Mater.* 22 (2010) 920–932. doi:10.1002/adma.200901407.
- [88] Q. Shao, S. Jiang, Molecular Understanding and Design of Zwitterionic Materials, *Adv. Mater.* 27 (2015) 15–26. doi:10.1002/adma.201404059.
- [89] P. Koeberle, A. Laschewsky, Hydrophobically Modified Zwitterionic Polymers: Synthesis, Bulk Properties, and Miscibility with Inorganic Salts, *Macromolecules.* 27 (1994) 2165–2173. doi:10.1021/ma00086a028.
- [90] P. Anton, A. Laschewsky, Zwitterionic polysoaps with reduced density of surfactant side groups, *Makromolekular Chem. Physics.* 194 (1993) 601–624. doi:10.1002/macp.1993.021940221.
- [91] H. Ringsdorf, J. Venzmer, F.M. Winnik, Fluorescence studies of hydrophobically modified poly(N-isopropylacrylamides), *Macromolecules.* 24 (1991) 1678–1686. doi:10.1021/ma00007a034.
- [92] S.L. Regen, A. Singh, G. Oehme, M. Singh, Polymerized phosphatidylcholine vesicles. Synthesis and characterization, *J. Am. Chem. Soc.* 104 (1982) 791–795. doi:10.1021/ja00367a023.
- [93] Y. Okamoto, Y. Kishi, K. Suga, H. Umakoshi, Induction of Chiral Recognition with Lipid Nanodomains Produced by Polymerization, *Biomacromolecules.* 18 (2017) 1180–1188. doi:10.1021/acs.biomac.6b01859.
- [94] Y. Kadoma, N. Nakabayashi, E. Masuhara, J. Yamauchi, Synthesis and hemolysis test of the polymer containing phosphorylcholine groups, *Soc. Polym. Sci. Japan.* 35 (1978) 423–427. doi:10.1295/koron.35.423.
- [95] K. Ishihara, T. Ueda, N. Nakabayashi, Preparation of Phospholipid Polymers and Their Properties as Polymer Hydrogel Membranes, *Polym. J.* 22 (1990) 355–360. doi:10.1295/polymj.22.355.

- [96] R.F. Zwaal, A.J. Schroit, Pathophysiologic implications of membrane phospholipid asymmetry in blood cells., *Blood*. 89 (1997) 1121–32.  
doi:<http://www.bloodjournal.org/content/89/4/1121.abstract>.
- [97] A. Mueller, D.F. O'Brien, Supramolecular Materials via Polymerization of Mesophases of Hydrated Amphiphiles, *Chem. Rev.* 102 (2002) 727–757.  
doi:10.1021/cr000071g.
- [98] S. Long, S. Clarke, M.C. Davies, A.L. Lewis, G.W. Hanlon, A.W. Lloyd, Controlled biological response on blends of a phosphorylcholine-based copolymer with poly(butyl methacrylate), *Biomaterials*. 24 (2003) 4115–4121.  
doi:10.1016/S0142-9612(03)00272-2.
- [99] A. Shukla, S.N. Avadhany, J.C. Fang, P.T. Hammond, Tunable vancomycin releasing surfaces for biomedical applications, *Small*. 6 (2010) 2392–2404.  
doi:10.1002/sml.201001150.
- [100] M.S. Rahaman, H. Thérien-Aubin, M. Ben-Sasson, C.K. Ober, M. Nielsen, M. Elimelech, Control of biofouling on reverse osmosis polyamide membranes modified with biocidal nanoparticles and antifouling polymer brushes, *J. Mater. Chem. B*. 2 (2014) 1724. doi:10.1039/c3tb21681k.
- [101] P. Gentile, M.E. Frongia, M. Cardellach, C.A. Miller, G.P. Stafford, G.J. Leggett, P. V. Hatton, Functionalised nanoscale coatings using layer-by-layer assembly for imparting antibacterial properties to polylactide-co-glycolide surfaces, *Acta Biomater.* 21 (2015) 35–43. doi:10.1016/j.actbio.2015.04.009.
- [102] D. Silva, H.C. de Sousa, M.H. Gil, L.F. Santos, G.M. Moutinho, A.P. Serro, B. Saramago, Antibacterial layer-by-layer coatings to control drug release from soft contact lenses material, *Int. J. Pharm.* 553 (2018) 186–200.  
doi:10.1016/j.ijpharm.2018.10.041.
- [103] J. Fu, J. Ji, D. Fan, J. Shen, Construction of antibacterial multilayer films containing nanosilver via layer-by-layer assembly of heparin and chitosan-silver ions complex, *J. Biomed. Mater. Res. Part A*. 79A (2006) 665–674.

doi:10.1002/jbm.a.30819.

- [104] A.K. Muszanska, H.J. Busscher, A. Herrmann, H.C. van der Mei, W. Norde, Pluronic–lysozyme conjugates as anti-adhesive and antibacterial bifunctional polymers for surface coating, *Biomaterials*. 32 (2011) 6333–6341.  
doi:10.1016/j.biomaterials.2011.05.016.
- [105] H.D.M. Follmann, A.F. Martins, A.P. Gerola, T.A.L. Burgo, C. V. Nakamura, A.F. Rubira, E.C. Muniz, Antiadhesive and Antibacterial Multilayer Films via Layer-by-Layer Assembly of TMC/Heparin Complexes, *Biomacromolecules*. 13 (2012) 3711–3722. doi:10.1021/bm3011962.
- [106] L. Huang, L. Zhang, S. Xiao, Y. Yang, F. Chen, P. Fan, Z. Zhao, M. Zhong, J. Yang, Bacteria killing and release of salt-responsive, regenerative, double-layered polyzwitterionic brushes, *Chem. Eng. J.* 333 (2018) 1–10.  
doi:10.1016/j.cej.2017.09.142.
- [107] A.K. Muszanska, M.R. Nejadnik, Y. Chen, E.R. van den Heuvel, H.J. Busscher, H.C. van der Mei, W. Norde, Bacterial Adhesion Forces with Substratum Surfaces and the Susceptibility of Biofilms to Antibiotics, *Antimicrob. Agents Chemother.* 56 (2012) 4961–4964.  
doi:10.1128/AAC.00431-12.
- [108] A.F. Radovic-Moreno, T.K. Lu, V.A. Puscasu, C.J. Yoon, R. Langer, O.C. Farokhzad, Surface Charge-Switching Polymeric Nanoparticles for Bacterial Cell Wall-Targeted Delivery of Antibiotics, *ACS Nano*. 6 (2012) 4279–4287.  
doi:10.1021/nn3008383.
- [109] B. Horev, M.I. Klein, G. Hwang, Y. Li, D. Kim, H. Koo, D.S.W. Benoit, pH-Activated Nanoparticles for Controlled Topical Delivery of Farnesol To Disrupt Oral Biofilm Virulence, *ACS Nano*. 9 (2015) 2390–2404.  
doi:10.1021/nn507170s.
- [110] I. Zhuk, F. Jariwala, A.B. Attygalle, Y. Wu, M.R. Libera, S.A. Sukhishvili, Self-Defensive Layer-by-Layer Films with Bacteria-Triggered Antibiotic

- Release, *ACS Nano*. 8 (2014) 7733–7745. doi:10.1021/nn500674g.
- [111] J. Borges, J.F. Mano, Molecular Interactions Driving the Layer-by-Layer Assembly of Multilayers, *Chem. Rev.* 114 (2014) 8883–8942. doi:10.1021/cr400531v.
- [112] R.K. Iler, Multilayers of colloidal particles, *J. Colloid Interface Sci.* 21 (1966) 569–594. doi:10.1016/0095-8522(66)90018-3.
- [113] G. Decher, J.D. Hong, J. Schmitt, Buildup of ultrathin multilayer films by a self-assembly process: III. Consecutively alternating adsorption of anionic and cationic polyelectrolytes on charged surfaces, *Thin Solid Films*. 210–211 (1992) 831–835. doi:10.1016/0040-6090(92)90417-A.
- [114] S. Kidambi, C. Chan, I. Lee, Selective Depositions on Polyelectrolyte Multilayers: Self-Assembled Monolayers of m-dPEG Acid as Molecular Template, *J. Am. Chem. Soc.* 126 (2004) 4697–4703. doi:10.1021/ja039359o.
- [115] S. Wijeratne, W. Liu, J. Dong, W. Ning, N.D. Ratnayake, K.D. Walker, M.L. Bruening, Layer-by-Layer Deposition with Polymers Containing Nitrilotriacetate, A Convenient Route to Fabricate Metal- and Protein-Binding Films, *ACS Appl. Mater. Interfaces*. 8 (2016) 10164–10173. doi:10.1021/acsami.6b00896.
- [116] A.P. Gomes, J.F. Mano, J.A. Queiroz, I.C. Gouveia, Layer-by-layer deposition of antimicrobial polymers on cellulosic fibers: a new strategy to develop bioactive textiles, *Polym. Adv. Technol.* 24 (2013) 1005–1010. doi:10.1002/pat.3176.
- [117] A.H. Brozena, C.J. Oldham, G.N. Parsons, Atomic layer deposition on polymer fibers and fabrics for multifunctional and electronic textiles, *J. Vac. Sci. Technol. A Vacuum, Surfaces, Film*. 34 (2016) 010801-1-010801-17. doi:10.1116/1.4938104.
- [118] J. Anzai, M. Nishimura, Layer-by-layer deposition of avidin and polymers on a solid surface to prepare thin films: significant effects of molecular geometry

- of the polymers on the deposition behaviour, *J. Chem. Soc. Perkin Trans. 2*. 2 (1997) 1887–1889. doi:10.1039/a704744d.
- [119] V. Selin, J. Ankner, S. Sukhishvili, Ionically Paired Layer-by-Layer Hydrogels: Water and Polyelectrolyte Uptake Controlled by Deposition Time, *Gels*. 4 (2018) 7. doi:10.3390/gels4010007.
- [120] S. Xiao, P. Xu, Q. Peng, J. Chen, J. Huang, F. Wang, N. Noor, Layer-by-Layer Assembly of Polyelectrolyte Multilayer onto PET Fabric for Highly Tunable Dyeing with Water Soluble Dyestuffs, *Polymers*. 9 (2017) 1–17. doi:10.3390/polym9120735.
- [121] K. Hyde, M. Rusa, J. Hinstroza, Layer-by-layer deposition of polyelectrolyte nanolayers on natural fibres: cotton, *Nanotechnology*. 16 (2005) 422S428. doi:10.1088/0957-4484/16/7/017.
- [122] M. Keeney, X.Y. Jiang, M. Yamane, M. Lee, S. Goodman, F. Yang, Nanocoating for biomolecule delivery using layer-by-layer self-assembly, *J. Mater. Chem. B*. 3 (2015) 8757–8770. doi:10.1039/C5TB00450K.
- [123] X. Zhang, H. Chen, H. Zhang, Layer-by-layer assembly: from conventional to unconventional methods, *Chem. Commun.* 14 (2007) 1395–1405. doi:10.1039/B615590A.
- [124] P. Bertrand, A. Jonas, A. Laschewsky, R. Legras, Ultrathin polymer coatings by complexation of polyelectrolytes at interfaces: suitable materials, structure and properties, *Macromol. Rapid Commun.* 21 (2000) 319–348. doi:10.1002/(SICI)1521-3927(20000401)21:7<319::AID-MARC319>3.0.CO;2-7.
- [125] P.K. Deshmukh, K.P. Ramani, S.S. Singh, A.R. Tekade, V.K. Chatap, G.B. Patil, S.B. Bari, Stimuli-sensitive layer-by-layer (LbL) self-assembly systems: Targeting and biosensory applications, *J. Control. Release*. 166 (2013) 294–306. doi:10.1016/j.jconrel.2012.12.033.
- [126] D. Choi, J. Hong, Layer-by-layer assembly of multilayer films for controlled

- drug release, *Arch. Pharm. Res.* 37 (2014) 79–87. doi:10.1007/s12272-013-0289-x.
- [127] S.S. Shiratori, M.F. Rubner, pH-Dependent Thickness Behavior of Sequentially Adsorbed Layers of Weak Polyelectrolytes, *Macromolecules*. 33 (2000) 4213–4219. doi:10.1021/ma991645q.
- [128] A.J. Chung, M.F. Rubner, Methods of Loading and Releasing Low Molecular Weight Cationic Molecules in Weak Polyelectrolyte Multilayer Films, *Langmuir*. 18 (2002) 1176–1183. doi:10.1021/la010873m.
- [129] S.A. Sukhishvili, S. Granick, Layered, Erasable, Ultrathin Polymer Films, *J. Am. Chem. Soc.* 122 (2000) 9550–9551. doi:10.1021/ja002410t.
- [130] S.A. Sukhishvili, S. Granick, Layered, Erasable Polymer Multilayers Formed by Hydrogen-Bonded Sequential Self-Assembly, *Macromolecules*. 35 (2002) 301–310. doi:10.1021/ma011346c.
- [131] S.A. Sukhishvili, E. Kharlampieva, V. Izumrudov, Where Polyelectrolyte Multilayers and Polyelectrolyte Complexes Meet, *Macromolecules*. 39 (2006) 8873–8881. doi:10.1021/ma061617p.
- [132] A. Laschewsky, B. Mayer, E. Wischerhoff, X. Arys, A. Jonas, M. Kauranen, A. Persoons, A New Technique for Assembling Thin, Defined Multilayers, *Angew. Chemie Int. Ed. English*. 36 (1997) 2788–2791. doi:10.1002/anie.199727881.
- [133] M. Koetse, A. Laschewsky, B. Mayer, O. Rolland, E. Wischerhoff, Ultrathin Coatings by Multiple Polyelectrolyte Adsorption/Surface Activation (CoMPAS), *Macromolecules*. 31 (1998) 9316–9327. doi:10.1021/ma980589a.
- [134] H.H. Rmaile, C.B. Bucur, J.B. Schlenoff, Polyzwitterions in Polyelectrolyte Multilayers: Formation and Applications, *Polym. Prepr.* 44 (2003) 1–2.
- [135] E. Kharlampieva, V.A. Izumrudov, S.A. Sukhishvili, Electrostatic Layer-by-Layer Self-Assembly of Poly(carboxybetaine)s: Role of Zwitterions in Film

- Growth, *Macromolecules*. 40 (2007) 3663–3668. doi:10.1021/ma062811e.
- [136] N. Ma, H. Zhang, B. Song, Z. Wang, X. Zhang, Polymer Micelles as Building Blocks for Layer-by-Layer Assembly: An Approach for Incorporation and Controlled Release of Water-Insoluble Dyes, *Chem. Mater.* 17 (2005) 5065–5069. doi:10.1021/cm051221c.
- [137] J. Cho, J. Hong, K. Char, F. Caruso, Nanoporous Block Copolymer Micelle/Micelle Multilayer Films with Dual Optical Properties, *J. Am. Chem. Soc.* 128 (2006) 9935–9942. doi:10.1021/ja062437y.
- [138] L. Xu, Z. Zhu, S.A. Sukhishvili, Polyelectrolyte Multilayers of Diblock Copolymer Micelles with Temperature-Responsive Cores, *Langmuir*. 27 (2011) 409–415. doi:10.1021/la1038014.
- [139] A. Palanisamy, S.A. Sukhishvili, Swelling Transitions in Layer-by-Layer Assemblies of UCST Block Copolymer Micelles, *Macromolecules*. 51 (2018) 3467–3476. doi:10.1021/acs.macromol.8b00519.
- [140] Y. Li, T. Pan, B. Ma, J. Liu, J. Sun, Healable Antifouling Films Composed of Partially Hydrolyzed Poly(2-ethyl-2-oxazoline) and Poly(acrylic acid), *ACS Appl. Mater. Interfaces*. 9 (2017) 14429–14436. doi:10.1021/acsami.7b02872.
- [141] T. He, D. Jańczewski, S. Guo, S.M. Man, S. Jiang, W.S. Tan, Stable pH responsive layer-by-layer assemblies of partially hydrolysed poly(2-ethyl-2-oxazoline) and poly(acrylic acid) for effective prevention of protein, cell and bacteria surface attachment, *Colloids Surfaces B Biointerfaces*. 161 (2018) 269–278. doi:10.1016/j.colsurfb.2017.10.031.
- [142] I. Geornaras, Y. Yoon, K.E. Belk, G.C. Smith, J.N. Sofos, Antimicrobial Activity of  $\epsilon$ -Polylysine against *Escherichia coli* O157:H7, *Salmonella* Typhimurium, and *Listeria monocytogenes* in Various Food Extracts, *J. Food Sci.* 72 (2007) M330–M334. doi:10.1111/j.1750-3841.2007.00510.x.
- [143] K. Ushimaru, Y. Hamano, H. Katano, Antimicrobial Activity of  $\epsilon$ -Poly-L-lysine after Forming a Water-Insoluble Complex with an Anionic Surfactant,

- Biomacromolecules. 18 (2017) 1387–1392. doi:10.1021/acs.biomac.7b00109.
- [144] H. Li, R. Cui, L. Peng, S. Cai, P. Li, T. Lan, Preparation of Antibacterial Cellulose Paper Using Layer-by-Layer Assembly for Cooked Beef Preservation at Ambient Temperature, *Polymers*. 10 (2017) 15. doi:10.3390/polym10010015.
- [145] Y. Lu, Y. Wu, J. Liang, M.R. Libera, S.A. Sukhishvili, Self-defensive antibacterial layer-by-layer hydrogel coatings with pH-triggered hydrophobicity, *Biomaterials*. 45 (2015) 64–71. doi:10.1016/j.biomaterials.2014.12.048.
- [146] Z. Li, D. Lee, X. Sheng, R.E. Cohen, M.F. Rubner, Two-Level Antibacterial Coating with Both Release-Killing and Contact-Killing Capabilities, *Langmuir*. 22 (2006) 9820–9823. doi:10.1021/la0622166.
- [147] L. Shen, B. Wang, J. Wang, J. Fu, C. Picart, J. Ji, Asymmetric Free-Standing Film with Multifunctional Anti-Bacterial and Self-Cleaning Properties, *ACS Appl. Mater. Interfaces*. 4 (2012) 4476–4483. doi:10.1021/am301118f.
- [148] J. Min, R.D. Braatz, P.T. Hammond, Tunable staged release of therapeutics from layer-by-layer coatings with clay interlayer barrier, *Biomaterials*. 35 (2014) 2507–2517. doi:10.1016/j.biomaterials.2013.12.009.
- [149] S. Veerachamy, T. Yarlagaadda, G. Manivasagam, P.K. Yarlagaadda, Bacterial adherence and biofilm formation on medical implants: A review, *Proc. Inst. Mech. Eng. Part H J. Eng. Med.* 228 (2014) 1083–1099. doi:10.1177/0954411914556137.
- [150] H.J. Busscher, H.C. van der Mei, G. Subbiahdoss, P.C. Jutte, J.J.A.M. van den Dungen, S.A.J. Zaat, M.J. Schultz, D.W. Grainger, Biomaterial-Associated Infection: Locating the Finish Line in the Race for the Surface, *Sci. Transl. Med.* 4 (2012) 153rv10-153rv10. doi:10.1126/scitranslmed.3004528.
- [151] A.S. Chitnis, J.R. Edwards, P.M. Ricks, D.M. Sievert, S.K. Fridkin, C. V. Gould, Device-Associated Infection Rates, Device Utilization, and

- Antimicrobial Resistance in Long-Term Acute Care Hospitals Reporting to the National Healthcare Safety Network, 2010, *Infect. Control Hosp. Epidemiol.* 33 (2012) 993–1000. doi:10.1086/667745.
- [152] M. Hoyos-Nogués, J. Buxadera-Palomero, M.P. Ginebra, J.M. Manero, F.J. Gil, C. Mas-Moruno, All-in-one trifunctional strategy: A cell adhesive, bacteriostatic and bactericidal coating for titanium implants, *Colloids Surfaces B Biointerfaces.* 169 (2018) 30–40. doi:10.1016/j.colsurfb.2018.04.050.
- [153] B.F. Bell, M. Schuler, S. Tosatti, M. Textor, Z. Schwartz, B.D. Boyan, Osteoblast response to titanium surfaces functionalized with extracellular matrix peptide biomimetics, *Clin. Oral Implants Res.* 22 (2011) 865–872. doi:10.1111/j.1600-0501.2010.02074.x.
- [154] D.-W. Lee, Y.-P. Yun, K. Park, S.E. Kim, Gentamicin and bone morphogenic protein-2 (BMP-2)-delivering heparinized-titanium implant with enhanced antibacterial activity and osteointegration, *Bone.* 50 (2012) 974–982. doi:10.1016/j.bone.2012.01.007.
- [155] A.K. Muszanska, E.T.J. Rochford, A. Gruszka, A.A. Bastian, H.J. Busscher, W. Norde, H.C. van der Mei, A. Herrmann, Antiadhesive Polymer Brush Coating Functionalized with Antimicrobial and RGD Peptides to Reduce Biofilm Formation and Enhance Tissue Integration, *Biomacromolecules.* 15 (2014) 2019–2026. doi:10.1021/bm500168s.
- [156] X. Cui, T. Murakami, Y. Tamura, K. Aoki, Y. Hoshino, Y. Miura, Bacterial Inhibition and Osteoblast Adhesion on Ti Alloy Surfaces Modified by Poly(PEGMA-*r*-Phosmer) Coating, *ACS Appl. Mater. Interfaces.* 10 (2018) 23674–23681. doi:10.1021/acsami.8b07757.
- [157] V. Bütün, S. Armes, N. Billingham, Synthesis and aqueous solution properties of near-monodisperse tertiary amine methacrylate homopolymers and diblock copolymers, *Polymer.* 42 (2001) 5993–6008. doi:10.1016/S0032-3861(01)00066-0.

- [158] V. Bütün, Selective betainization of 2-(dimethylamino)ethyl methacrylate residues in tertiary amine methacrylate diblock copolymers and their aqueous solution properties, *Polymer*. 44 (2003) 7321–7334.  
doi:10.1016/j.polymer.2003.09.027.
- [159] M.A. Rahim, H. Ejima, K.L. Cho, K. Kempe, M. Müllner, J.P. Best, F. Caruso, Coordination-driven multistep assembly of metal-polyphenol films and capsules, *Chem. Mater.* 26 (2014) 1645–1653. doi:10.1021/cm403903m.
- [160] M. Haktaniyan, S. Atilla, E. Cagli, I. Erel-Goktepe, pH- and temperature-induced release of doxorubicin from multilayers of poly(2-isopropyl-2-oxazoline) and tannic acid, *Polym. Int.* 66 (2017) 1851–1863.  
doi:10.1002/pi.5458.
- [161] A. Mero, M. Campisi, Hyaluronic Acid Bioconjugates for the Delivery of Bioactive Molecules, *Polymers*. 6 (2014) 346–369.  
doi:10.3390/polym6020346.
- [162] T. Shutava, M. Prouty, D. Kommireddy, Y. Lvov, pH Responsive Decomposable Layer-by-Layer Nanofilms and Capsules on the Basis of Tannic Acid, *Macromolecules*. 38 (2005) 2850–2858.  
doi:10.1021/ma047629x.
- [163] N.J. Baxter, T.H. Lilley, E. Haslam, M.P. Williamson, Multiple Interactions between Polyphenols and a Salivary Proline-Rich Protein Repeat Result in Complexation and Precipitation, *Biochemistry*. 36 (1997) 5566–5577.  
doi:10.1021/bi9700328.
- [164] A. Quinn, E. Tjipto, A. Yu, T.R. Gengenbach, F. Caruso, Polyelectrolyte Blend Multilayer Films: Surface Morphology, Wettability, and Protein Adsorption Characteristics, *Langmuir*. 23 (2007) 4944–4949.  
doi:10.1021/la0634746.
- [165] R.N. Wenzel, Resistance of solid surfaces to wetting by water, *Ind. Eng. Chem.* 28 (1936) 988–994. doi:10.1021/ie50320a024.

- [166] Z. Gui, J. Qian, Q. Zhao, Y. Ji, Y. Liu, T. Liu, Q. An, Controllable disintegration of temperature-responsive self-assembled multilayer film based on polybetaine, *Colloids Surfaces A Physicochem. Eng. Asp.* 380 (2011) 270–279. doi:10.1016/j.colsurfa.2011.02.049.
- [167] P.F. Ren, H.C. Yang, H.Q. Liang, X.L. Xu, L.S. Wan, Z.K. Xu, Highly stable, protein-resistant surfaces via the layer-by-layer assembly of poly(sulfobetaine methacrylate) and tannic acid, *Langmuir*. 31 (2015) 5851–5858. doi:10.1021/acs.langmuir.5b00920.
- [168] E. Kharlampieva, S.A. Sukhishvili, Hydrogen-Bonded Layer-by-Layer Polymer Films, *J. Macromol. Sci. Part C Polym. Rev.* 46 (2006) 377–395. doi:10.1080/15583720600945386.
- [169] P. Thevenot, W. Hu, L. Tang, Surface chemistry influence implant biocompatibility, *Curr Top Med Chem.* 8 (2008) 270–280. doi:10.1016/j.nano.2008.04.001.
- [170] M. J. Schick, *Colloidal Polymers*, CRC Press, Lyon, France, 2003. doi:10.1201/9780203911488.
- [171] T.R. Kyriakides, Molecular Events at Tissue–Biomaterial Interface, in: *Host Response to Biomater.*, Elsevier, 2015: pp. 81–116. doi:10.1016/B978-0-12-800196-7.00005-0.
- [172] M.J. Jones, N.P. Donegan, I. V. Mikheyeva, A.L. Cheung, Improving transformation of *Staphylococcus aureus* belonging to the CC1, CC5 and CC8 clonal complexes, *PLoS One*. 10 (2015) 1–14. doi:10.1371/journal.pone.0119487.
- [173] A. Ducret, G.G. Hardy, Y. V Brun, Negative Bacteria, *Microbiol. Spectr.* 3 (2015) 1–45. doi:10.1128/microbiolspec.MB-0018-2015.Adhesins.
- [174] G. Xu, P. Liu, D. Pranantyo, L. Xu, K. Neoh, E. Kang, Antifouling and Antimicrobial Coatings from Zwitterionic and Cationic Binary Polymer Brushes Assembled via “Click” Reactions, *Ind. Eng. Chem. Res.* 56 (2017)

14479–14488. doi:10.1021/acs.iecr.7b03132.

- [175] S.Y. Wang, X.F. Sun, W.J. Gao, Y.F. Wang, B.B. Jiang, M.Z. Afzal, C. Song, S.G. Wang, Mitigation of membrane biofouling by D-amino acids: Effect of bacterial cell-wall property and D-amino acid type, *Colloids Surfaces B Biointerfaces*. 164 (2018) 20–26. doi:10.1016/j.colsurfb.2017.12.055.
- [176] S. Shaikh, D. Singh, M. Subramanian, S. Kedia, A.K. Singh, K. Singh, N. Gupta, S. Sinha, Femtosecond laser induced surface modification for prevention of bacterial adhesion on 45S5 bioactive glass, *J. Non. Cryst. Solids*. 482 (2018) 63–72. doi:10.1016/j.jnoncrysol.2017.12.019.
- [177] K. Bazaka, M. V. Jacob, R.J. Crawford, E.P. Ivanova, Efficient surface modification of biomaterial to prevent biofilm formation and the attachment of microorganisms., *Appl. Microbiol. Biotechnol.* 95 (2012) 299–311. doi:10.1007/s00253-012-4144-7.
- [178] Y. Chang, S. Chen, Z. Zhang, S. Jiang, Highly protein-resistant coatings from well-defined diblock copolymers containing sulfobetaines, *Langmuir*. 22 (2006) 2222–2226. doi:10.1021/la052962v.
- [179] E. Ostuni, R.G. Chapman, M.N. Liang, G. Meluleni, G. Pier, D.E. Ingber, G.M. Whitesides, Self-assembled monolayers that resist the adsorption of proteins and the adhesion of bacterial and mammalian cells, *Langmuir*. 17 (2001) 6336–6343. doi:10.1021/la010552a.
- [180] J. Gallo, M. Holinka, C. Moucha, Antibacterial Surface Treatment for Orthopaedic Implants, *Int. J. Mol. Sci.* 15 (2014) 13849–13880. doi:10.3390/ijms150813849.
- [181] S. Sanchez-Salcedo, M. Colilla, I. Izquierdo-barba, M. Vallet-Regi, Preventing bacterial adhesion on scaffolds for bone tissue engineering, *Int. J. Bioprinting*. 2 (2016) 20–34. doi:http://dx.doi.org/10.18063/IJB.2016.01.008.
- [182] K. Bruellhoff, M. Moeller, R.E. Brenner, Novel surface coatings modulating eukaryotic cell adhesion and preventing implant infection, 32 (2009) 655–662.

- [183] I. Izquierdo-barba, S. Sánchez-salcedo, M. José, *Acta Biomaterialia* Inhibition of bacterial adhesion on biocompatible zwitterionic SBA-15 mesoporous materials, *Acta Biomater.* 7 (2011) 2977–2985.  
doi:10.1016/j.actbio.2011.03.005.
- [184] J. Lam, N.F. Truong, T. Segura, Design of Cell-Matrix Interactions in Hyaluronic Acid Hydrogel Scaffolds, 10 (2015) 1571–1580.  
doi:10.1016/j.actbio.2013.07.025.
- [185] M. Sin, Y. Sun, Y. Chang, Zwitterionic-Based Stainless Steel with Well-Defined Polysulfobetaine Brushes for General Bioadhesive Control, (2014).
- [186] X. Liu, Z. Xu, Osteogenesis in calcified aortic valve disease: From histopathological observation towards molecular understanding, *Prog. Biophys. Mol. Biol.* 122 (2016) 156–161.  
doi:10.1016/j.pbiomolbio.2016.02.002.